CHAPTER - 2

Synthesis and study of aza[n]helicene based chiral amines

2.1 Azahelicenes

The helicenes grafted with *N* atom are called azahelicenes which belong to the subgroup of heterohelicenes.[1] They are composed of *ortho* fused benzene and *N*-heterocyclic rings. Various heterocycles such as pyridine, pyrrole, pyridazine or pyrazine can be incorporated into the helical skeleton to form azahelicenes (**Figure 2.1**).

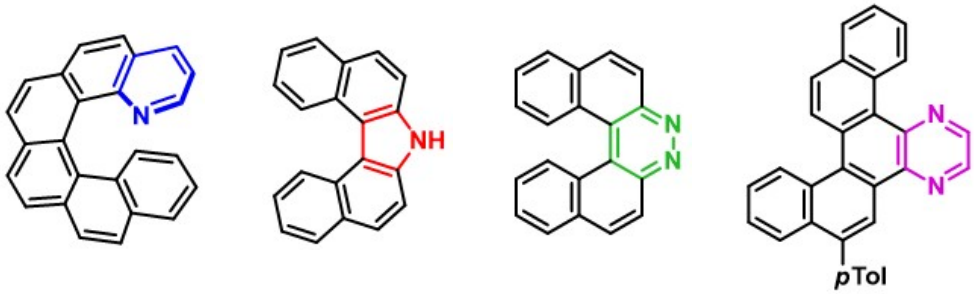

***Figure 2.1**: N-incorporating helicenes*

The presence of nitrogen and its lone pair strongly modifies the characteristics of an aromatic ring. The electronegativity of *N* atom alters the inherent properties of the whole ring such as its electron density, its redox potentials, its aromaticity, and also reactivity towards electrophiles and nucleophiles. The lone pair of *N* in pyridyl unit is not involved in the π-conjugation and is thus available for reacting with other systems (basicity, oxidation, coordination, and so on), whereas in pyrroles the lone pair of *N* is engaged in the ring aromaticity and is thus unavailable directly for reactions. All these factors directly affect the photophysical, chiroptical and other properties of azahelicenes such as complexation, conduction, or catalysis.

2.2 Approaches for incorporating *N* within the helical scaffold

2.2.1. Photochemical approach

The photochemical approach for the synthesis of aza[n]helicenes can be divided into two main subgroups, where: First group utilizes the light-induced cyclization of stilbene moiety containing C=C double bond substituted by various aromatic *N*-heterocycles, whereas the second one uses photocyclization of arylimines or hydroxamic acids.

The oxidative photocyclization is one of the most widely used methods for the synthesis of aza[n]helicenes. Many derivatives of aza[n]helicenes have been synthesized by this method

ranging from five membered to larger analogues. In 2005, Carrona group carried out the oxidative photocyclization of stilbene derivatives to obtain a series of aza or diaza[5]helicenes.[2] Stillbene derivatives were prepared by a Wittig reaction between the corresponding aldehydes and phosphonium salts. After oxidative photocyclization, aza[5]helicenes, where nitrogens placed at different positions respectively, were prepared with high regioselectivity and high yields. (**Scheme 2.1**)

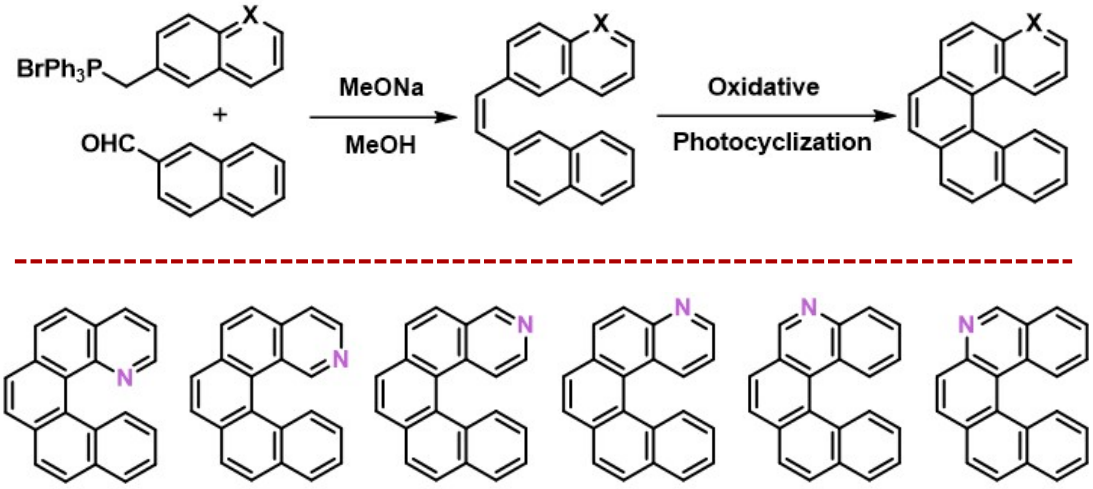

***Scheme 2.1**: Synthesis of aza[5]helicenes by oxidative photocyclization*

Aza[5]helicenes are good models for the study of configurational stability. Corrona and group observed that these aza[5]helicenes showed lower activation barriers compared to carbo[5]helicene. Also, a similar observation was made by Starý and Stará group.[3] Later, Daehen and co-workers also failed to resolve aza[5]helicenes due to their rapid racemization under ambient conditions.[4] The same oxidative photochemical approach was used by Hassine for the synthesis of aza[6]helicene.[5] (**Scheme 2.2**) Enantiomers were separated by chrial HPLC and chiroptical properties of compound **2** were reported.

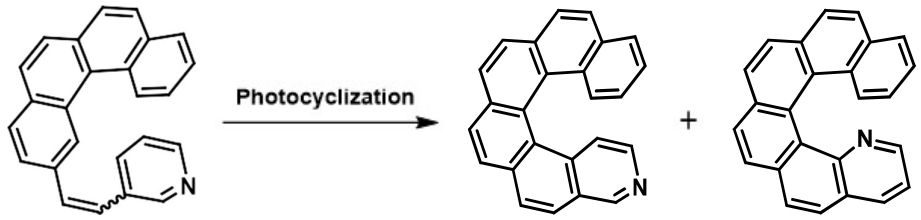

***Scheme 2.2**: Synthesis of aza[6]helicene by oxidative photocyclization*

Howarth attempted the photochemical synthesis of 8,11-diaza[7]heptahelicene from the

bis-imine precursor for the first time in 1997.[6] Unfortunately, the low yield of the reaction discouraged the use of aromatic imines as precursors for azahelicenes. The poor reactivity of imines caused by the thermal instability of *Z*-conformers results in the lower yield of such reactions. Later, Murase came up with an idea to use the boron complexes of *N*-phenylbenzohydroxamic acid **4** possessing a fixed *Z*-conformation minimizing the influence of lone electron pair on the nitrogen atom, thus leading to successful photocyclization on cleavage of N–O bond.[7] (**Scheme 2.3a**) Recently, Alabugin, Církva, and Sýkora reported a Brønsted acid-promoted photocyclization of arylimine.[8] (**Scheme 2.3b**) Unfortunately, higher aza[n]helicenes ($n > 6$) remained inaccessible by using this approach.

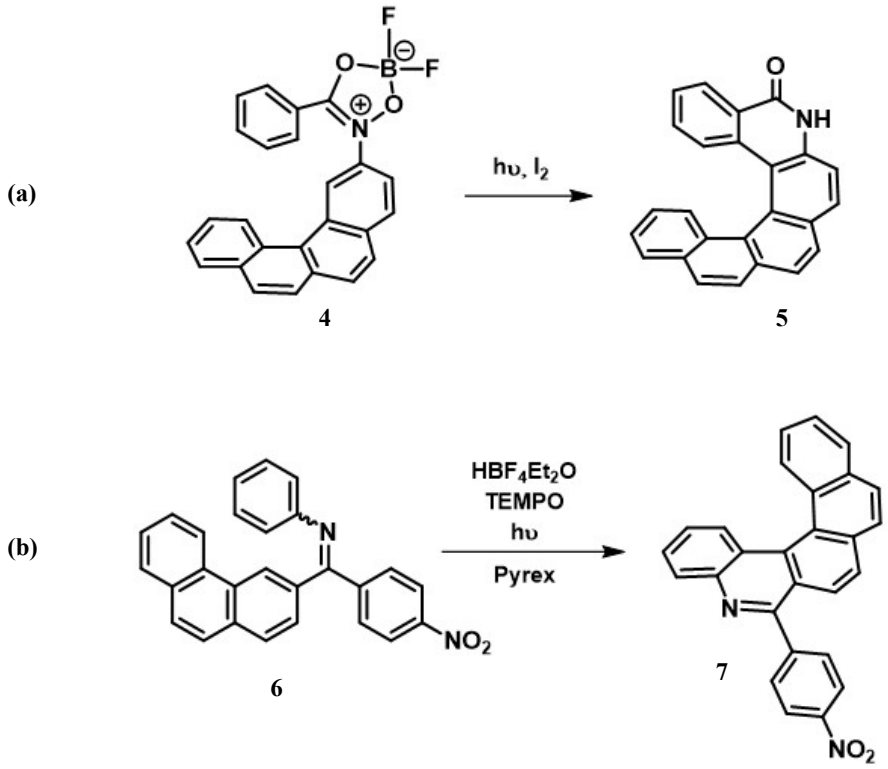

***Scheme 2.3**: Photocyclization of (a) hydroxamic acid and (b) arylimine*

2.2.2. Non photochemical approaches

The first diaza[6]helicene **10** was synthesized in 1927 by Fuchs and Niszel via double Bucherer carbazole synthesis, a nonphotochemical approach.[9] Later, Pischel and co-workers prepared the corresponding tetramethyl derivative **11** by using the same method and separated its enantiomers using chiral HPLC.[10] (**Scheme 2.4**)

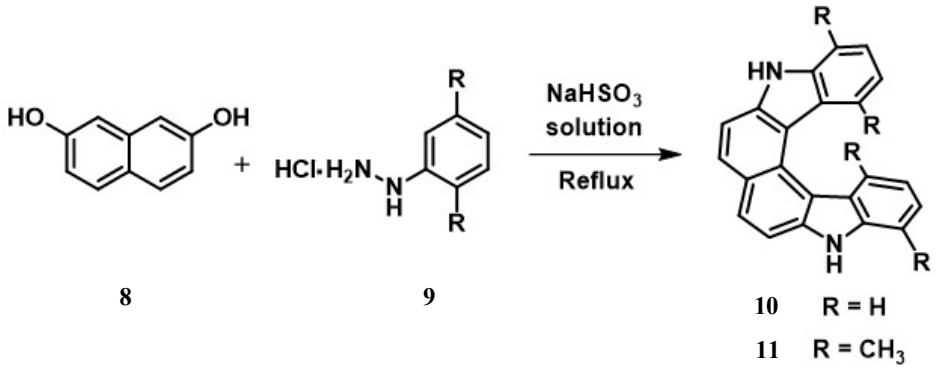

8 **9** **10** R = H **11** R = CH_3

***Scheme 2.4**: Preparation of diaza[6]helicenes by double Bucherer carbazole synthesis*

The use of transition metal catalysed [2+2+2] cycloisomerisation of aromatic triynes is a highly versatile nonphotochemical methodology for the synthesis of azahelicenes.[11] Utilising this strategy, Stará, Starý and co-workers reported the syntheses of 1-aza[6]helicene **16** and 2-aza[6]helicene **17** (**Scheme 2.5**).[12] Here, cobalt-catalysed [2+2+2] cyclotrimerisation of aromatic pyridotriynes was used to prepare the helical scaffolds. Also, they were successful in obtaining the enantiomers of **16** and **17**, assigning their absolute configuration and obtaining the X-ray crystal structures of their corresponding silver complexes.

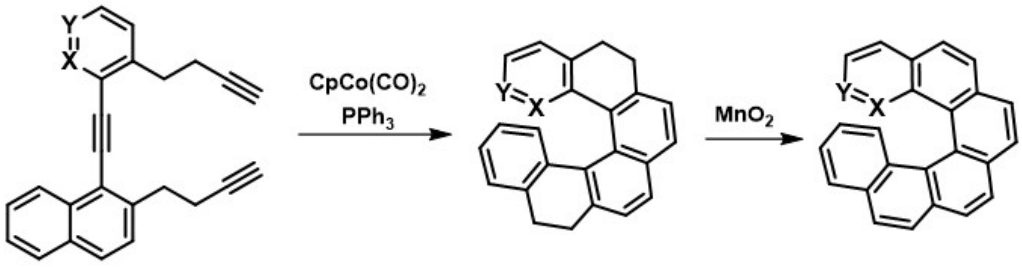

12 X=N, Y=H
13 X= H, Y=N

14 X=N, Y=H (82%)
15 X= H, Y=N (89%)

16 X=N, Y=H (65%)
17 X=H, Y=N (53%)

***Scheme 2.5**: Synthesis of aza[6]helicenes by [2+2+2] cycloisomerization*

Takenaka and co-workers developed synthetic route to a series of 1-aza[5]- and [6]helicene oxides based on the key Stille-Kelly coupling reaction to form an internal benzene ring of the helical skeleton (**Scheme 2.6**).[13] A highly Z-selective Wittig olefination reaction was performed by combining benzo[h]quinoline- derived aldehyde **19** with the phosphonium salt **18** to obtain the dihalogenated olefin **20**. The subsequent Stille-Kelly reaction of this olefin **20** resulted in the formation of 1-aza[6]helicene **21**. Two more derivatives- aza[5]helicene oxide and a variant of aza[6]helicene oxide were also synthesized in good yields. Racemic helicenes were subsequently converted to helicenic *N*-oxides **22** (a family of asymmetric catalysts) using *m*-CPBA and the enantiomers were separated with the help of chiral HPLC.

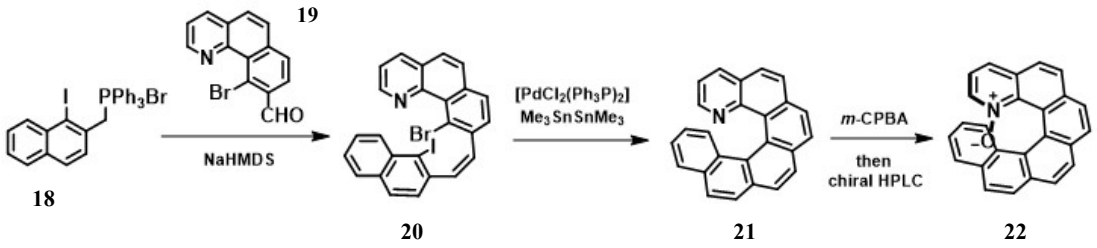

***Scheme 2.6**: Synthesis of enantiopure aza[6]helicene oxide*

Fuchter and co-workers devised a scalable route for the synthesis of 1-aza[6]helicene derivatives utilizing a Pt-catalyzed alkyne-arene cycloisomerisation (**Scheme 2.7**).[14] It is the shortest and most practical synthetic route to obtain 1-aza[6]helicene. By employing cycloisomerization process with [$PtCl_4$] in dichloroethane, axially chiral precursors **23** were transformed to chiral helicenes **24**. Here, the enantioenriched axially chiral precursors **23** were obtained *via* a chiral HPLC resolution step.

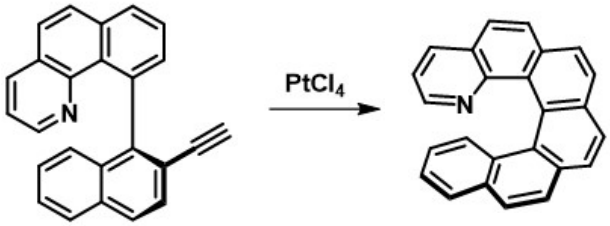

***Scheme 2.7**: Synthesis of 1-aza[6]helicene by alkyne-arene cycloisomerization*

Asymmetric synthesis of azahelicenes was uncommon until the significant achievements were made by Nozaki and coworkers by synthesizing enantiopure aza[7]helicene. A Pd-catalyzed double *N*-arylation of primary amine with the nonaflate derivative of enantiopure 4,4'-biphenanthryl- 3,3'-diol (*S*)-**40** was used for the synthesis of enantiopure carbazole derived aza[7]helicene (*P*)-**26** (**Scheme 2.8**).[15]

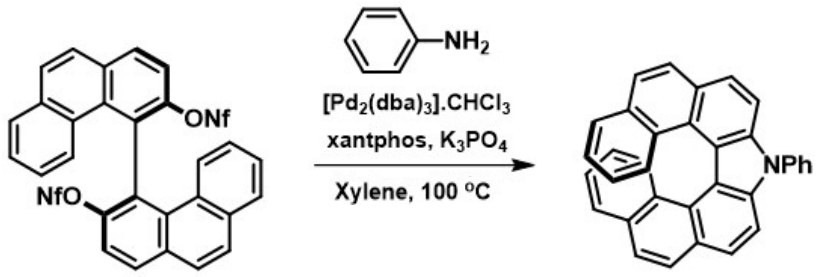

***Scheme 2.8**: Enantiopure synthesis of aza[7]helicene by intramolecular N-arylation*

In 2014, List and co-workers reported an asymmetric organocatalytic synthetic approach to obtain indole/carbazole-derived azahelicenes (**Scheme 2.9**).[16] An enantioselective Fischer indolisation reaction catalyzed by a chiral SPINOL-derived phosphoric acid containing extended π-substituents (*S*)-**29** was employed to prepare the helical skeleton in good yield.

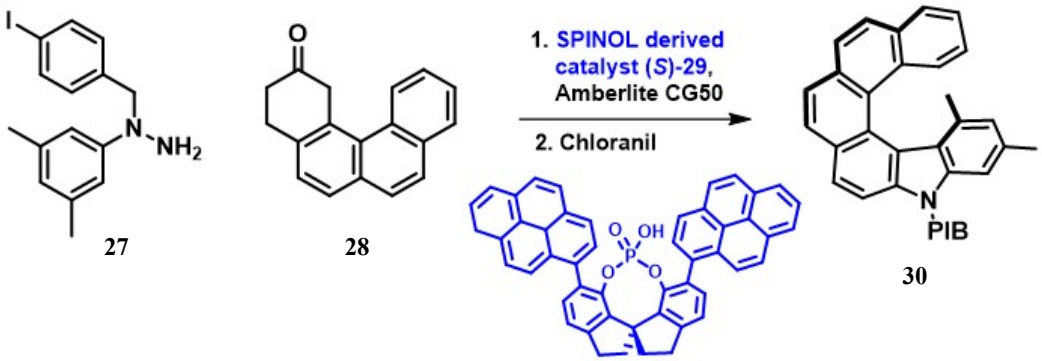

***Scheme 2.9**: Asymmetric synthesis of aza[6]helicene by enantioselective Fischer Indolization*

Osuka and co-workers reported the use of oxidative fusion reactions of 1,2-phenylene-bridged tripyrrolic precursors for the formation of pseudo-triaza[5]helicene and a series of triaza[7]helicenes. Here, multiple oxidative fusion followed by a 1,2-aryl shift resulted into the formation of helicene **32** (**Scheme 2.10**).[17]

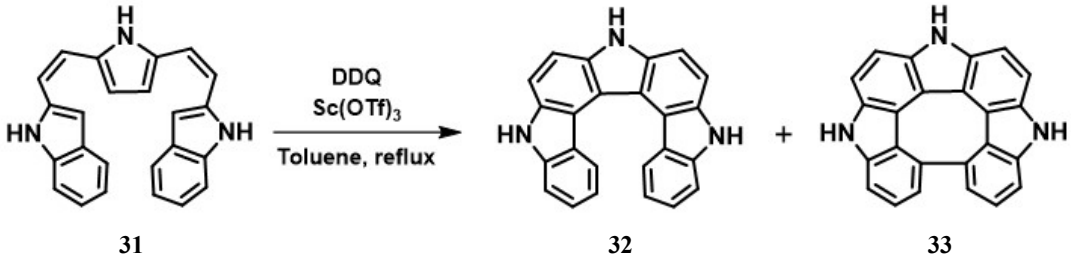

***Scheme 2.10**: Synthesis of trisaza[7]helicene by oxidative fusion of pyrroles*

Most of the reported azahelicenes are derivatives of pyridine or pyrrole. Azahelicenes show potential applications in the fields of light-emitting devices, chemosensors, asymmetric catalysis and self-assembly.[18] In our present study, we have synthesized aza[n]helicenes using carbazole as a structural motif by oxidative photocyclization approach. Carbazole was chosen as our starting point for the synthesis of helical skeleton due to several reasons: its easy availability, presence of three inbuilt rings, cheap starting material and regioselective functionalization.

CHAPTER - 2A

Synthesis and resolution of unsymmetrical 2-amino-5-aza[6]helicene

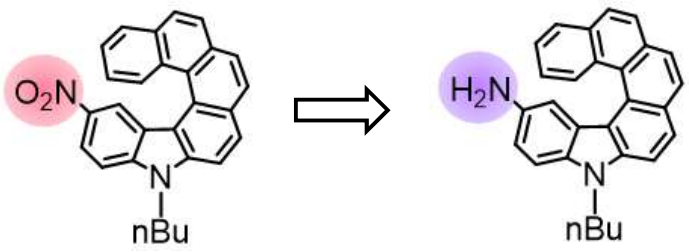

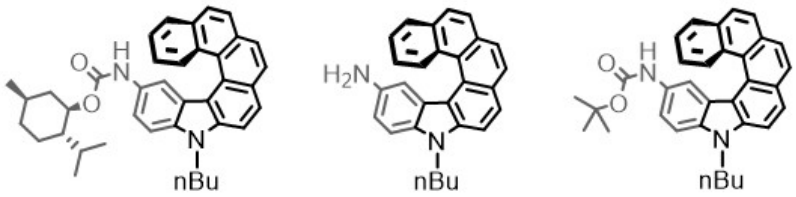

$[\alpha]_D$ + 1183 $[\alpha]_D$ + 1105 $[\alpha]_D$ + 1120

Table of Contents

2A.1 Chemistry of Amino-Substituted Helicenes: Literature Insight

Because of the incompatibility of amino group with the classical oxidative photocyclization process to synthesize amino-substituted helicenes, other methods have been developed in order to access this class of helical compounds. In some cases, either a protected amino group or a group easily convertible to amino is installed at an early stage of synthesis before the photocyclization step.

Starý, Stará and co-workers recently prepared the nonracemic 2-amino[6]helicene derivatives. An enantioselective [2+2+2] cycloisomerization of an achiral triyne under [Ni(COD)$_2$]/(R)-QUINAP catalysis was used to obtain (*P*)-(+)-**2** and its Boc-protected analogue **1** in 67% ee. A "point-to-helical" chirality transfer occurred during the cyclization reaction of enantiopure triynes mediated by [Ni(CO)$_2$(PPh$_3$)$_2$] to afford (*M*)-(−)- or (*P*)-(+)-hexahelicen-2-amine **4**, its benzoderivative **6** along with their Boc-protected analogues (**3** and **5**) in >99% ee (**Figure 2A.1**).[19] Later, aminohelicene **4** (racemic and enantiopure) was examined for its behavior in self-assembly at the air-water interface by the use of Langmuir-Blodgett (LB) method. It was observed that despite of the absence of long alkyl chains, (rac)-, (*M*)-(−)-, and (*P*)- (+)-7,8-bis(*p*-tolyl)hexahelicen-2-amines **4** formed Langmuir monolayers at the air-water interface. AFM microscopy was used to characterize the LB films on quartz or silicon substrates.

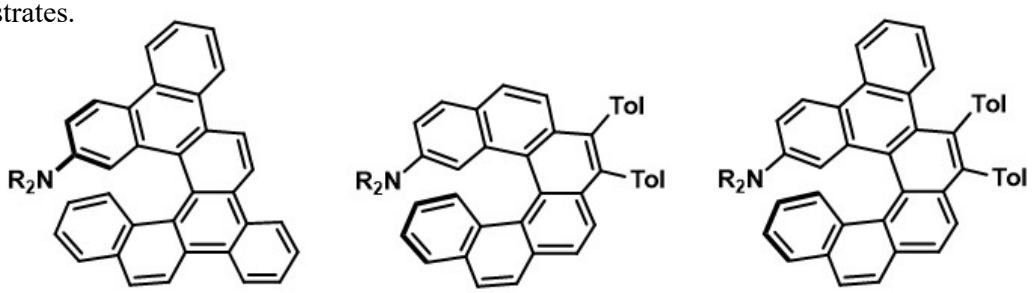

(*P*)-**1** (R = Boc)
(*P*)-**2** (R = H)
67% ee

(*M*)-**3** (R = Boc)
(*M*)-**4** (R = H)
>99% ee

(*M*)-**5** (R = Boc)
(*M*)-**6** (R = H)
>99% ee

***Figure 2A.1**: Derivatives of 2-amino[6]helicenes prepared by [2+2+2]cycloisomerization*

In 2016, Kellogg and co-workers prepared 5-amino-carbo[6]helicene by cycloisomerization using [PtCl$_2$] (**Scheme 2A.1**).[20] Several attempts were made for the resolution of amino helicene **9** by crystallization of diastereomeric salts with various chiral acids which resulted in failure. Then, the separation of enantiomers was achieved by performing chiral HPLC on a Chiralcel OD-H column. Authors also attempted the enantioselective

cycloisomerization but did not meet with much success.

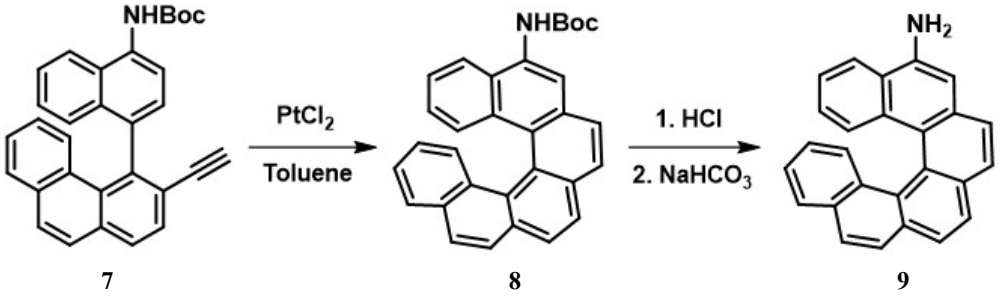

***Scheme 2A.1**: Synthesis of 5-amino[6]helicene by cycloisomerization*

Also, Kellogg's group examined the self-assembly of enantiopure as well as on racemic sample of 5-aminohelicene **9** at liquid-solid interface. A solution of **9** in 1,2,4- trichlorobenzene (TCB) was applied on a Au(111) surface and observed the formation of a "three-dot" p3-(P3) pattern (**Figure 2A.2 (1)**), along with the partial spontaneous resolution of (*M*)- and (*P*)-**9** on the surface.[21] The self-assembly was also examined under ultrahigh vacuum (UHV) conditions by scanning tunneling microscopy (STM) (**Figure 2A.2 (2)**).[20] It was observed that two rotational domains formed by the rows of dimers oriented along the ⟨1−11⟩ Au crystallographic directions were formed for the enantiopure aminohelicene. The racemic compound showed the emergence of two enantiomorphous domains which were rotated by 6° with respect to the ⟨1−11⟩ crystallographic directions and exhibited a double-row structure. This assembly of double rows appeared remarkably different from the triangular structures formed at the Au(111)/1,2,4-trichlorobenzene (TBC) interface.

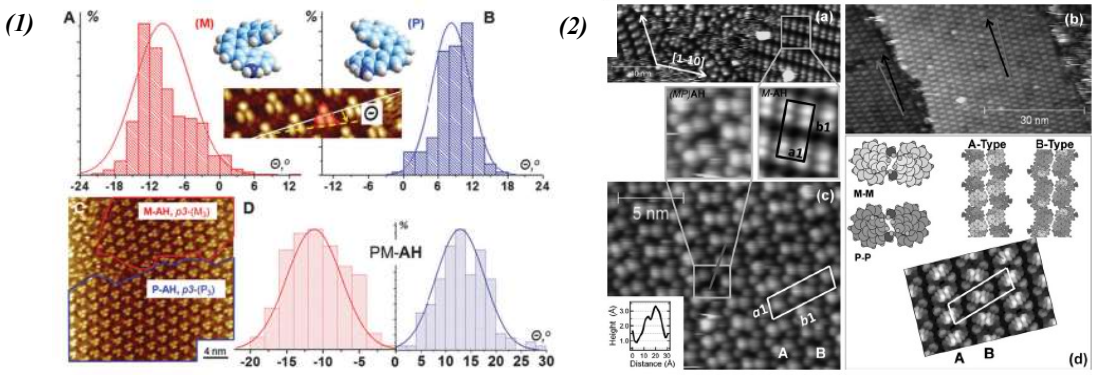

***Figure 2A.2**: **(1)** Self-assembly of 9 formed at Au(111)/TCB interface. (A, B, D) Distribution of tilt angles (Θ) between the sides of helicene trimers and the unit cell vectors in p3-(2973) patterns of (M)-, (P)- and (rac)- 9, respectively. (C) STM image of homochiral conglomerates (p3-(M3) and p3-(P3), red and blue, respectively) formed from racemic 9.[21] **(2)** (a) STM image of (M)-9 on Au(111) at UHV. (b, c) STM images of racemic 9 on Au(111). (b) Two enantiomorphous domains separated by a monatomic step of the surface. (c) High-resolution image of the molecular structure developed by the racemate (d) DFT-based molecular model of the racemic structure in (c) that highlights the presence of M−M and P−P dimers in the A- and B-type molecular row model. Different colors indicate different chirality: light gray for (M)-9 and dark gray for (P)- 9.[20]*

Later, Ascolani, Fuhr, Lingenfelder and co-workers reported the assembly of (*M*)-5-amino-helicene **9** on Cu(100) and Au(111) under UHV conditions studied by STM. It was observed that the amino group does not induce polar interactions by hydrogen bonding but rather maximizes van der Waals interactions which directs the formation of the self-assembly.[22]

Crassous and co-workers converted helicene-boronate (*M*)-**10** to a variety of amino derivatives (**Scheme 2A.2**).[23] Carbo[6]helicenyl boronate was synthesized by using oxidative photocyclization as the key step and the enantiomers were separated by chiral HPLC. 2-Aminocarbo[6]helicene (*M*)-**12** was synthesized by Cu-catalyzed azidation yielding (*M*)-**11**, followed by hydrogenation. Further, the secondary *N*-benzyl helicenyl amine (*M*)-**13** was synthesized from (*M*)-**10** by converting it to the helicenic dichloroborane followed by in situ treatment with benzyl azide. A Chan-Lam amination was used to prepare the piperidino derivative (*M*)-**13**. Also, (*M*)-**10** was transformed to an amino ester derivative **15** by a three-component Petasis condensation using glyoxylic acid and morpholine, followed by (trimethylsilyl)diazomethane mediated esterification reaction. This condensation resulted in the formation of the mixture of two diastereomeric compounds with a good stereocontrol (dr: 7/ 3).

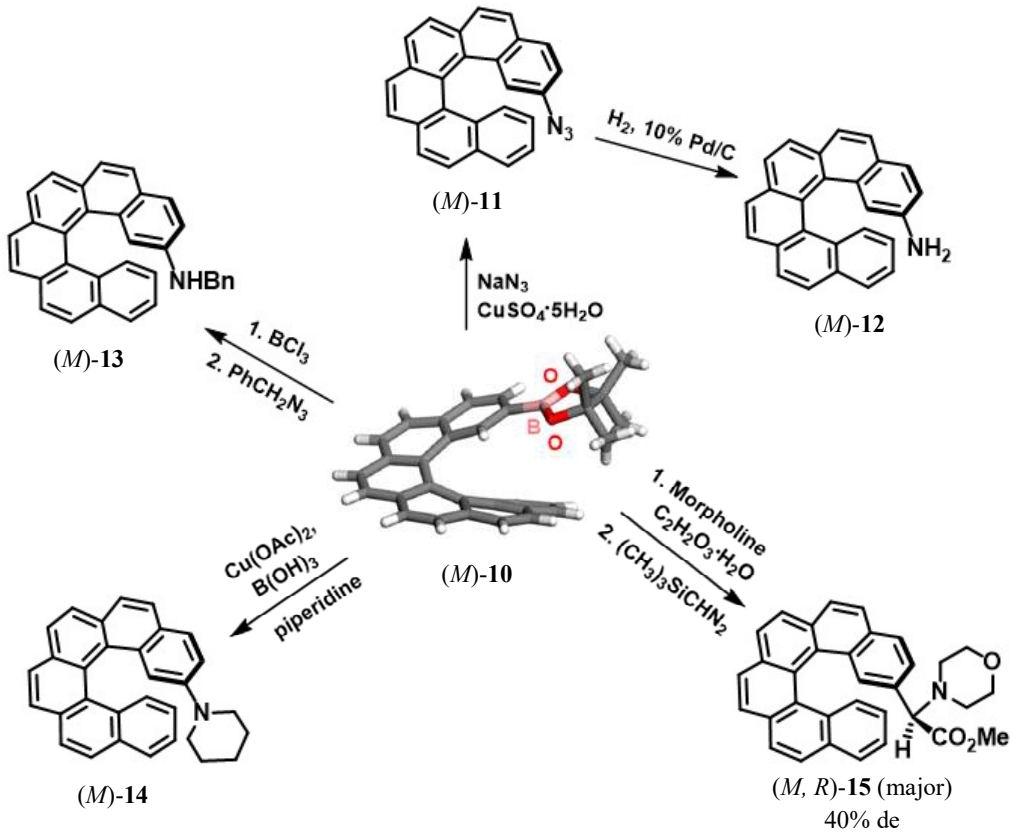

***Scheme 2A.2**: Synthesis of amino helicenyl derivatives from helicene-boronate (M)-10*

Sugiyama group studied the effect of functionalities on the helical skeletons.[24] When these helicenes were added to solution of Z-DNA or B-DNA, it was observed that the helicene **16** exhibited the selectivity in binding with Z-DNA and effectively converted B-DNA into Z-DNA (**Figure 2A.3 (a)**). The associate constant for (*P*)-**16** was five times larger compared to (*M*)-**16**. In comparison, the helicene **17** did not show any selectivity, which indicated that the presence of amino groups on the helical skeleton were essential for the interaction with Z-DNA.

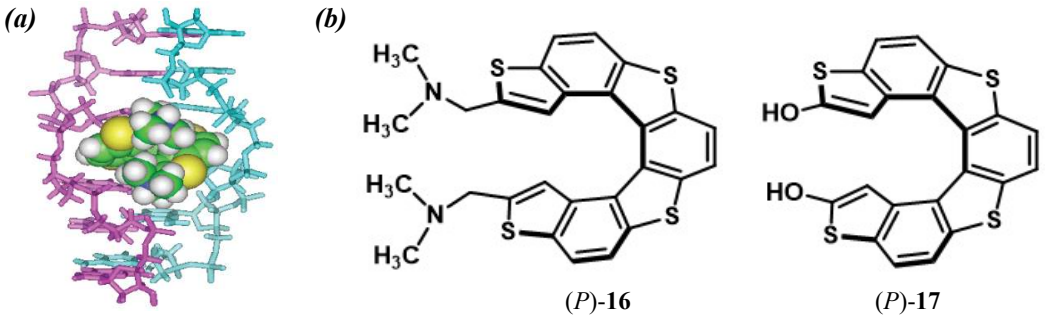

***Figure 2A.3**: (a) Schematic representation of Z-DNA with (P)-2 (b) structures of different functionalized thiahelicenes.[24]*

Starý, Stará and co-workers reported a non-photochemical synthetic approach to 3-hexahelicenol **18**. Ni(0)-catalyzed intramolecular [2+2+2] cycloisomerization of aromatic triynes was used as the key step for the synthesis of helical scaffold. Here, the cyclization proceeded enantioselectively as the chiral ligand (*R*)-(+)-BINAP was used in the reaction but failed to observe any kinetic resolution. Further functional group transformations led to the formation of a series of 3-substituted hexahelicenes. A Buchwald-Hartwig amination method was applied to prepare the amino derivatives (**Scheme 2A.3**).[25]

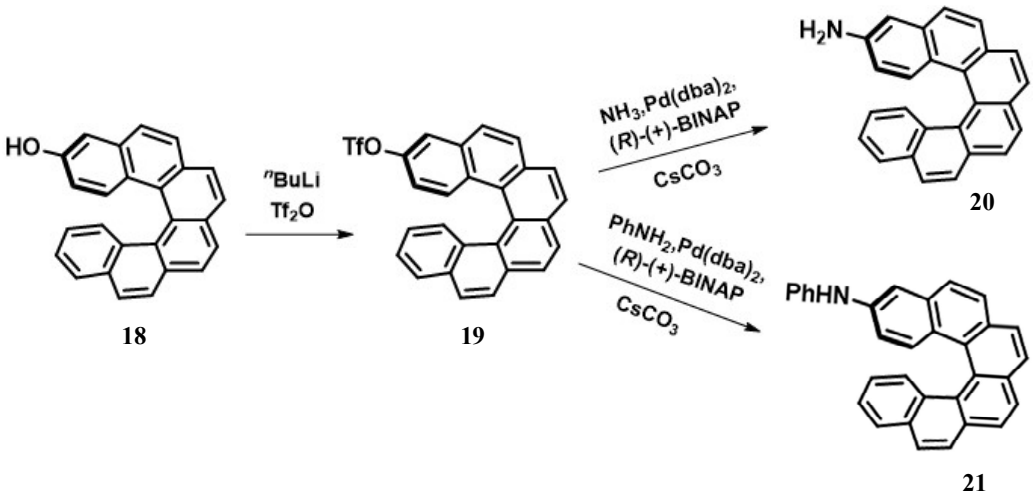

***Scheme 2A.3**: Synthesis of amino helicenyl derivatives by Buchwald-Hartwig amination*

Yamaguchi and co-workers reported the synthesis of stable [4]helicene derivatives. They first synthesized 1,12-dimethylbenzo[c]phenanthrene-5,8-dicarboxylate **22** and carried out its resolution by forming diastereomeric (−)-quinine salts via repeated recrystallization. They also explored the chemical reactivity of the chiral helical diacid (*P*)-**22** in order to access a large variety of functional groups: electron accepting groups like nitro and nitrile groups and electron donating groups like amino and hydroxyl. In 2001, they synthesized 5,8-bis-amino-1,12-dimethyl-[4]helicene (*P*)-**23** from dicarboxylic acid (*P*)-**22** via Curtius rearrangement (**Scheme 2A.4**).[26] The functionalized [4]helicenes were investigated for their behavior in chiral recognition. The electron deficient tetranitro derivative of [4]helicene (*P*)-**24** formed charge-transfer (CT) complex with an electron rich diamino derivative (*P*)-**23** in solution.[26] Later in 2011, Yamaguchi and co-workers further synthesized enantiopure oligomer (*P*,*P*,*P*)-**25** from diamino helicene (*P*)-**23** in order to investigate their aggregation behavior in different solvents, and at varying concentration and temperature conditions.[27]

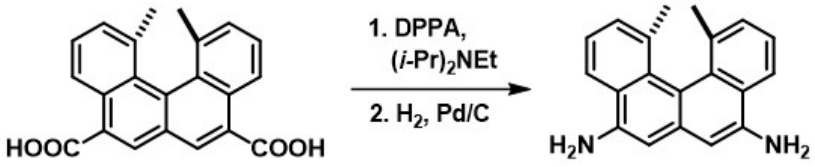

(*P*)-**22** (*P*)-**23**

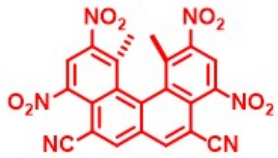

(*P*)-**24**

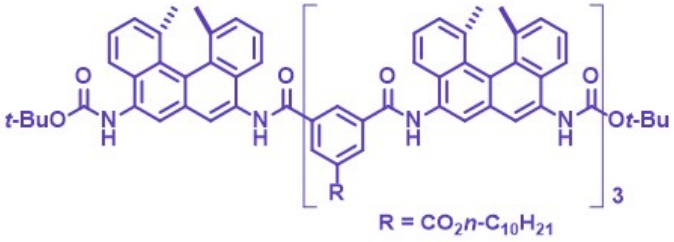

(*P*,*P*,*P*)-**25**

***Scheme 2A.4**: Synthesis of diamino[4]helicene; 5,8-dicyano-1,12-dimethyl-2,4,9,11-tetranitro[4]helicene (in red); helicene oligomer (in blue)*

Lacour and co-workers reported the regioselective post-functionalization of racemic and enantiopure cationic diaza [4]helicenes (**Scheme 2A.5**).[28] Variation in the peripheral auxochrome substituents, allowed a general tuning of their electrochemical, photophysical and chiroptical properties. The functionalized helicenes exhibits stronger circular dichroism in the visible region compared to the parent helicene **26**. Helicenes *M*-**27** and *M*-**28** displayed

absorption of circularly polarized light in the range of 400-600 nm, which corresponds to the first and second low energy absorption transitions. The amino helicene *M*-**29** appeared to be a rare example of purely organic helicene showing ECD in the far-red and NIR region of the electromagnetic spectrum.

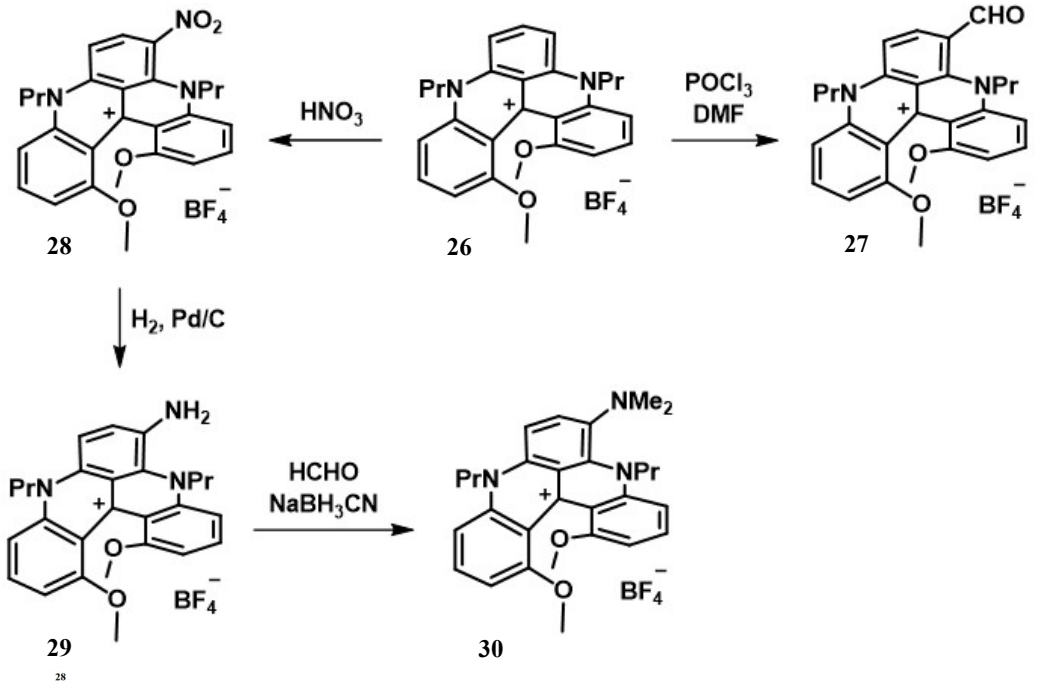

***Scheme 2A.5**: Functionalization of [4]helicene*

In 2017, Starý and Stará reported a straightforward route to access optically pure 2-aminooxa[5]helicenes and 2-aminooxa[6]helicene by using [2+2+2] cycloisomerization of chiral functionalized triynes as the key step.[29] Helicene-amine derivatives (*M*,*R*,*R*)-(−)-**32** and chloro-substituted (*M*,*R*,*R*)-(−)-**34** were prepared by diastereoselective [2+2+2] cycloisomerization process, then **32** was hydrolyzed to obtain (*M*,*R*,*R*)-(−)-**33**, while (*M*,*R*,*R*)-(−)-**34** was further subjected to Suzuki coupling using different arylboronic acid or aryl-boronates, yielding (*M*,*R*,*R*)-(−)-**35b−g** which on hydrolysis gives (*M*,*R*,*R*)-(−)-**36b−g** (**Scheme 2A.6**).

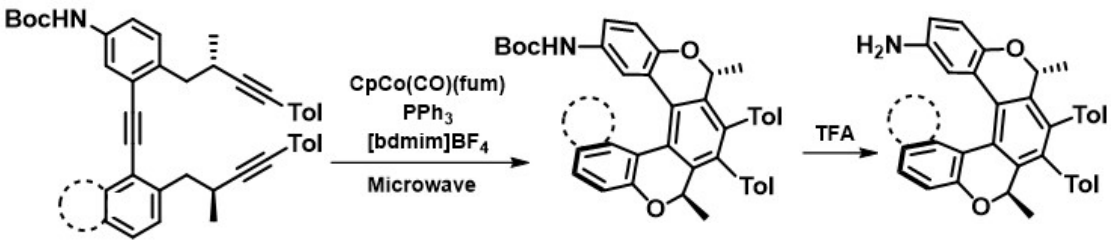

(*R*,*R*)-(-)-**31** (*M*,*R*,*R*)-(-)-**32** (*M*,*R*,*R*)-(-)-**33**

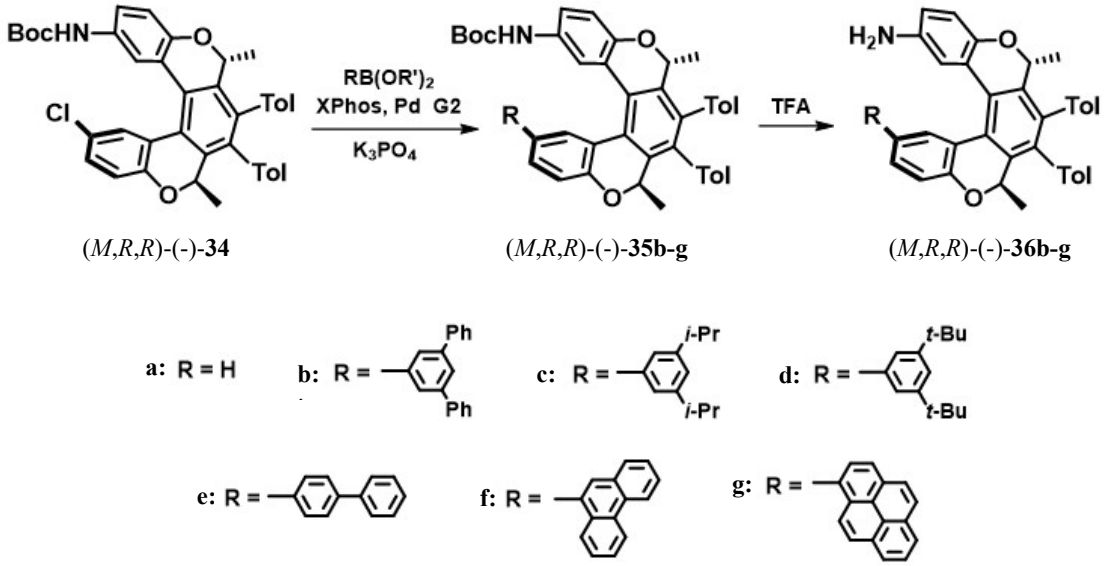

***Scheme 2A.6**: Synthesis of 2-amino derivatives of oxa[5]- and oxa[6]helicene*

These amino oxahelicenes were further converted to the imidazolium salts (*M*,*R*,*R*)-(−)-**37** and (*M*,*R*,*R*),(*M*,*R*,*R*)-(−)-**38** by two different ways as depicted in **Scheme 2A.7**, depending on which either the monohelicenic or bis-helicenic structure is obtained.

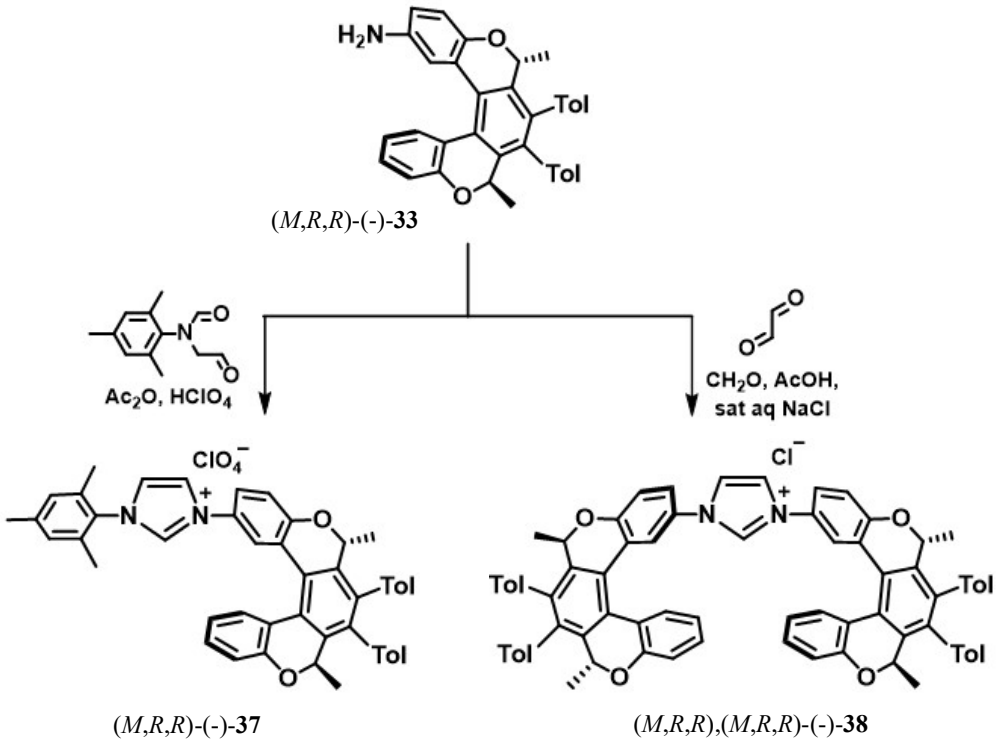

***Scheme 2A.7**: Synthesis of imidazolium salts from 2-amino derivatives of oxa[5]- and oxa[6]helicene*

Enantiopure helical NHC ligand precursors (*M*,*R*,*R*)-(−)-**37** and (*M*,*R*,*R*),(*M*,*R*,*R*)-(−)-**38** were used in the enantioselective Ni(0)-catalyzed [2+2+2] cycloisomerization of the aromatic triynes to obtain the helicene derivatives in upto 86% ee (**Scheme 2A.8**).

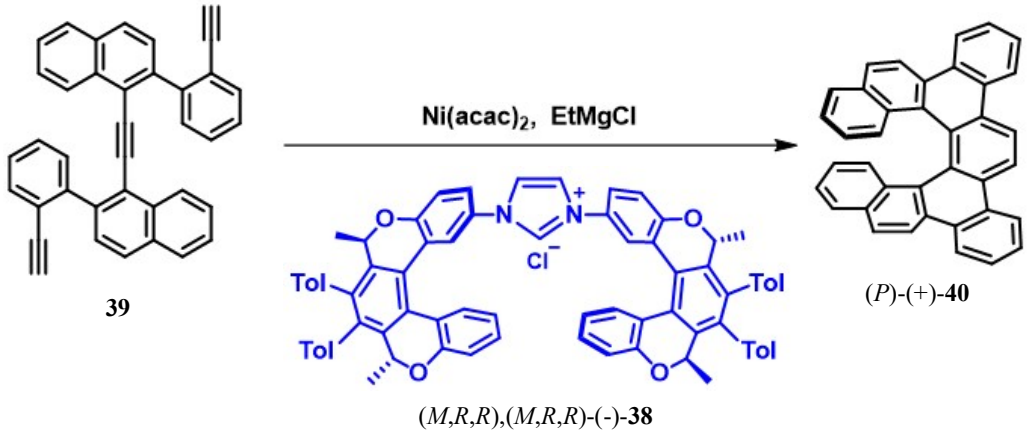

39

(*M*,*R*,*R*),(*M*,*R*,*R*)-(-)-**38**

(*P*)-(+)-**40**

***Scheme 2A.8**: Non-racemic synthesis of helicenes mediated by enantiopure helicene NHC ligand precursor*

The synthesis and studies of amino-substituted azahelicenes are relatively less explored as seen in the available literature. The presence of primary amino group on aromatic rings of helical system can be useful to introduce various functional groups for suitable modifications as well as it can be helpful in searching applications as observed in the literature. The amino group is also adequate to form salts with chiral acids to prepare diastereomers or to conveniently attach chiral modifiers to make diastereomeric derivatives for easy separation of isomers. The introduction of an amino group can be achieved via several means, reduction of nitro group, coupling with aryl halides, Hoffmann rearrangement of primary amides or from some name reactions like Curtius, Lossen etc. In this chapter we shall discuss the preparation of 2-amino-5-aza[6]helicene via reduction of its corresponding nitro derivative and elaborate on our efforts to isolate it in optically pure form.

2A.2 Results and Discussion

2A.2.1 *Synthesis of 2-nitro-5-aza[6]helicene*

The synthetic route to 2-nitro aza[6]helicene **47** started with the *N*-butylation of carbazole (**Scheme 2A.9**). This *n*-Bu group was introduced in order to improve the solubility of carbazole.[30] The butylated carbazole **42** was formylated using Vilsmeier-Haack conditions to obtain 3-formyl-*N*-butylcarbazole **43** which was subjected to nitration to get 6-nitro-3-formyl derivative **44** in good yield. One of the effective methods to construct phenanthrene and benzo[*c*]phenanthrene substructure of poly aromatic hydrocarbons is the photochemical dehydrogenative oxidative cyclization of the corresponding stilbene derivatives.[31] Commonly, the photochemically induced cyclization is performed in the presence of iodine as the oxidant and the propylene oxide[31c] or THF[32] as the scavenger of the byproduct, hydroiodic acid. With the view to adopt this strategy to construct the angularly shaped aza[6]helicene, the stilbenenoid **46** was synthesized from nitroaldehyde **44** by Wittig olefination with triphenylphosphonium salt **45**, prepared from 2-bromomethyl naphthalene.

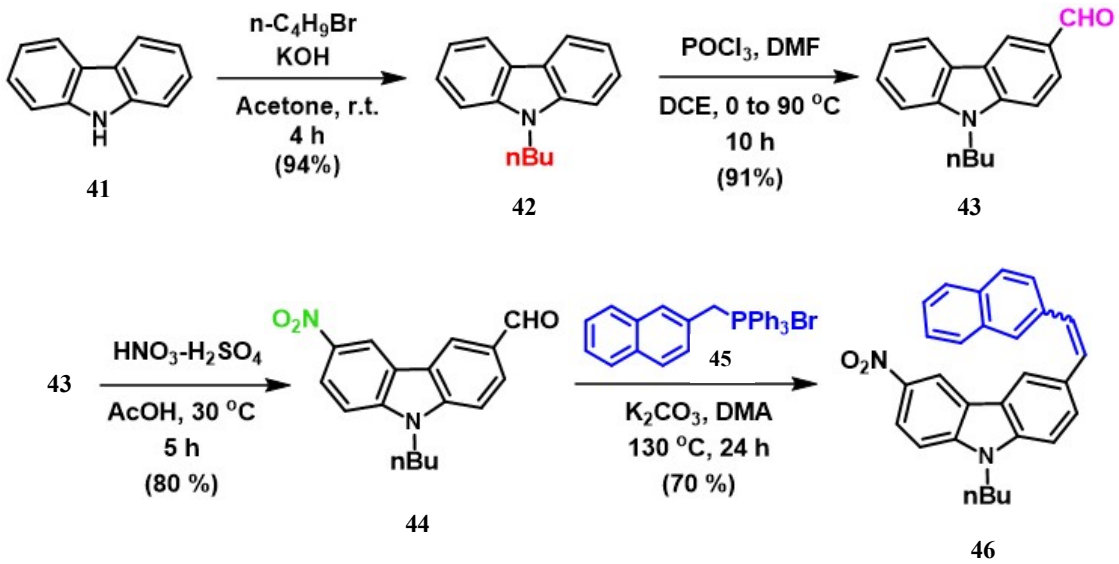

***Scheme 2A.9**: Synthesis of stilbenoid 45 – a precursor of 2-nitro aza[6]helicene*

The stilbenoid **46** was isolated mostly in its E-isomer, and subjected to the photochemical cyclization in the presence of I_2-THF in toluene and irradiation with high pressure mercury vapour lamp (125 W) (**Scheme 2A.10**). The cyclization of such systems with bulkier aromatic substituents, often lead to the products of both the possible ring closing modes. The angular cyclization will lead to desired product **47**, while the linear mode of cyclization will give **48**. In our previous study of the photocyclization of the carbazole derived bis-stilbene

attached with naphthalene units, we have established that the cyclization directed to the angular position is favoured at very low concentration.[33] Accordingly, the photocyclization was performed in toluene with 9.9 X 10^{-4} mol/L solution.

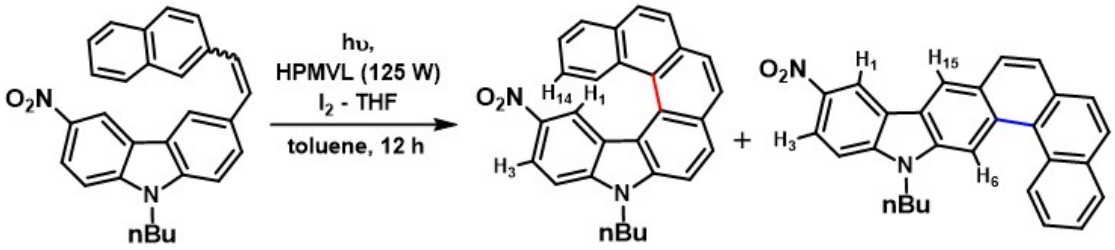

46 **47 (31%)** **48 (3%)**

***Scheme 2A.10**: Photocyclization of stilbenoid 46*

The products obtained on the cyclization of **46** were carefully separated and characterized by ^{1}H NMR analysis. The ^{1}H NMR of the crude reaction mixture showed the presence of angularly cyclized isomer **47** as major product, while the linear one **48** was formed in minor amount (85.5:14.5) (**Figure 2A.4**). The structure of **47** was confirmed by the presence of hydrogen attached to C1 (H_1) at upfield region of 7.58 ppm as a "d", as it is shielded by the last aromatic ring of the helix. The hydrogen on C3 (H_3) appeared at 8.28 ppm as a "dd," while one attached at C14 (H_{14}) showed a "m" at 7.13 ppm, also indicating the formation of **47**. The linearly cyclized isomer **48** showed a "d" at 9.21 ppm for the hydrogen attached to C1 (H_1) and "dd" at 8.51 ppm for hydrogen at C3 (H_3). This structure was further established by the presence of two singlets in the downfield region (8.80 and 9.16 ppm) for H_6 and H_{15}.

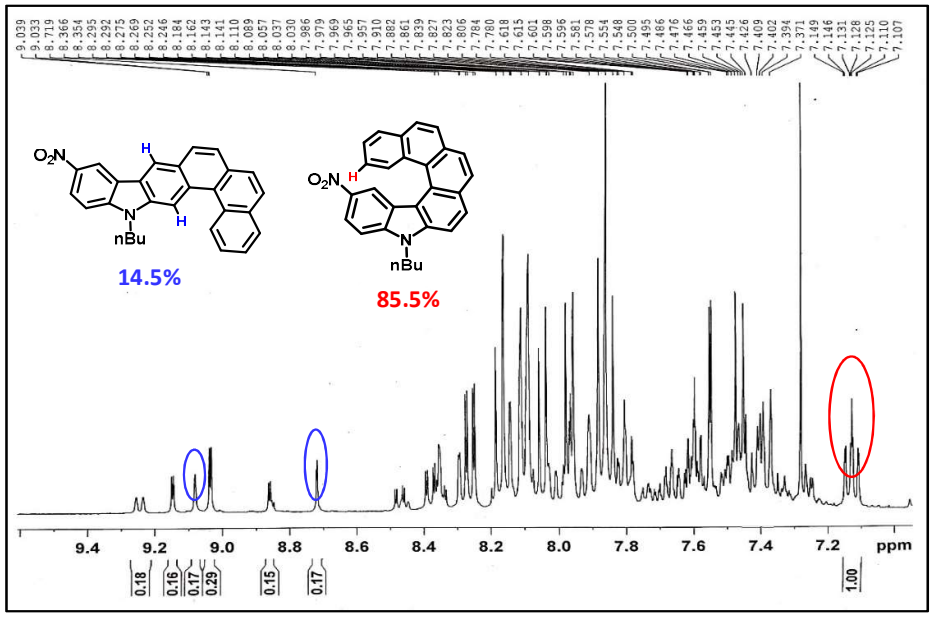

***Figure 2A.4**: Aromatic region of ^{1}H NMR of crude reaction mixture of 2-nitro aza[6]helicene*

2A.2.2 *Understanding regioselectivity of photocyclization*

In a polynuclear system with more than one site for photocyclization, the regioselectivity is governed by two major considerations: the electronic and the steric factors.[34] In cases where steric hindrance is not very severe, the product formed usually depends on the stability of the intermediate, leading to greater aromatic stabilization. If the electronically favorable pathway is sterically hindered, then the alternative pathway with less steric hindrance is preferred.[35] In some cases, despite of the favorable theoretical predictions, the actual photocyclization may result in different outcome.[36] The two available sites A and B in the carbazole based stilbene derivatives, directs the photocyclization to obtain either angular or linear regiomer (**Scheme 2A.11**). Here, the position A is electronically more favorable for electrocyclization in comparision to the position B. The two possible dihydro intermediates **IA** and **IB** upon oxidation leads to aromatized angular product **IIA** and linear product **IIB**. In case of angular mode of cyclization, the dihydro intermediate **IA** is formed where the aromatic character of the pyrrole ring present in the parent carbazole moiety remains intact, whereas it is compromised in the intermediate **IB** formed in case of linear mode. A similar observation was made by Katz and co-workers for the intermediates generated in the Diels−Alder cycloaddition of vinyl carbazole.[37] They observed that the angular intermediate is 8.6 kcal/mol more stable compared to the corresponding linear intermediate. The electronic effects direct the cyclization in an angular manner as the aromatic character of the pyrrole ring in **IA** remains intact. However, this is partially balanced by the steric effect generated by an aromatic ring of naphthalene moiety favoring the formation of intermediate **IB**, also leading to the formation of linear regiomer **IIB**.

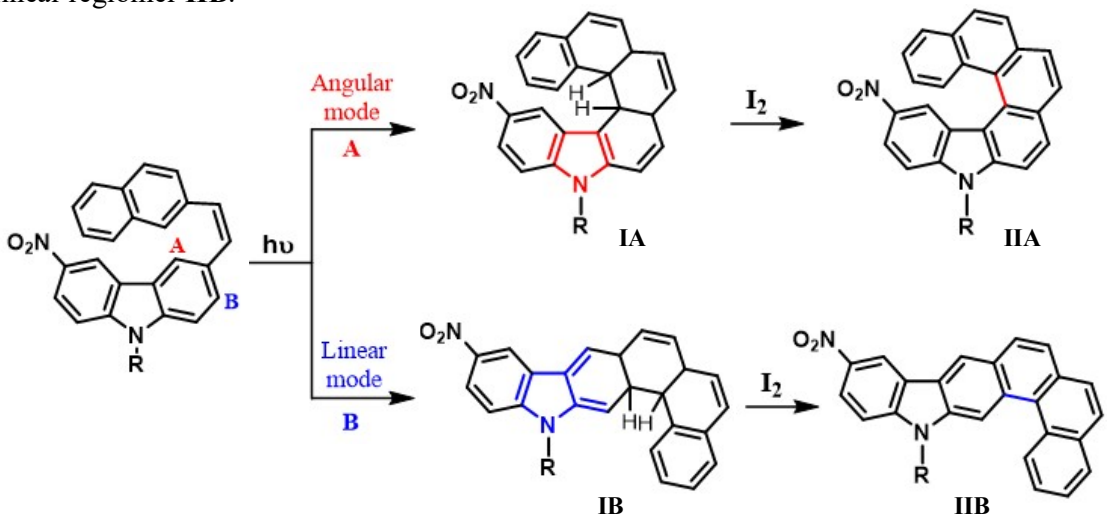

***Scheme 2A.11**: Possible modes of photocyclization*

2A.2.3 X-ray Structure Analysis of compound 47

Helicene **47** showed good solubility in majority of organic solvents. A good quality crystal of **47** was obtained by slow evaporation of its solution in acetonitrile. The single crystal X-ray diffraction study confirmed the structure of angular isomer (**Figure 2A.5**). The crystal was grown in the space group of P 2_1/n with four molecules packed in the unit cell, two each as *P* and *M* conformation indicating lack of enrichment of isomers (**Figure 2A.6**). As expected for such helical systems, the inner aromatic carbon-carbons were found to be slightly elongated compared to the flat polycyclic aromatic hydrocarbons (1.404-1.450 Å), on the other hand the outside peripheral bonds were slighted compressed (1.343-1.361 Å). The observed torsion angles were 19.51° (φ1 = C15-C15a-C15b-C15c), 32.00° (φ2 = C15a-C15b-C15c-C15d), 15.31° (φ3 = C15b-C15c-C15d-C15e), while the distortion in the molecule was found to be 66.82° (φ1 + φ2 + φ3) resulting in a dihedral angle of 51.70° (θ).

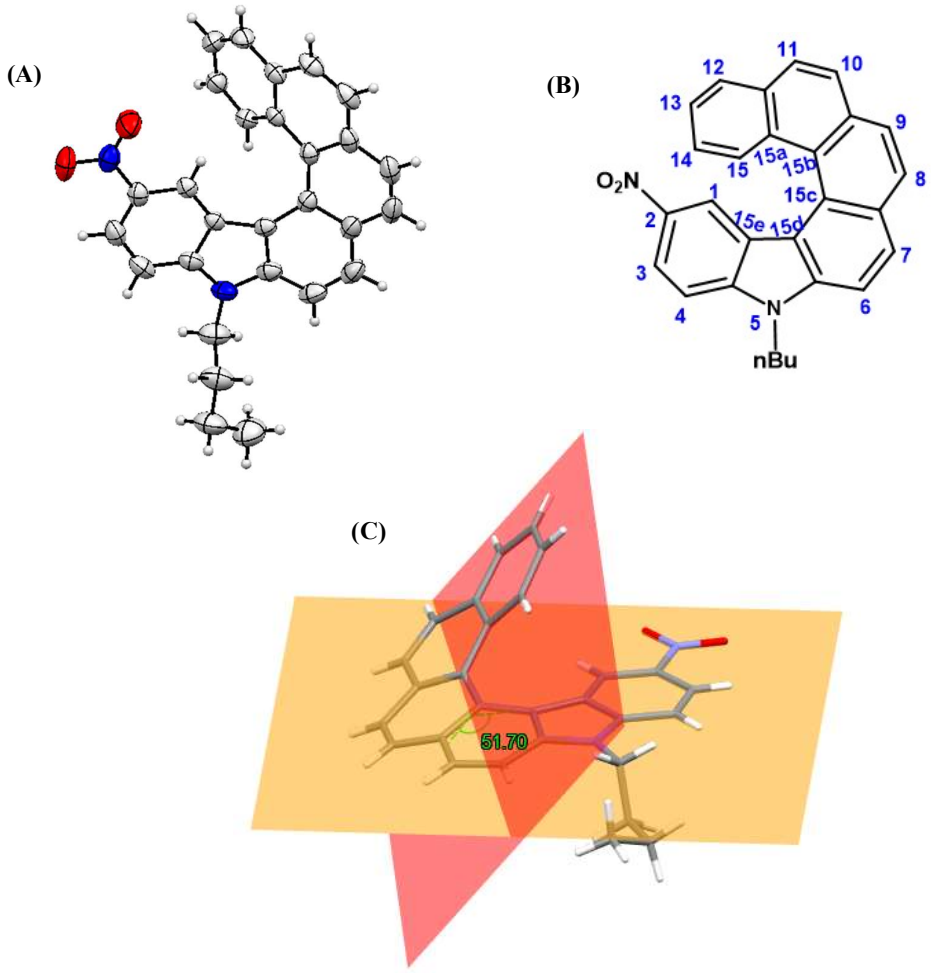

***Figure 2A.5**: (A) ORTEP plot of compound 47 CCDC 1848325 (B) Molecular structure and numbering scheme for 47 (C) figure showing interplanar angle*

Inner carbon-carbon bond length (Å)	
C15-C15a	1.404
C15a-C15b	1.450
C15b-C15c	1.443
C15c-C15d	1.429
Outer carbon-carbon bond length (Å)	
C6-C7	1.360
C8-C9	1.343
C10-C11	1.352
C12-C13	1.361
Torsion angle (º)	
φ1 = C15-C15a-C15b-C15c	19.51
φ2 = C15a-C15b-C15c-C15d	32.00
φ3 = C15b-C15c-C15d-C15e	15.31
Distortion of the molecular structure (º)	
φ1 + φ2 + φ3	66.82
Dihedral angle (º)	
θ	51.70

***Table 2A.1**: Crystallographic properties of compound 47*

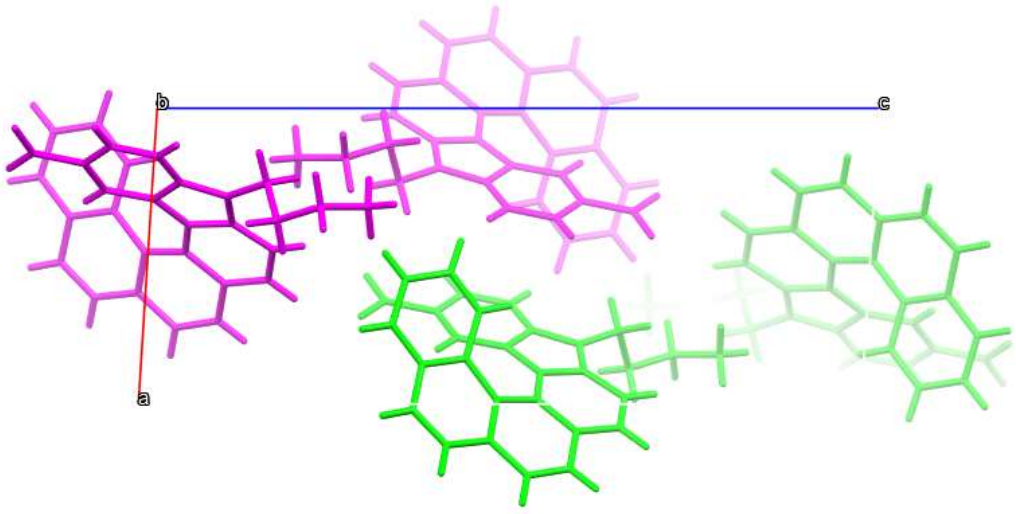

***Figure 2A.6**: Crystal packing structure of compound 47 along b axis*

2A.2.4 *Synthesis of 2-amino-5-aza[6]helicene*

The objective of the present study is to prepare optically pure isomers of amino-substituted aza[6]helicene. Two approaches of separation of diastereomeric derivatives were explored: one involving salt formation of amines with chiral acids and other one by attaching chiral auxiliary. With this aim we attempted to convert the nitro group of **47** to primary amine **49**. For this conversion several conditions were explored and summarized here (**Scheme 2A.12** and **Table 2A.2**). The known method of reduction with iron powder in glacial acetic acid[38a] resulted in moderate conversion, which marginally improved at higher temperature. Slightly better results were obtained with $NaBH_4$ reduction in presence of $NiCl_2$ as catalyst,[38b] however good conversion of **47** was observed with Sn-HCl conditions.[38c] The reduced amino helicene **49** was isolated and showed satisfactory spectral analysis. The formation of **49** was confirmed by the presence of hydrogen attached to C1 (H_1) at upfield region of 5.97 ppm as a "s", compared to that in **47** which appeared at downfield region of 7.58 ppm. This shielding effect was observed in **49** because of the presence of electron releasing amino group *ortho* to C1.

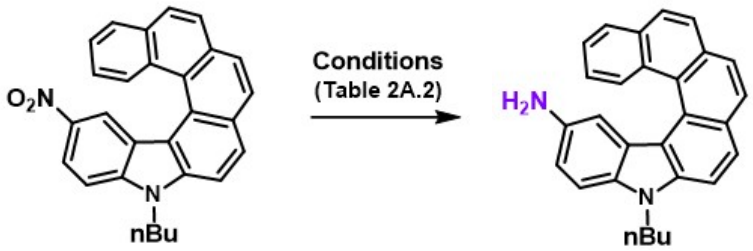

47 **49**

Scheme 2A.12: Reduction of 2-nitroaza[6]helicene

No.	Reagent	Solvent	Temperature	Isolated yield of 49 (%)
1	Fe	AcOH	r.t.	53
2	Fe	AcOH	100 °C	48
3	$NaBH_4$-$NiCl_2$	MeOH, THF	r.t.	61
4	Sn, HCl	MeOH, THF	r.t.	86

Table 2A.2: Conditions for the reduction of 47

2A.2.5 Resolution of 2-amino-5-aza[6]helicene

2A.2.5.1 Resolution by diastereomeric salt formation with chiral acids

As the amino helicene **49** was relatively less stable for further experiments of separation of isomers with chiral acids, it was converted to its dimethylamino derivative **50** using paraformaldehyde and sodium cyanoborohydride (**Scheme 2A.13**).[39] The 2-*N*,*N*-dimethylamino-5-aza[6]helicene **50** was characterized by usual spectral analysis and single crystal X-ray analysis. The ^{1}H NMR at ambient conditions ($CDCl_3$, 22 °C) showed only one singlet of two methyl groups of -NMe_2, indicating fast rotation of the aromatic C-N bond. The hydrogen at C3 (H_3) appeared as "dd" at 7.06 ppm, which has upfield shift compared to **47**.

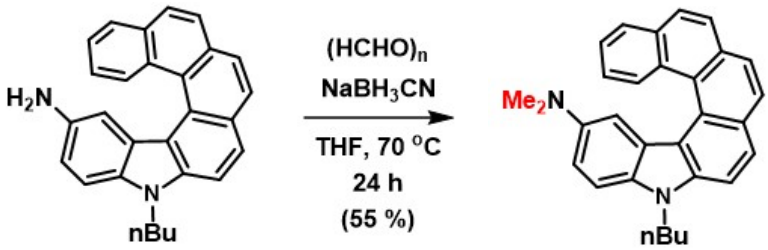

49 **50**

***Scheme 2A.13**: Preparation of dimethylamine derivative 50*

The amino helicene **49** also did not possess crystalline nature, which was achieved by converting it to the dimethylamino derivative **50**. Helicene **50** exhibited good crystalline nature and a single crystal was obtained from its solution in a mixture of chloroform and petroleum ether (60:40). The single crystal study revealed the structural aspects, consistent with the proposed structure. The X-ray analysis showed the space group of P 2_1/c where four molecules were packed in the unit cell, containing two isomers of each *P* and *M* conformation. The detailed revealed that the inner aromatic carbon-carbon bonds were found to be slightly elongated as compared to the flat polycyclic aromatic hydrocarbons (1.409-1.430 Å), whereas the outer peripheral bonds were slighted compressed (1.352-1.358 Å), which is a characteristic observation for these compounds. The torsion angles were observed to be 16.16° (φ1 = C15-C15a-C15b-C15c), 30.09° (φ2 = C15a-C15b-C15c-C15d), 18.69° (φ3 = C15b-C15c-C15d-C15e), leading to 64.94° (φ1 + φ2 + φ3) of overall distortion in the molecule and the dihedral angle (θ) was calculated to be of 52.49° (**Figure 2A.7** and **Table 2A.3**).

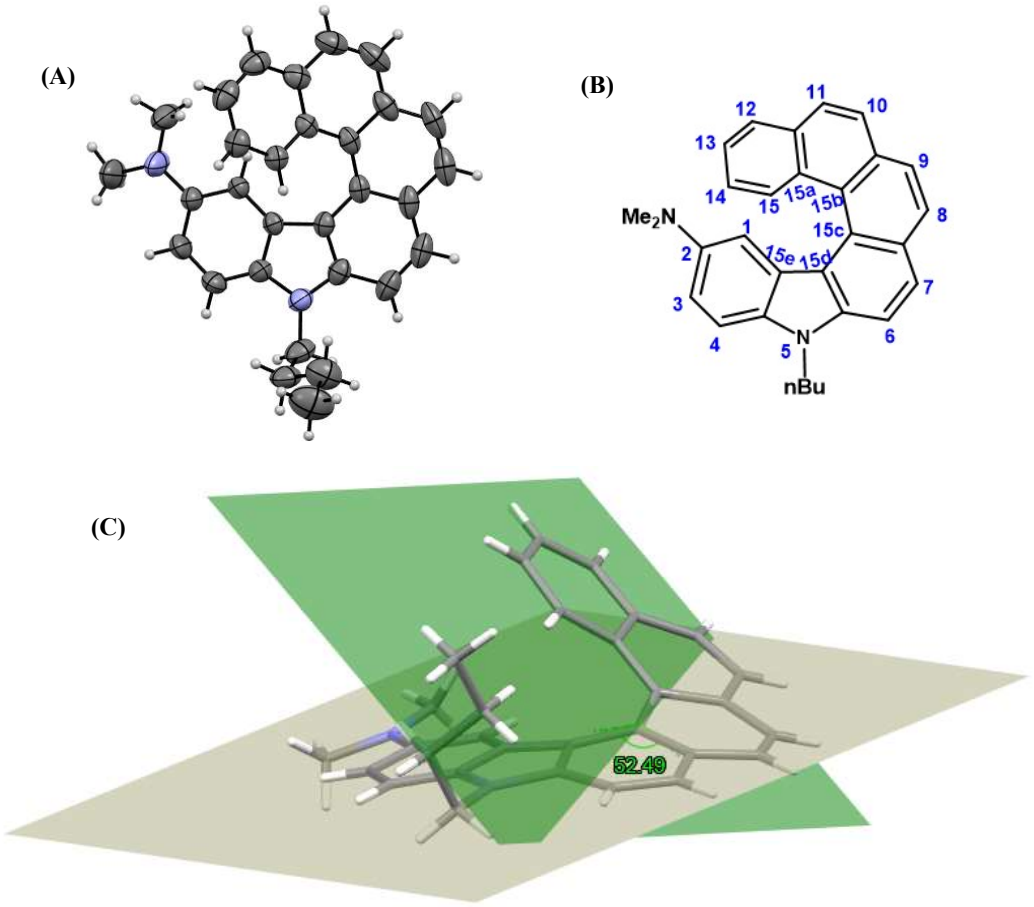

Figure 2A.7: (A) ORTEP plot of 50 CCDC 1921710 (B) Molecular structure and numbering scheme for 50 (C) figure showing interplanar angle

Torsion angle (º)	Distortion of the molecular structure (º)	Dihedral angle (º)
φ1 = C15-C15a-C15b-C15c = 16.16 φ2 = C15a-C15b-C15c-C15d = 30.09 φ3 = C15b-C15c-C15d-C15e = 18.69	φ1 + φ2 + φ3 = 64.94	θ = 52.49

Table 2A.3: Crystallographic properties of compound 50

The sample of dimethylamine **50** was subjected for co-crystallization with (*R*)-(-)-mandelic acid, (1*R*)-(-)-camphorsulfonic acid etc. in different solvents. However, either amorphous solid fell out or oily material was obtained. Analysis of this material revealed lack of enrichment of isomer of **50**.

2A.2.5.2 *Resolution by attaching chiral auxiliary*

The chiral compounds with primary amino group can be resolved by converting them into diastereomeric carbamates.[40] This method was adopted to separate the isomers of **49**, by converting it to diastereomeric menthyl carbamate **51** by attaching the amino group with a chiral auxiliary, (1*R*)-(-)-menthylchloroformate (**Scheme 2A.14**).

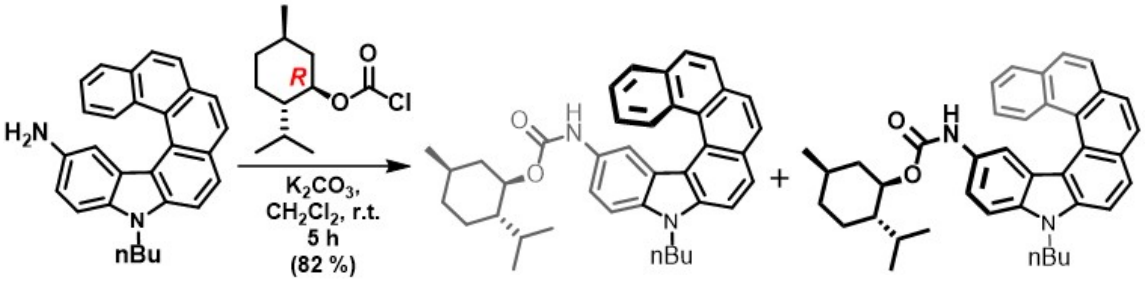

49

(*P*)-**51**

99.3 % d.e.

[α]D + 1183

(*M*)-**51**

100 % d.e.

[α]D - 1648

***Scheme 2A.14**: Conversion of 49 to diastereomeric carbamates (P)-(+)-51 and (M)-(-)-51*

The mixture of isomers of **51** was obtained in 82% yield and was analyzed by ^{1}H NMR. It was observed that both the diastereomers were present in almost equal proportion (based on the values of integration of the marked protons) (**Figure 2A.8**).

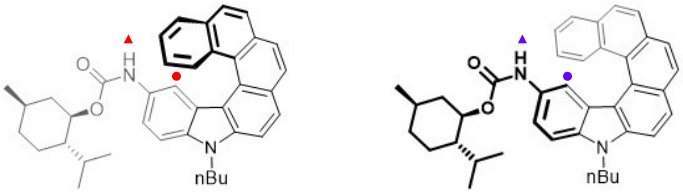

(*P*)-**51** (*M*)-**51**

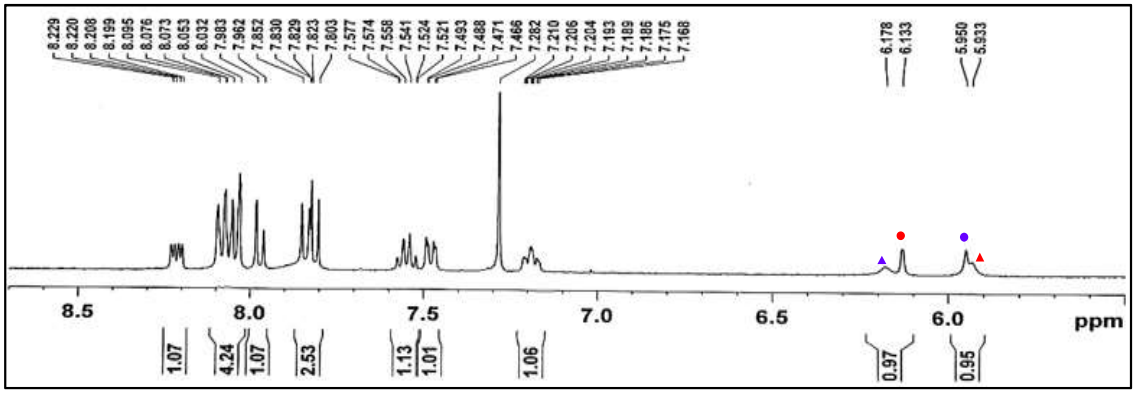

***Figure 2A.8**: ^{1}H NMR spectrum of mixture of diastereomers 51 (enlarged aromatic region)*

Further, a careful column chromatography over alumina resulted in the elution of faster moving isomer, which showed positive optical rotation, indicating it to be the *P* isomer. We were able to separate both isomers in pure form, confirmed by HPLC analysis on chiral stationary phase (Chiralcel OD-H) (**Figure 2A.9**).

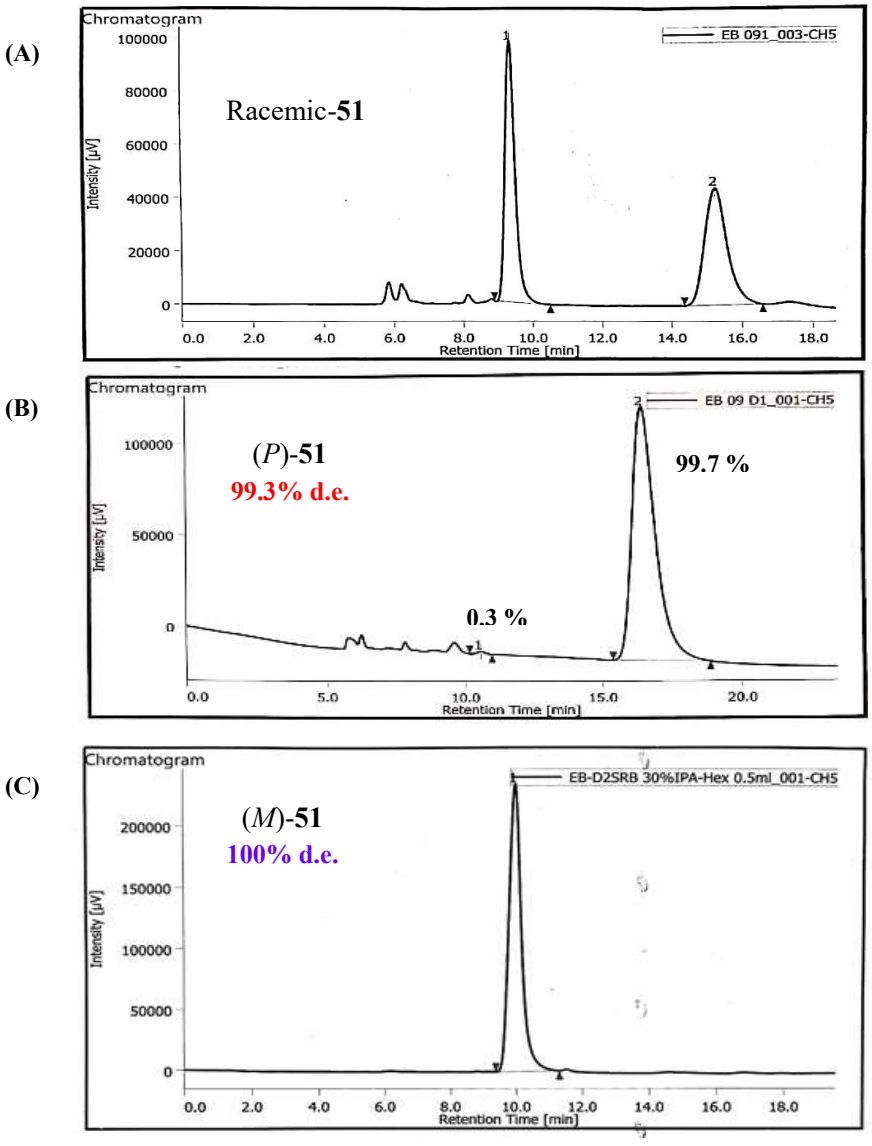

***Figure 2A.9**: HPLC chromatograms of (A) mixture of diastereomers; (B) (P)-51; (C) (M)-51*
HPLC Conditions: Chiral Column: Chiralcel OD-H Column,
Solvent System: Hexane: IPA(70:30), Flow rate: 0.5 mL/min

One of the important features of the optically pure helical isomers is their considerably high values of specific optical rotations. The specific and molar rotations of the pure (*P*)-**51** (99.3% d.e.): $[\alpha]_D$ = + 1183, $[\phi]_D$ = + 6743; (*M*)-**51** (100% d.e.): $[\alpha]_D$ = - 1648, $[\phi]_D$ = - 9393, measured as solution in chloroform (c = 1.7 X 10^{-2} M). The rotation values are opposite, but

not exactly similar. This could be due to the small contribution to SOR from (*R*)-menthyl moiety.

Both the isomers of **51** were characterized by ^{1}H and ^{13}C NMR. The ^{1}H NMR spectra showed specific signals for helical unit and menthyl group. As diastereomers have different physical and chemical properties, they exhibit some differences in their NMR spectra also. A noticeable difference was observed for the proton attached to C1 of the helical unit and NH of carbamate moiety, whereas only a marginal difference in their chemical shifts was observed for other protons.

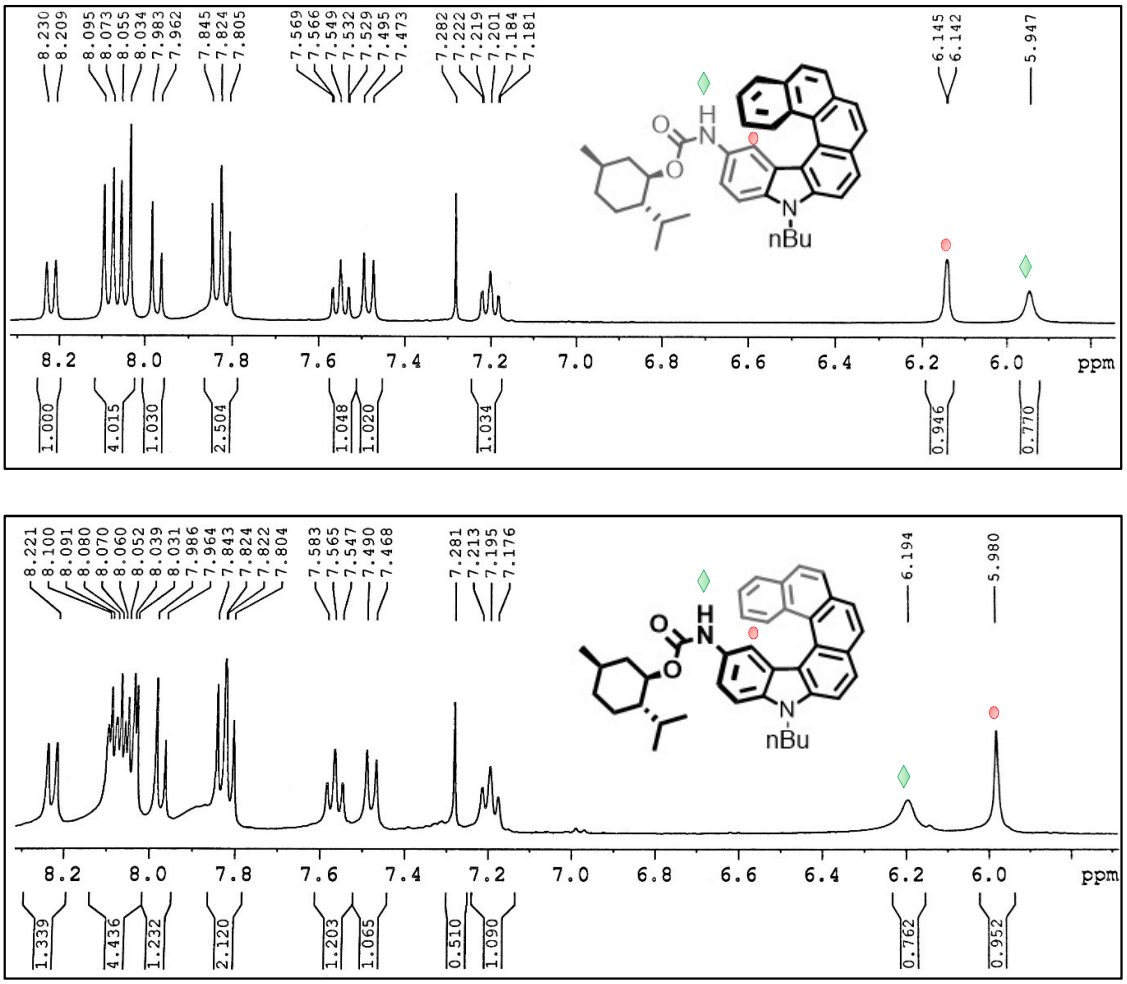

***Figure 2A.10**: Comparision of ^{1}H NMR Spectra of (P)-51 (top) and (M)-51 (bottom) after purification (enlarged aromatic region)*

We further studied the circular dichroism (CD) of the separated diastereomers (**Figure 2A.11**). They displayed opposite cotton effect in the spectra. Since the menthyl group showed no significant response in this UV-Vis range, this mirror image relationship was mainly due to

the helical framework of the two isomers.[41] The presence of positive bisignate couplets at around 281 and 325 nm and a negative at 247 nm, confirms the (*P*)-isomer.

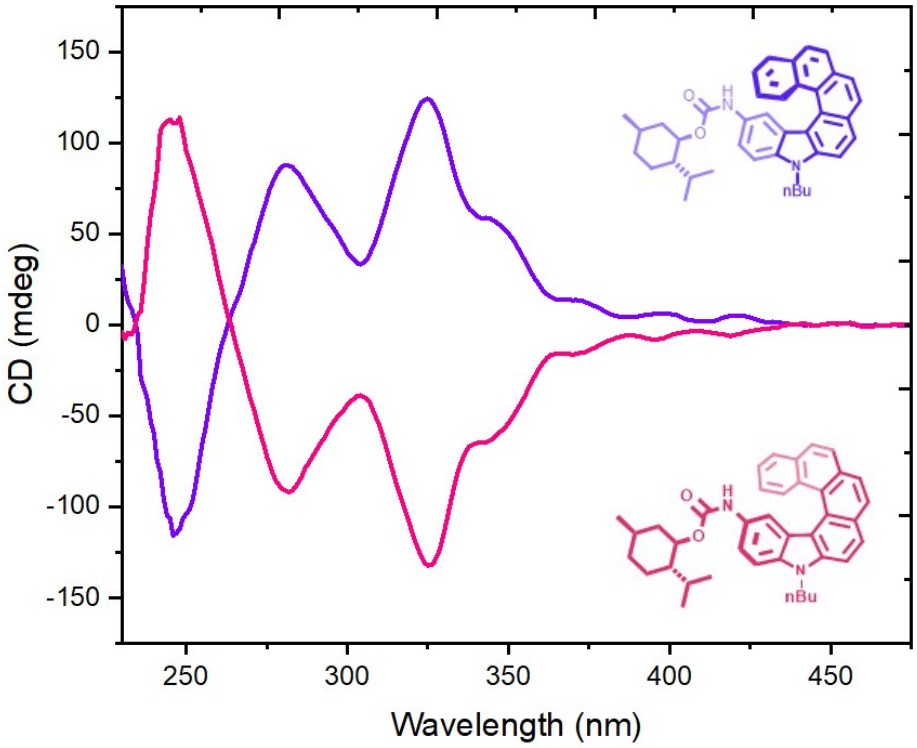

***Figure 2A.11**: CD Spectra of diastereomers (P)-51(pink) and (M)-51(blue) (1.0 x 10^{-5} M in $CHCl_3$)*

2A.2.5.3 Deprotection of carbamate

For accessing optically pure helical amines the deprotection of carbamate was investigated. The pure sample of (*P*)-**51** was subjected to the standard deprotection condition of TBAF in dry THF.[42] The reaction was sluggish at ambient conditions, but proceeded smoothly at elevated temperature (**Scheme 2A.15**). The amine sample was obtained by a quick chromatography over neutral alumina. We observed that the amine was slightly unstable and we could not check its optical purity by HPLC analysis. It was then converted to more stable *N*-Boc derivative (*P*)-**52**, by reaction with $(Boc)_2O$ at room temperature. The HPLC analysis on chiral stationary phase (Chiralcel OD-H) revealed only moderate purity (56% ee; $[\alpha]_D$ +747, c = 0.15 in $CHCl_3$) of (*P*)-**52** (**Figure 2A.12**). We believe the conformational isomerization of the helical framework may have happened at higher temperature during the deprotection of the carbamate. This was confirmed when the deprotection was conducted at lower temperature, the amine **49** was obtained in lesser yield; it was converted to *N*-Boc derivative and analyzed. Its optical purity was established to be 87% ee ($[\alpha]_D$ +1120, c = 0.15 in $CHCl_3$).

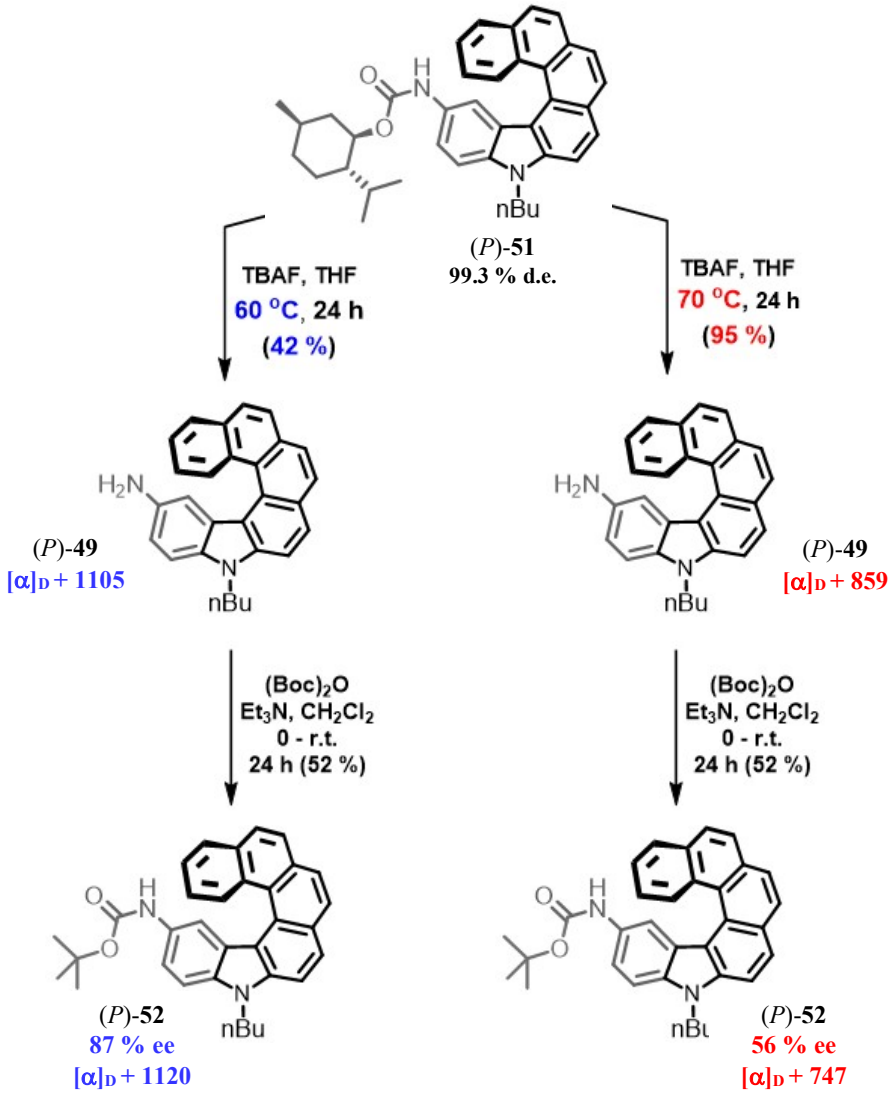

***Scheme 2A.15**: Attempted conversion of (P)-51 to optically pure amine (P)-49 and its boc-derivative (P)-52.*

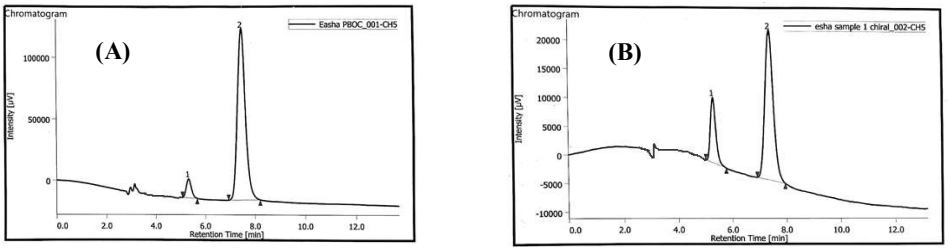

***Figure 2A.12**: HPLC chromatogram of (P)-52 with (A) 87 % ee and (B) 56 % ee*

HPLC Conditions: Chiral Column: Chiralcel OD-H

Solvent System: Hexane: IPA(70:30) Flow rate: 1.0 mL/min

It is believed that the isomerization of helical structure is not taking place during the introduction of Boc group, but must be during the deprotection of carbamate. Our efforts to attempt deprotection of carbamate with TBAF at lesser temperature (50-55 °C) resulted in negligible conversion. We also investigated other known methods of deprotection of carbamate, trifluoroacetic acid in dichloromethane,[43a] diethylenetriamine,[43b] and aqueous phosphoric acid (85 wt%),[43c] but did not result in the cleavage.

2A.3 Conclusion

In this chapter we present the synthesis of amino derivatives of aza[6]helicene where the basic helical skeleton was built by photochemical cyclodehydrogenation as the key step. The 2-amino-5-aza[6]helicene was converted to diastereomeric carbamate by reaction with (*R*)-(-)-menthyl chloroformate, which could be physically separated by column chromatography. The optically pure amines were regenerated and their chiroptical properties were measured. The diastereomeric derivatives were analyzed by CD spectroscopy, while the 2-nitro-5-aza[6]helicene and 2-*N*,*N*,-dimethylamino-5-aza[6]helicene were characterized by single crystal X-ray diffraction analysis.

2A.4 Experimental Data

All reactions were carried out in oven-dried glassware with magnetic stirring. Reagents purchased from commercial sources were used without further purification. All the solvents used were stored on oven-dried molecular sieves (4 Å). All reactions were carried out under inert atmosphere (nitrogen) unless other conditions are specified. Thin Layer Chromatography was performed on Merck 60 F254 Aluminium coated plates. The spots were visualized under UV light or with iodine vapor. Purification of all the compounds were done by column chromatography using SRL silica gel (60-120 mesh). ^{1}H NMR spectra were recorded on a 400 MHz Bruker Advance 400 spectrometer (100 MHz for ^{13}C) with $CDCl_3$ as solvent and TMS as an internal standard. IR spectra were recorded on a Perkin-Elmer FTIR RXI spectrometer as KBr pallets. High-resolution mass spectra (HRMS) were measured using electronspray ionization (ESI) method. HPLC was performed using CHIRALCEL OD-H column. Specific optical rotations were measured on JASCO P-2000 polarimeter. Melting points were measured in Thiele's tube using paraffin oil and are uncorrected.

Synthetic procedures and analytical data

9-Butyl-9*H*-carbazole (42)

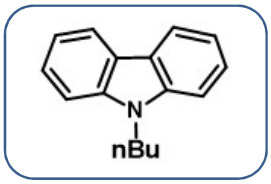

Molecular formula: $C_{16}H_{17}N$
Molecular weight: 223.31
Physical state: white crystalline solid
M.p = 58 °C

In a dry round bottom flask, carbazole (5 g, 29.9 mmol) was dissolved in acetone (25 mL). To this homogenous solution, KOH (6.7 g, 119.4 mmol) was added and the solution was allowed to stir at room temperature for 30 minutes. To this solution, 1-bromobutane (5.32 g, 4.2 mL, 38.9 mmol) was added. The mixture was allowed to stir for 4-5 hours at room temperature. After the completion of reaction (which is monitored by TLC), the reaction mixture was poured on ice cold water (50 mL) and extracted using ethyl acetate (3 x 50 mL). Combined organic layer was washed with water (50 mL) and dried over anhydrous sodium sulfate and concentrated at reduced pressure. Compound was purified by performing column chromatography over silica gel using petroleum ether as eluent. White solid of N-butyl carbazole **42** was obtained. The analytical data were in complete agreement with the previously published data.[30] **Yield:** 6.27g (94%)

^{1}H NMR (400 MHz, $CDCl_3$): δ 8.15 (d, *J* = 8.0 Hz, 2H), 8.52-7.48 (m, 2H), 7.45 (d, *J* = 8.0 Hz, 2H), 7.29-7.25 (m, 2H), 4.36-4.32 (t, *J* = 7.2 Hz, 2H), 1.93-1.86 (m, 2H), 1.0- 0.96 (t, *J* = 7.2 Hz, 3H)

3-Formyl *N*-butyl carbazole (43)

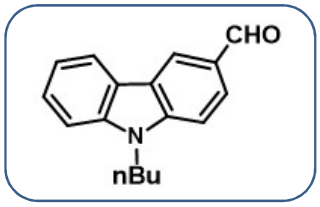

Molecular formula: $C_{17}H_{17}NO$
Molecular weight: 251.32
Physical state: viscous liquid
M.p = 60 °C

In a dry two neck round bottom flask phosphoryl chloride (13.76 g, 8.36 mL, 89.0 mmol) was added slowly in DMF (16.36 g, 17.22 mL, 224 mmol) which was purged with nitrogen and cooled to 0 °C. The reactant was warmed to room temperature and stirred for 1 hour and cooled again to 0 °C. To this mixture was added N-butyl carbazole (10.0 g, 44.8 mmol) in 1, 2-dichloroethane (50 mL). In 1 hour, the reaction temperature was raised to 90 °C and then kept for 8 hours. The cooled solution was poured into ice water and extracted with dichloromethane (3X100 mL). The organic layer was washed with water, dried over anhydrous sodium sulfate and concentrated at reduced pressure. The purification of compound was performed by column chromatography over silica gel using 10 % ethyl acetate pet ether as eluent to obtain **43** as viscous liquid which solidifies as brown solid on standing at low temperature. The analytical data were in complete agreement with the previously published data.[44] **Yield:** 10.24 g (91%)

^{1}H NMR (400 MHz, $CDCl_3$): δ 10.11 (s, 1H), 8.62 (d, *J* = 1.2 Hz, 1H), 8.14 (d, *J* = 8.8 Hz, 1H), 8.03-8.01 (m, 1H), 7.57-7.55 (m, 1H), 7.53-7.47 (m, 1H), 7.46-7.32 (m, 2H), 4.35 (t, *J* = 7.2 Hz, 2H), 1.91-1.87 (m, 2H), 0.98 (t, *J* = 7.2 Hz, 3H).

3-Formyl-6-nitro *N*-butyl carbazole (44)

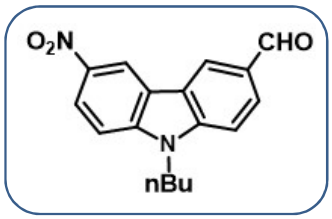

Molecular formula: $C_{17}H_{16}N_2O_3$
Molecular weight: 296.32
Physical state: yellow solid
M.p = 98 °C

A solution of 3-formyl-9-butylcarbazole (**43**, 3.0 g, 11.95 mmol) in glacial acetic acid (20 mL) was cooled to 0 °C. To this solution, a 2 mL nitrating mixture (3:1 conc HNO_3: conc H_2SO_4)

was added and stirred at room temperature for 5 hours. After 5 h, the cooled reaction mixture was poured into ice water, neutralized with sodium bicarbonate solution and extracted with dichloromethane (3X100 mL). The organic layer was washed with water, dried over anhydrous sodium sulfate and concentrated at reduced pressure. The purification of compound was performed by column chromatography over silica gel using 20 % ethyl acetate pet ether as eluent to obtain **44** as yellow solid. The analytical data were in complete agreement with the previously published data.[45] **Yield:** 2.83 g (80%)

^{1}H NMR (400 MHz, $CDCl_3$): δ 10.15 (s, 1H), 9.08 (s, 1H), 8.68 (s, 1H), 8.45 (d, *J* = 8.8 Hz,1H), 8.13 (d, *J* = 7.7 Hz, 1H), 7.58 ((d, *J* = 7.9 Hz, 1H), 7.50 (d, *J* = 8.8 Hz, 1H), 4.12 (t, *J* = 7.2 Hz, 2H), 1.91-1.87 (m, 2H), 0.98 (t, *J* = 7.2 Hz, 3H).

2-(Bromomethyl) naphthalene

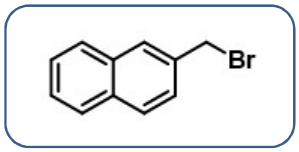

Molecular formula: $C_{11}H_9Br$
Molecular weight: 221.09
Physical state: brown solid
M.p = 50-52 °C

In round bottom flask equipped with a magnetic stirrer and reflux condenser 2-methyl naphthalene was (2.0 g, 14.0 mmol) dissolved in carbon tetrachloride (25 mL). To this solution, the mixture of N-bromo succinimide (2.62g, 14.7 mmol) and benzoyl peroxide (0.169g, 0.7 mmol) was added. The mixture was stirred in presence of tungsten filament domestic light for 5-6 hrs. After the completion of reaction (TLC), succinimide was filtered and the solvent was removed under the reduced pressure. Solid material after distillation was recrystallised from petroleum ether as brown solid. The analytical data were in complete agreement with the previously published data.[46] **Yield:** 2.44 g (83%)

^{1}H-NMR (400 MHz, $CDCl_3$): δ 7.81-7.78 (m, 4H), 7.49-7.46 (m, 3H), 4.64 (s, 2H).

Bromo(naphthalen-2-ylmethyl)triphenylphosphorane (45)

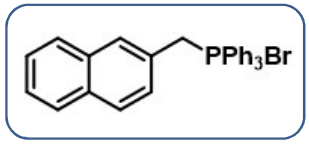

Molecular formula: $C_{29}H_{24}BrP$
Molecular weight: 483.38
Physical state: white solid
M.p = 253.8 °C

Add triphenylphosphine (2.61 g, 9.95 mmol) to the solution of 2-bromine methyl naphthalene

(2.0 g, 9.05 mmol) in 20 mL of xylene. Heat the reaction mixture at 85 °C for 7 hours. The white solid is formed, indicate the formation of Wittig's salt. Allow the reaction mixture to cool. Filter the reaction mixture. Wash the solid residue with xylene or petroleum ether (15 mL × 3). Dry the product under vacuum. The analytical data were in complete agreement with the previously published data.[47] **Yield:** 4.24 g (97%)

^{1}H (400 MHz, $CDCl_3$): δ 7.78–7.67 (m, 10H), 7.62–7.51 (m, 9H), 7.44–7.35 (m, 2H), 7.16 (d, *J* = 8.4 Hz, 1H), 5.58 (s, 1H), 5.53 (s, 1H).

9-butyl-3-(2-(naphthalen-2-yl)vinyl)-6-nitro-9*H*-carbazole (46)

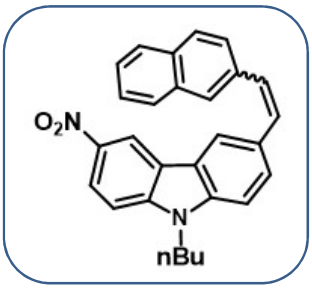

Molecular formula: $C_{28}H_{24}N_2O_2$
Molecular weight: 420.51
Physical state: yellow solid
M.p = 208-209 °C

In a 100 mL Flask equipped with a reflux condenser were placed 9-butyl-6-nitro-9*H*-carbazole-3-carbaldehyde (0.5 g, 1.68 mmol), (2-naphthalenylmethyl)triphenylphosphonium bromide **45** (0.979 g, 2.02 mmol), dry potassium carbonate (0.70 g, 5.06 mmol), and *N,N*-dimethylacetamide (20 mL). This mixture was heated under reflux for 48 h. After cooling, the mixture was poured to water and extracted with ethyl acetate (3×100 mL). The combined organic phase was washed with water and brine and dried over anhydrous sodium sulfate. The solvent was removed under reduced pressure, and the crude product was purified by column chromatography on silica gel using ethyl acetate/petroleum ether (10:90 – 30:70) as eluent to afford a Z/E mixture of 9-butyl-3-(2-(naphthalen-2-yl)vinyl)-6-nitro-9H-carbazole as yellow solid. **Yield:** 0.595 g (70%).

(E)-isomer,

^{1}H NMR (400 MHz, $CDCl_3$): δ 9.08 (d, *J* = 2.4 Hz, 1H), 8.41 (dd, *J* = 8.8, 2.4 Hz, 1H), 8.35 (d, *J* = 1.6 Hz, 1H), 7.93-7.81(m, 6H), 7.51-7.42 (m, 5H), 7.37 (d, *J* = 16.4 Hz, 1H), 4.38 (t, *J* = 7.2 Hz, 2H), 1.95-1.88 (m, 2H), 1.47-1.39 (m, 2H), 1.00 (t, *J* = 7.4 Hz, 3H).

^{13}C NMR (100 MHz, $CDCl_3$): δ 143.8, 141.2, 140.6, 135.0, 133.8, 132.9, 130.5, 128.9, 128.3, 128.0, 127.7, 127.5, 126.4, 126.3, 126.1, 125.8, 123.4, 123.2, 122.5, 121.7, 119.0, 117.4, 109.9, 108.4, 43.5, 31.1, 20.5, 13.9.

IR (KBr): 3055, 2958, 2859, 1625, 1597, 1510, 1482, 1327, 1279, 1207, 1091, 967, 822, 746, 475 cm^{-1}.

HRMS (ESI+): *m/z* calcd for $C_{28}H_{25}N_2O_2$ $[M + H]^+$ 421.1910, found 421.1909.

Photocyclization of 46. In an immersion wall photoreactor equipped with a water cooling jacket and a stir bar, a *Z*/*E* mixture of 9-butyl-3-(2-(naphthalen-2-yl)vinyl)-6-nitro-9*H*-carbazole **46** (0.250 g, 0.59 mmol), iodine (0.166 g, 0.65 mmol), and THF (2.146 g, 2.41 mL, 29.76 mmol) was dissolved in toluene (600 mL). Nitrogen gas was bubbled through the solution within 10 min under sonication for removal of the dissolved oxygen prior to irradiation using a 125 W high-pressure mercury vapour (HPMV) lamp (11 h monitored by TLC). After completion of the reaction, the excess of iodine was removed by washing with aqueous $Na_2S_2O_3$ followed by distilled water. The organic layer was concentrated under the reduced pressure to obtain the crude product. The crude product purified by column chromatography over silica gel using ethyl acetate/petroleum ether (10:90) as eluent to obtain a yellow solid.

Overall yield = 0.0998 g (40%, mixture of two regioisomers **47** and **48**). Ratio of angular and linear isomer, 11:12 = 85.47:14.5, calculated by integration from signals at 7.12 and 8.71 in the ^{1}H NMR spectrum of the crude product.

Separation and purification of regioisomers 11 and 12: Separation of the regioisomers was done by enrichment of the compound using column chromatography followed by crystallization. The reaction mixture was subjected to column chromatography where the initial fractions were collected and crystallized using ethyl acetate and pet ether to obtain orangish yellow crystals yielding linear isomer **48**. The fractions obtained later were concentrated and crystallized in ethyl acetate and pet ether to obtain yellow needle like crystals of the desired angular isomer **47**. The isolated yields were less than that determined from ^{1}H NMR as some mixture remains in the mother liquor of respective regiomers.

Angular isomer, 7-butyl-10-nitro-7*H*-phenanthro[3,4-*c*]carbazole (47)

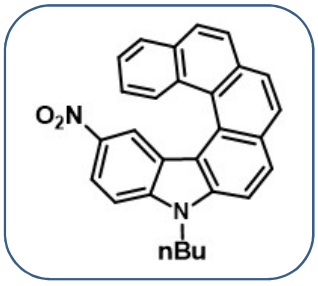

Molecular formula: $C_{28}H_{22}N_2O_2$
Molecular weight: 418.49
Physical state: yellow solid
M.p = 273-274 °C
Yield = 0.077 g, 31%

^{1}H NMR (400 MHz, $CDCl_3$): δ 8.28 (dd, *J* = 8.8, 2.0 Hz, 1H), 8.19 (d, *J* = 8.8 Hz, 1H), 8.16

(d, *J* = 8.0 Hz, 1H), 8.11 (dd, *J* = 8.4, 2.8 Hz, 2H), 8.06 (d, *J* = 8.0 Hz, 1H), 7.98 (d, *J* = 8.8 Hz, 1H), 7.89 (d, *J* = 8.4 Hz, 1H), 7.88 (d, *J* = 8.8 Hz, 1H), 7.62-7.58 (m, 2H, including a d at δ 7.58, *J* = 2.0 Hz), 7.50 (d, *J* = 8.8 Hz, 1H), 7.15-7.11 (m, 1H), 4.56 (t, *J* = 7.2 Hz, 2H), 2.06-1.98 (m, 2H), 1.56-1.52 (m, 2H), 1.06 (t, *J* = 7.2 Hz, 3H).

^{13}C NMR (100 MHz, $CDCl_3$): δ 142.3, 141.2, 139.1, 132.7, 132.0, 129.8, 129.1, 128.7, 128.5, 128.3, 128.2, 127.8, 126.4, 126.1, 125.5, 125.4, 124.7, 124.6, 122.6, 122.2, 119.8, 118.3, 110.4, 107.9, 43.6, 31.4, 20.6, 13.9.

IR (KBr): 3047, 2956, 2867, 1616, 1580, 1506, 1477, 1452, 1318, 1286, 1145, 1072, 835, 782, 746, 625, 541 cm^{-1}.

HRMS (ESI+): *m/z* calcd for C28H23N2O2 $[M + H]^+$ 419.1754, found 419.1752.

Linear isomer, 14-butyl-11-nitro-14*H*-phenanthro[4,3-*b*]carbazole (48)

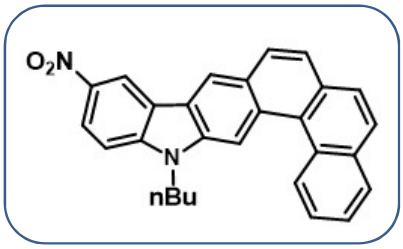

Molecular formula: $C_{28}H_{22}N_2O_2$
Molecular weight: 418.49
Physical state: yellow solid
M.p = 276 °C
Yield = 0.0084 g, 3%

^{1}H NMR (400 MHz, $CDCl_3$): δ 9.28 (d, *J* = 8.4 Hz, 1H), 9.21 (d, *J* = 2.4 Hz, 1H), 9.16 (s, 1H), 8.8 (s, 1H), 8.51 (dd, *J* = 8.8, 2.4 Hz, 1H), 8.12 (t, *J* = 8.4 Hz, 2H), 7.99 (d, *J* = 8.8 Hz, 1H), 7.91 (d, *J* = 8.4 Hz, 1H), 7.82 (d, *J* = 8.8 Hz, 1H), 7.76-7.67 (m, 2H), 7.48 (d, *J* = 9.2 Hz, 1H), 4.52 (t, *J* = 7.2 Hz, 2H), 2.08-2.01 (m, 2H), 1.60-1.53 (m, 2H), 1.06 (t, *J* = 7.2 Hz, 3H).

^{13}C NMR (100 MHz, $CDCl_3$): δ 145.9, 141.2, 140.5, 133.5, 130.5, 129.9, 128.9, 128.6, 128.2, 127.7, 127.0, 126.98, 126.91, 126.2, 125.7, 124.9, 123.0, 122.9, 122.5, 120.3, 117.8, 107.9, 106.8, 43.6, 30.9, 20.6, 13.9.

IR (KBr): 3426, 2924, 2854, 1680, 1636, 1602, 1508, 1485, 1461, 1331, 1249, 1205, 1136, 1091, 880, 832, 814, 743 cm^{-1}.

HRMS (ESI+): *m/z* calcd for $C_{28}H_{22}N_2O_2K$ $[M + K]^+$ 457.1313, found 457.1316.

7-butyl-7*H*-phenanthro[3,4-*c*]carbazol-10-amine (49)

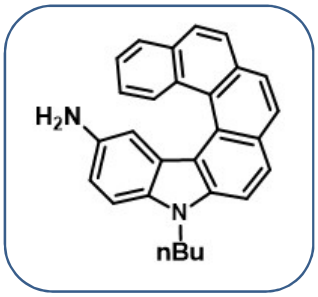

Molecular formula: $C_{28}H_{24}N_2$
Molecular weight: 388.51
Physical state: yellow solid
M.p = 194-196 °C

To a suspension of 7-butyl-10-nitro-7H-phenanthro[3,4-*c*]carbazole **47** (0.075 g, 0.17 mmol) in methanol (6 ml) and tetrahydrofuran (2 mL) was added hydrochloric acid (1.5 mL). Then tin powder (0.106 g, 0.89 mmol) was added in several times at room temperature. The mixture was stirred at room temperature for 10 h. Then the reaction mixture was poured into ice-water, and aqueous solution of NaOH (2M) was added until the pH reaches 10. The mixture was extracted with ethyl acetate (3×50 mL). The combined organic layer was dried over anhydrous Na_2SO_4, filtered and concentrated under reduced pressure. The crude reaction mass was filtered over alumina gel column chromatography using ethyl acetate/ petroleum ether (15:85) as eluent to obtain brownish orange mass which was used instantly for the next step. **Yield:** 0.060 g (86%).

^{1}H NMR (400 MHz, $CDCl_3$): δ 8.23 (d, *J* = 8.4 Hz, 1H), 8.06-8.02 (m, 2H), 7.99-7.93 (m, 3H), 7.80 (t, *J* = 7.6 Hz, 2H), 7.53 (t, *J* = 7.6 Hz, 1H), 7.36 (d, *J* = 8.8 Hz, 1H), 7.23 (t, *J* = 7.2 Hz, 1H), 6.95 (d, *J* = 8.8 Hz, 1H), 5.97 (s, 1H), 4.47 (t, *J* = 7.2 Hz, 2H), 2.00-1.93 (m, 2H), 1.57-1.47 (m, 2H), 1.03 (t, *J* = 7.2 Hz, 3H).
IR (KBr): 3019, 2959, 2929, 1732, 1683, 1581, 1525, 1483, 1214, 1155, 909, 835, 782, 742, 668, 626 cm^{-1}.
MS (DIP-EI): *m/z* 388 (M+, 7%), 234 (11%), 184 (25%), 147 (34%), 129 (78%), 84 (38%), 83 (63%), 73 (72%), 71 (100%).

7-butyl-*N*,*N*-dimethyl-7*H*-phenanthro[3,4-*c*]carbazol-10-amine (50)

Molecular formula: $C_{30}H_{28}N_2$
Molecular weight: 416.56
Physical state: orangish yellow solid
M.p = 221-223 °C

To a solution of 7-butyl-7H-phenanthro[3,4-*c*]carbazol-10-amine **49** (0.062 g, 0.16 mmol) in

tetrahydrofuran (THF) was added paraformaldehyde (0.012 g, 0.399 mmol) and sodium cyanoborohydride (0.01g, 0.16 mmol). The reaction mixture was heated to reflux for 24 hours. After completion of reaction water (20 mL) was added and aqueous phase was extracted with ethyl acetate (3×50 mL). The combined organic layer was dried over anhydrous Na_2SO_4, filtered and concentrated under reduced pressure. The crude product was purified by column chromatography over alumina using ethyl acetate/petroleum ether (10:90) as eluent to obtain orangish yellow solid. **Yield:** 0.034 g (55%).

^{1}H NMR (400 MHz, $CDCl_3$): δ 8.33 (d, *J* = 8.4 Hz, 1H), 8.05-8.01 (m, 4H), 7.96 (d, *J* = 8.8 Hz, 1H), 7.82-7.77 (m, 2H), 7.51-7.47 (m, 1H), 7.42 (d, *J* = 8.8 Hz, 1H), 7.26-7.21 (m, 1H), 7.06 (dd, *J* = 8.8 Hz, 2.4 Hz, 1H), 6.22 (d, *J* = 2.4 Hz, 1H), 4.48 (t, *J* = 7.2 Hz, 2H), 2.45 (s, 6H), 2.07-1.94 (m, 2H), 1.61-1.51 (m, 2H), 1.04 (t, *J* = 7.2 Hz, 3H).
^{13}C NMR (100 MHz, $CDCl_3$): δ 143.5, 140.3, 133.7, 132.31, 131.6, 130.6, 128.9, 128.2, 127.9, 127.5, 127.4, 126.45, 126.4, 125.7, 125.5, 125.4, 124.8, 123.7, 123.1, 117.7, 114.7, 111.6, 110.5, 108.6, 43.2, 42.5, 31.6, 20.7, 14.0.
IR (KBr): 3441, 3040, 2953, 2865, 2787, 1620, 1579, 1523, 1490, 1455, 1354, 1321, 1269, 1220, 1131, 1016, 954, 899, 864, 829, 781, 742, 626, 592, 545 cm^{-1}.
HRMS (ESI+): *m/z* calcd for C30H29N2 $[M + H]^+$ 417.2325, found 417.2323.

(1*R*,2*S*,5*R*)-2-isopropyl-5-methylcyclohexyl (7-butyl-7*H*-phenanthro[3,4-*c*]carbazol-10-yl)carbamate ((±)51)

To a solution of 7-butyl-7H-phenanthro[3,4-*c*]carbazol-10-amine **49** (0.108 g, 0.27 mmol) and potassium carbonate (0.042 g, 0.30 mmol), in dichloromethane was added (1R,2S,5R)-(-)-menthyl chloroformate (0.073 g, 0.07 mL, 0.33 mmol) drop wise at 0 ℃ under N_2 atmosphere. After completion of the reaction, the reaction mixture was poured in ice cold water. The aqueous layer was extracted with dichloromethane (2×75 mL), the extracts were combined and the organic layer was dried over Na_2SO_4 and evaporated to obtain a crude mass. The crude product was purified by column chromatography over alumina using ethyl acetate/petroleum ether (10:90) as eluent to obtain pale yellow solid. **Overall yield** = 0.130 g, (82%, mixture of two diastereomers (*P*)-**51** and (*M*)-**51**).

HPLC conditions for (*P*)-**51** and (*M*)-**51**: two well separated peaks [column: Chiralcel OD-H; isopranol/n-hexane (30/70), 0.5 mL/min, UV 254 nm, t_R (*P*)-**51** = 15.19 and t_R (*M*)-**51** = 9.32 min].

HRMS (ESI+): *m/z* calcd for $C_{39}H_{42}N_2O_2Na$ $[M + Na]^+$ 593.3138, found 593.3138.

(*P*)-51

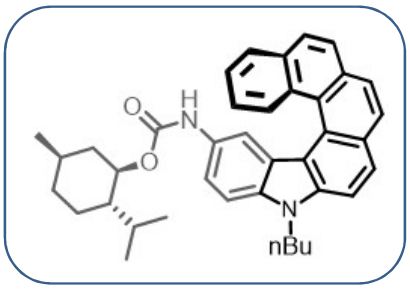

Molecular formula: $C_{39}H_{42}N_2O_2$
Molecular weight: 570.77
Physical state: yellowish brown sticky solid
M.p = 107-111 °C

de = 99.3%. **$[\alpha]_D$** = +1183, **$[\phi]_D$** = +6743 (*c* = 1.0 in $CHCl_3$).

^{1}H NMR (400 MHz, $CDCl_3$): δ 8.22 (d, *J* = 8.4 Hz, 1H), 8.09-8.03 (m, 4H), 7.97 (d, *J* = 8.4 Hz, 1H), 7.82 (t, *J* = 8.4 Hz, 2H), 7.57-7.53 (m, 1H), 7.48 (d, *J* = 8.8 Hz, 1H), 7.22-7.18 (m, 1H), 6.14 (s, 1H), 5.94 (s, 1H), 4.62-4.59 (m, 1H), 4.50 (t, *J* = 7.2 Hz, 2H), 2.06-1.94 (m, 4H), 1.70 (d, *J* = 11.6 Hz, 2H), 1.55-1.49 (m, 3H), 1.28 (s,1H), 1.1 (m, 1H), 1.03 (t, *J* = 7.2 Hz, 5H), 0.99-0.89 (m, 9H).

^{13}C NMR (100 MHz, $CDCl_3$): δ 154.0, 140.4, 136.4, 132.3, 131.6, 130.2, 128.9, 128.3, 128.0, 127.7, 127.5, 127.0, 126.4, 125.6, 125.4, 125.1, 124.7, 123.4, 123.0, 117.8, 117.4,116.8, 114.4, 110.4, 108.5, 74.7, 47.4, 43.3, 41.4, 34.4, 31.6, 29.9, 26.5, 23.9, 22.1, 20.9, 20.6, 16.8, 14.0.

IR (KBr): 3438, 3401, 3046, 2954, 2924, 2865, 1723, 1623, 1583, 1526, 1487,1448, 1313, 1211, 1046, 990, 834, 780, 765, 626, 543 cm^{-1}.

(*M*)-51

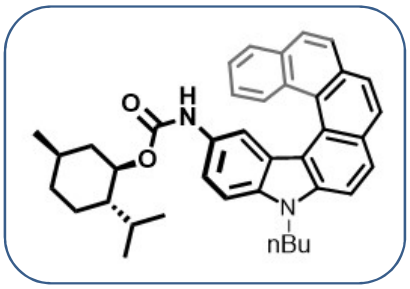

Molecular formula: $C_{39}H_{42}N_2O_2$
Molecular weight: 570.77
Physical state: yellowish brown sticky solid
M.p = 104-106 °C

de = 100%. **$[\alpha]_D$** = -1648, **$[\phi]_D$** = -9393 (*c* = 1.0 in $CHCl_3$).

^{1}H NMR (400 MHz, $CDCl_3$): δ 8.23 (d, *J* = 8.4 Hz, 1H), 8.10-8.03 (m, 4H), 7.97 (d, *J* = 8.8 Hz, 1H), 7.82 (t, *J* = 7.6 Hz, 2H), 7.56 (t, *J* = 7.2 Hz, 1H), 7.47 (d, *J* = 7.2 Hz, 1H), 7.19 (t, *J* = 7.2 Hz, 1H), 6.19 (s, 1H), 5.98 (s, 1H), 4.63-4.60 (m, 1H), 4.50 (t, *J* = 7.2 Hz, 2H), 2.01-1.94 (m, 2H), 1.89-1.86 (m, 1H), 1.71-1.63 (m, 4H), 1.54-1.49 (m, 2H), 1.28 (s, 1H), 1.07-1.01 (m,

6H), 0.96 (d, *J* = 6.4 Hz, 3H), 0.92-0.86 (m, 4H), 0.74 (d, *J* = 6.8 Hz, 3H).

^{13}C NMR (100 MHz, $CDCl_3$): δ 153.9, 140.4, 136.3, 132.3, 131.6, 130.2, 128.9, 128.8, 128.5, 128.3, 127.9, 127.7, 127.6, 127.0, 126.4, 125.6, 125.5, 125.1, 124.7, 123.4, 123.1, 117.4, 116.37, 110.4, 108.4, 74.6, 47.2, 43.2, 41.4, 34.3, 31.4, 29.7, 26.0, 23.3, 22.1, 20.8, 20.6, 16.2, 13.9.

7-butyl-7*H*-phenanthro[3,4-*c*]carbazol-10-amine ((*P*)-49)

[**Deprotection of pure (P)-13 diastereomer**, de = 99.3%].

A solution of (*P*)-**51** (0.054 g, 0.09 mmol) and tetra-*n*-butylammonium fluoride (TBAF) (0.47 mL, 1M in THF, 0.47 mmol) in dry THF (5 mL) was heated at 70 ℃ for 24 hours. After completion of reaction water (20 mL) was added and aqueous phase was extracted with ethyl acetate (3×20 mL). The combined organic layer was dried over anhydrous Na_2SO_4, filtered and concentrated under reduced pressure. The crude reaction mass was filtered over alumina gel column chromatography using ethyl acetate/ petroleum ether (15:85) as eluent to obtain brownish orange mass. **Yield:** 0.035 g (95%).

[α]$_D$ = +859 (*c* = 0.202 in $CHCl_3$). Rest of the data was same as that described earlier for 7-butyl-7H-phenanthro[3,4-*c*]carbazol-10-amine **49**.

tert-butyl (7-butyl-7*H*-phenanthro[3,4-*c*]carbazol-10-yl)carbamate ((*P*)-52)

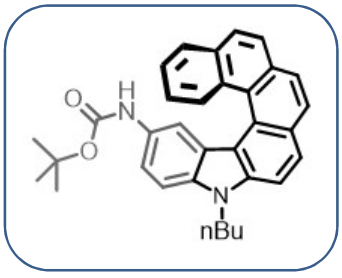

Molecular formula: $C_{33}H_{32}N_2O_2$
Molecular weight: 488.24
Physical state: brown solid
M.p = 178-181 °C

To a solution of (*P*)-**49** (0.040 g, 0.08 mmol) and triethylamine (0.009 g, 0.01 mL, 0.09 mmol) in dichloromethane was added Boc anhydride (0.017 g, .018 mL, 0.08 mmol) drop wise at 0 ℃ under N_2 atmosphere and stirred at room temperature. After completion of the reaction, the reaction mixture was poured in ice cold water. The aqueous layer was extracted with dichloromethane (2×20 mL), the extracts were combined and the organic layer was dried over Na_2SO_4 and evaporated to obtain a crude mass. The crude product was purified by column

chromatography over alumina using ethyl acetate/petroleum ether (10:90) as eluent to obtain pale yellow solid. **Yield:** 0.021 g (52%).

ee = 56%. **$[\alpha]_D$** = +747 (*c* = 0.15 in $CHCl_3$).

^{1}H NMR (400 MHz, $CDCl_3$): δ 8.22 (d, J = 8.4 Hz, 1H), 8.08-8.02 (m, 4H), 7.96 (d, *J* = 8.4 Hz, 1H), 7.82 (t, *J* = 8.8 Hz, 2H), 7.58-7.54 (m, 1H), 7.45 (d, *J* = 8.8 Hz, 1H), 7.21-7.17 (m, 1H), 6.17 (s, 1H), 5.88 (s, 1H), 4.50 (t, *J* = 7.2 Hz, 2H), 2.01-1.93 (m, 2H), 1.56-1.46 (m, 2H merged with s, 9H), 1.02 (t, *J* = 7.2 Hz, 3H).

IR (KBr): 3439, 2957, 2923, 2852, 1723, 1623, 1582, 1524, 1482, 1366, 1314, 1225, 1159, 1053, 1022, 834, 800, 765, 627, 543 cm^{-1}.

HRMS (ESI+): *m/z* calcd for $C_{33}H_{32}N_2O_2Na$ $[M + Na]^+$ 511.2356, found 511.2355.

2A.5 Spectral Data

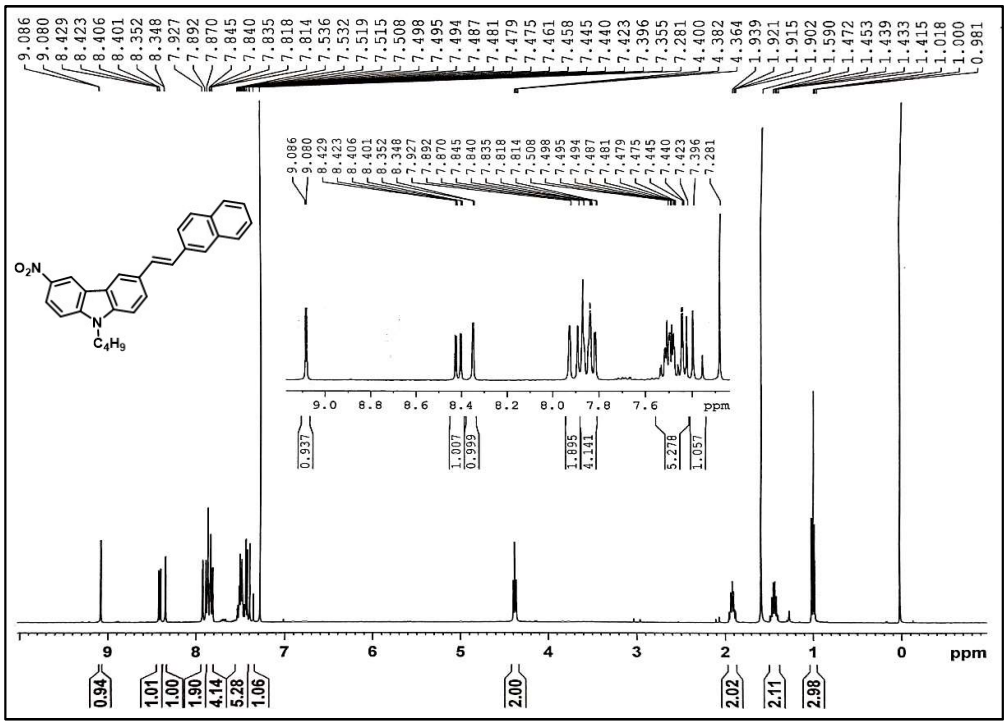

^{1}H NMR Spectrum of 46 ($CDCl_3$, 400 MHz)

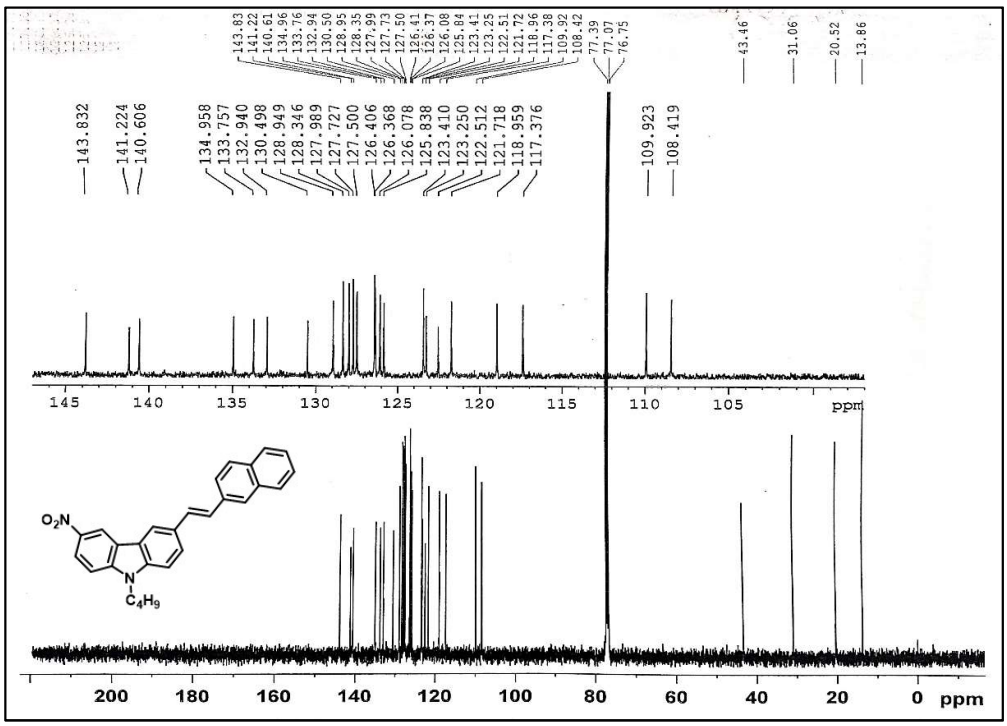

^{13}C NMR Spectrum of 46 ($CDCl_3$, 100 MHz)

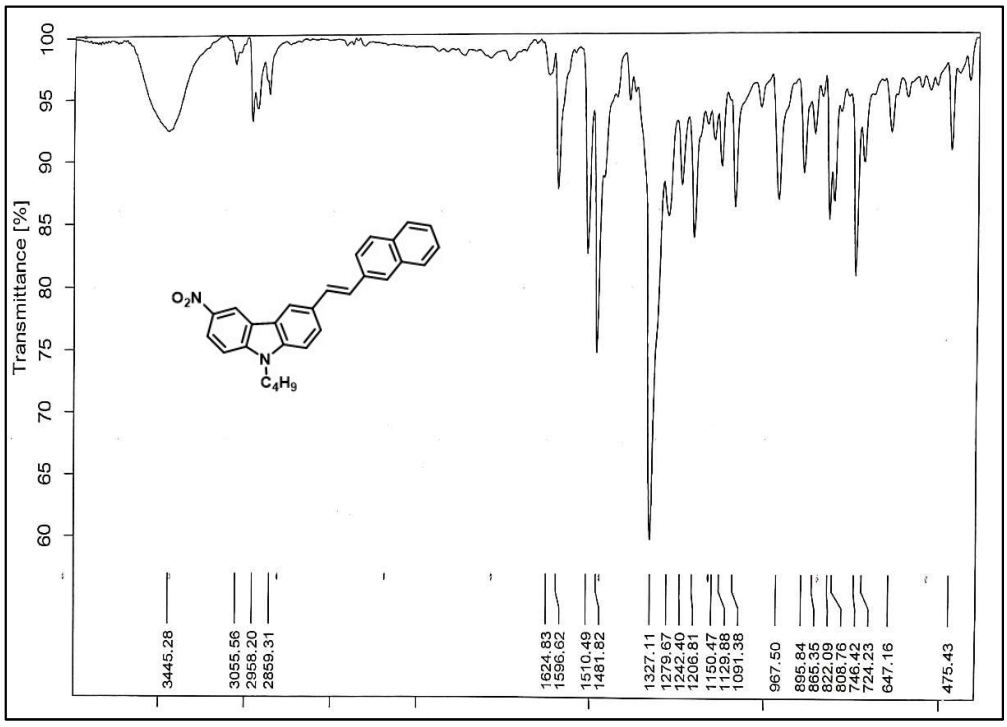

IR Spectrum of 46

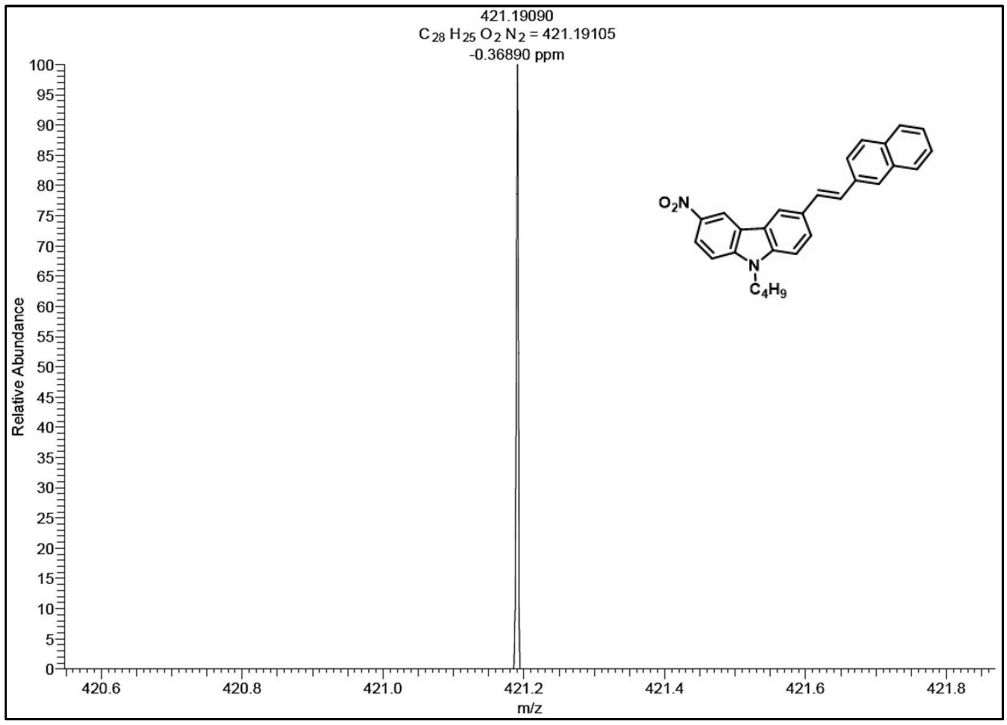

HRMS Spectrum of 46

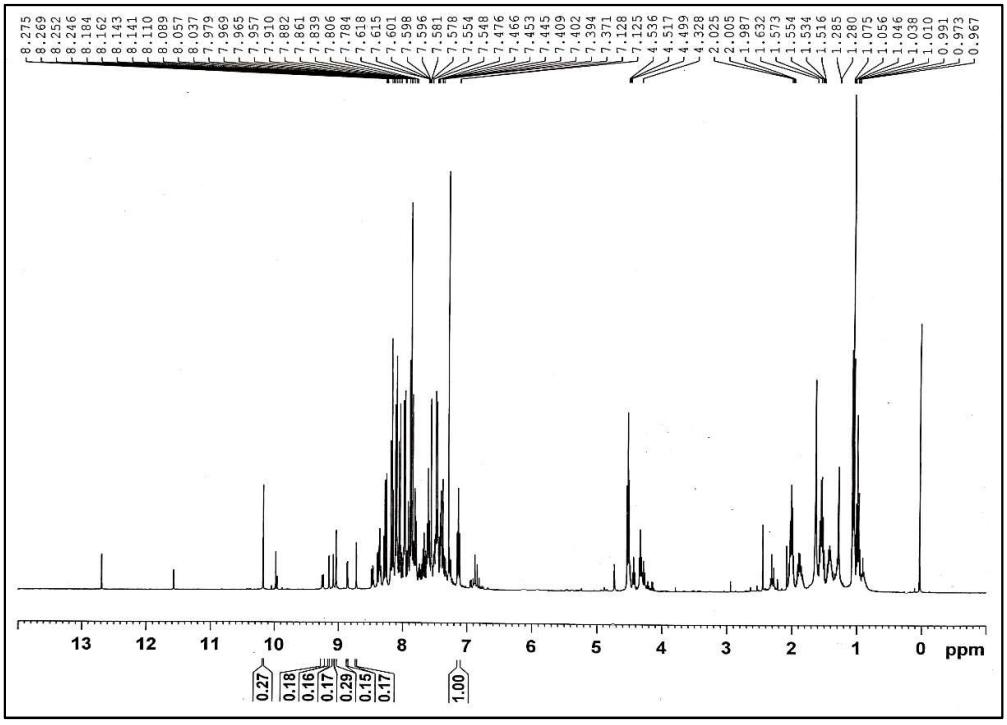

^{1}H NMR Spectrum of crude reaction mixture of photocyclization of 46

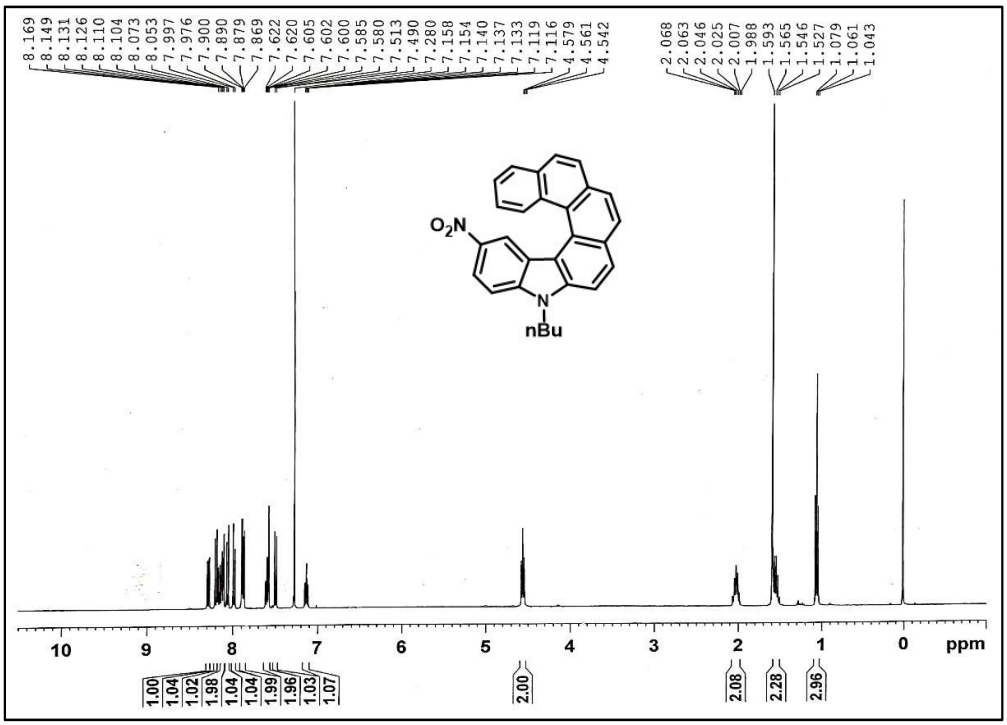

^{1}H NMR Spectrum of 47 ($CDCl_3$, 400 MHz)

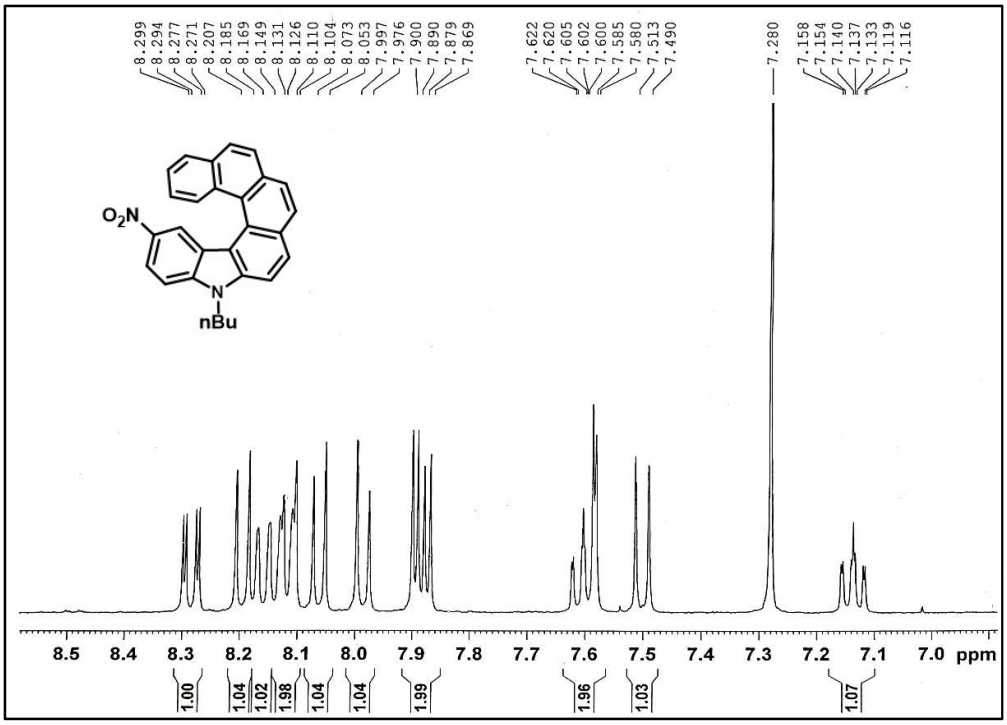

^{1}H NMR Spectrum of 47 (aromatic region) ($CDCl_3$, 400 MHz)

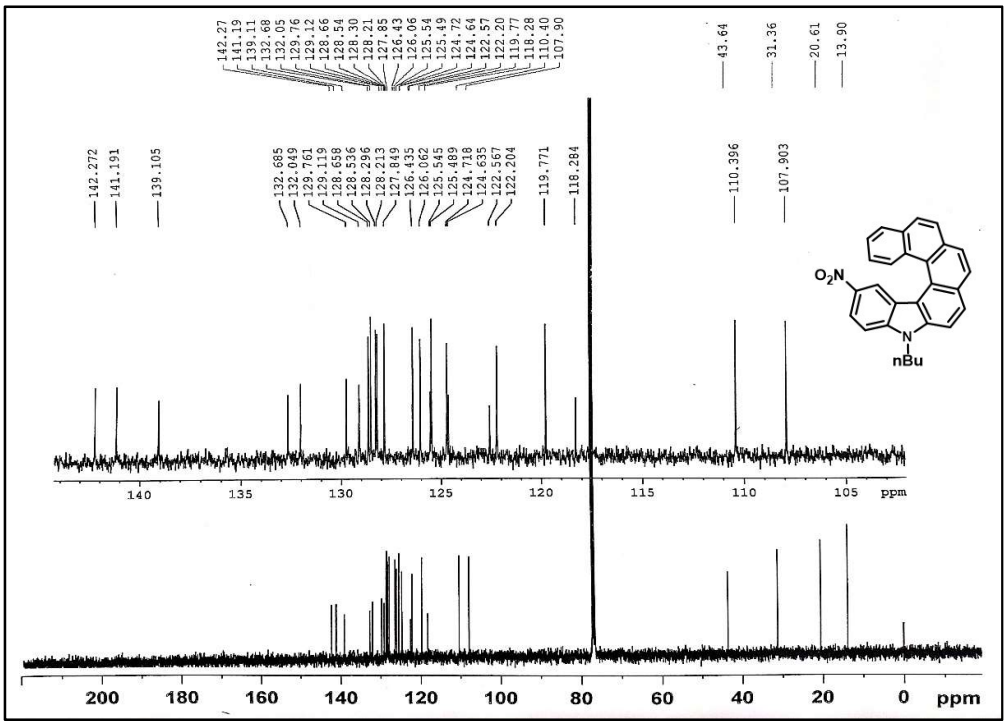

^{13}C NMR Spectrum of 47 ($CDCl_3$, 100 MHz)

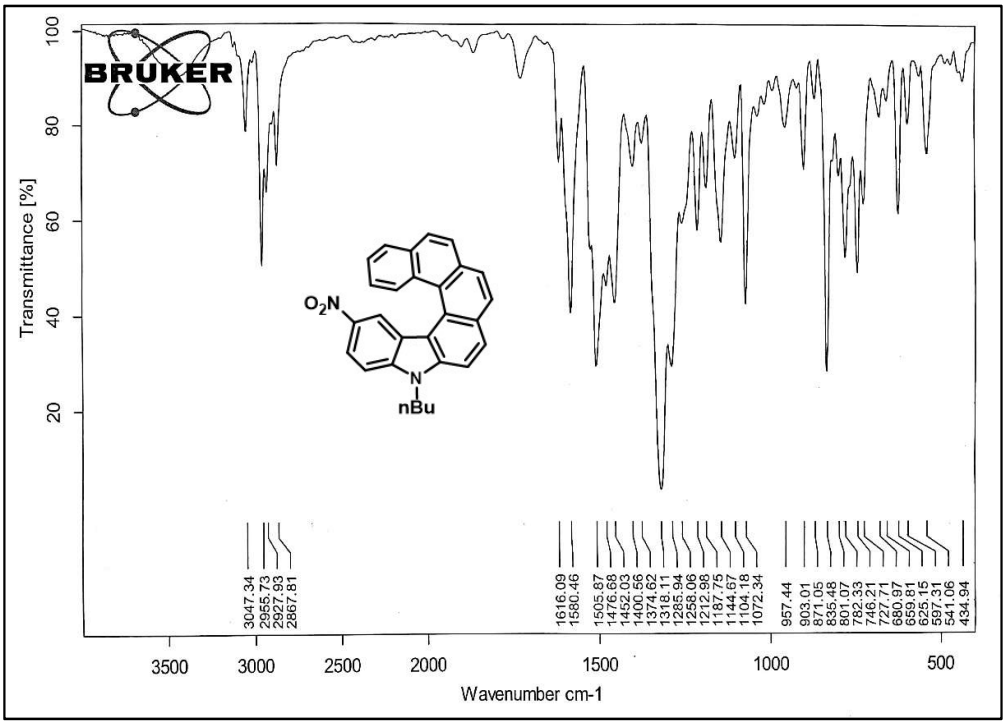

IR Spectrum of 47

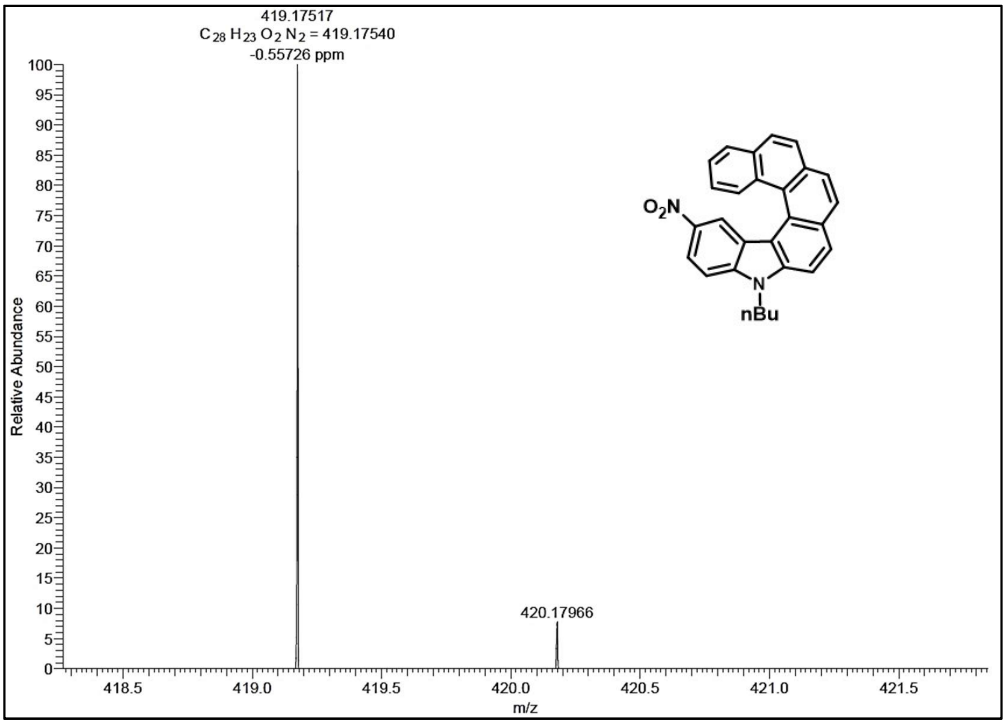

HRMS Spectrum of 47

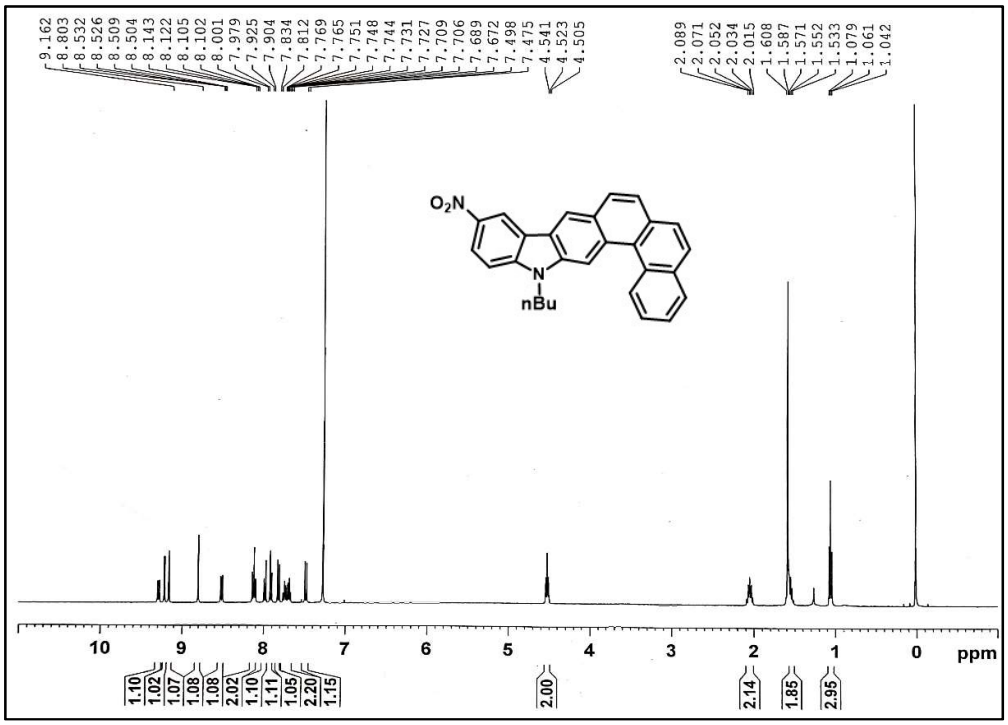

^{1}H NMR Spectrum of 48 ($CDCl_3$, 400 MHz)

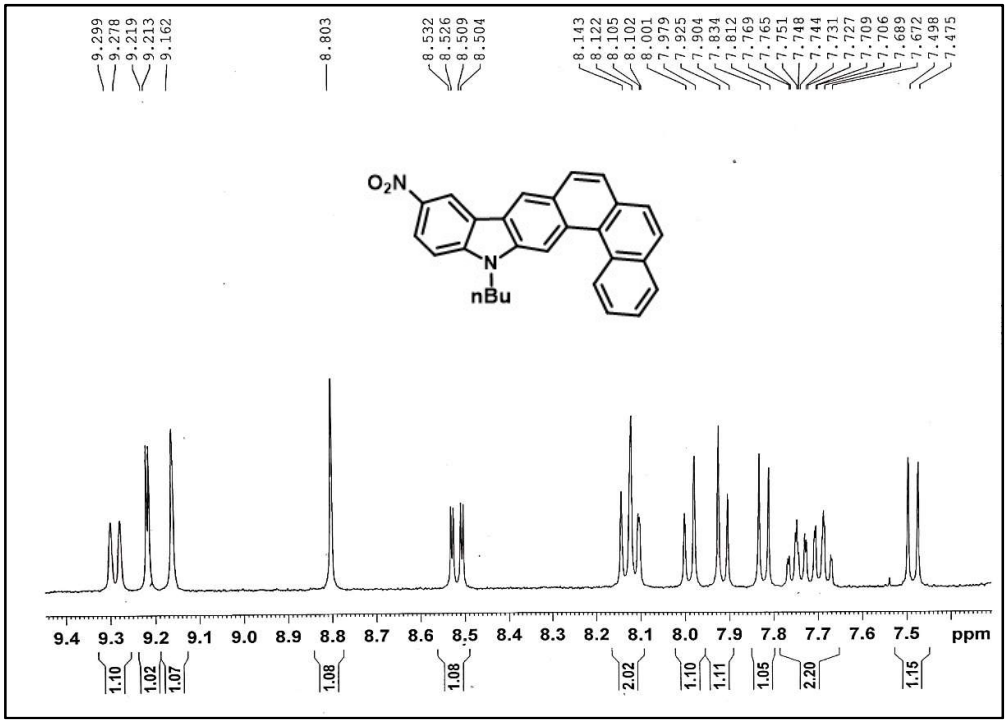

^{1}H NMR Spectrum of 48 (aromatic region) ($CDCl_3$, 400 MHz)

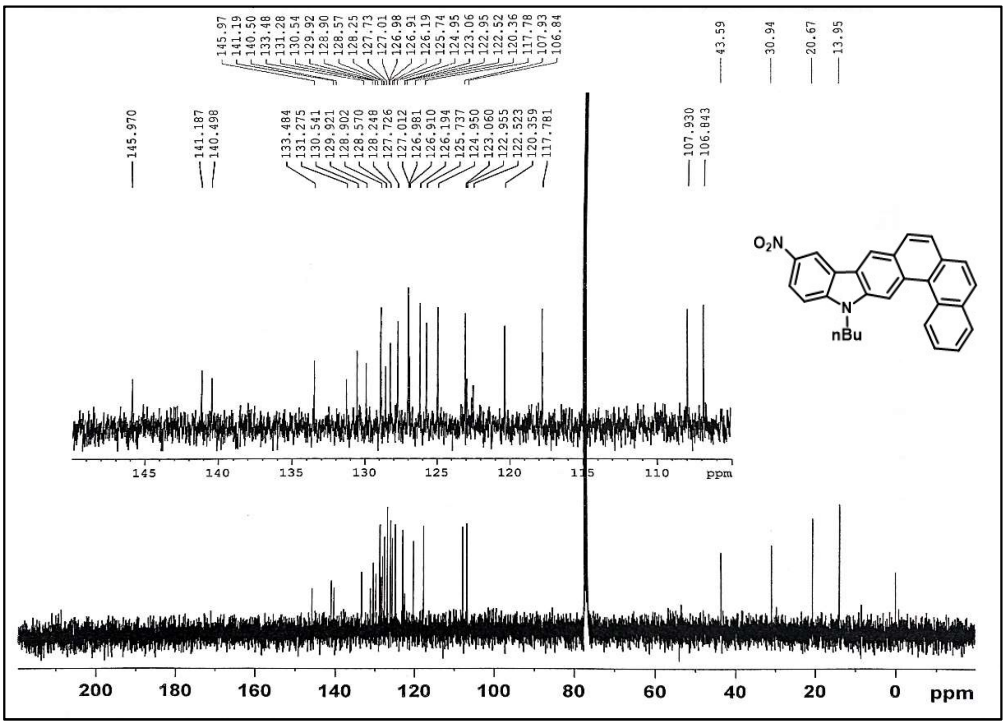

^{13}C NMR Spectrum of 48 ($CDCl_3$, 100 MHz)

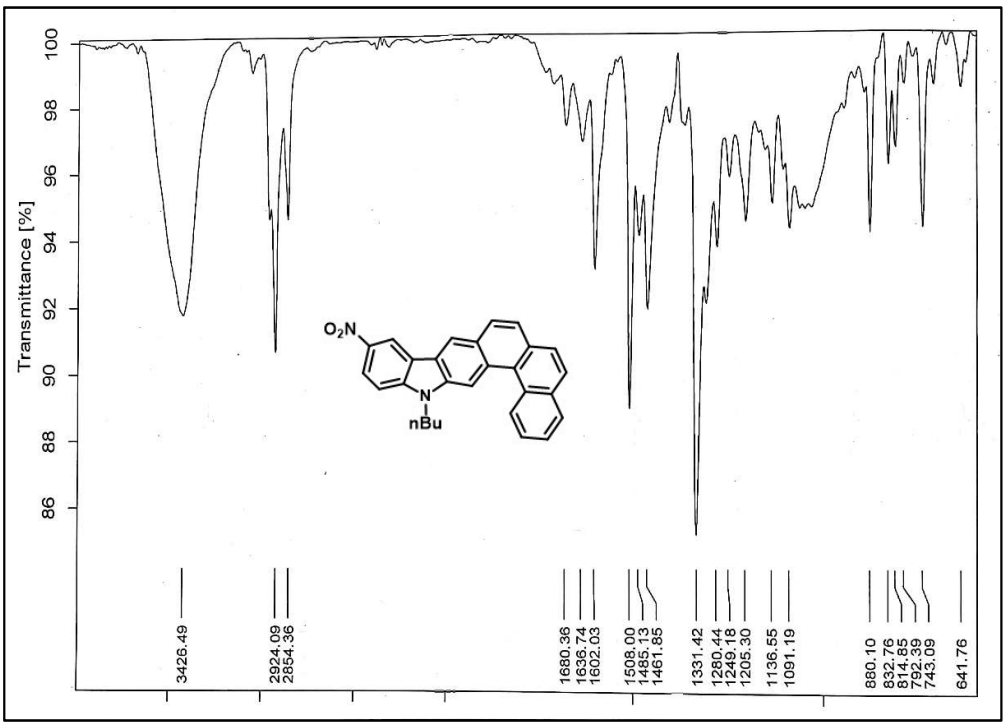

IR Spectrum of 48

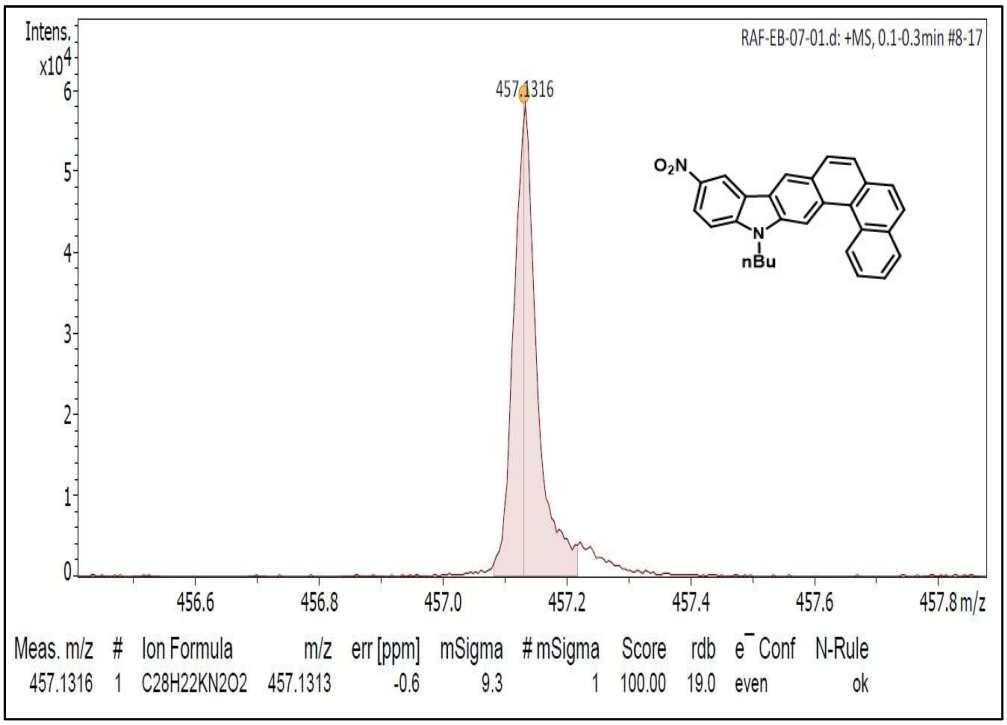

HRMS Spectrum of 48

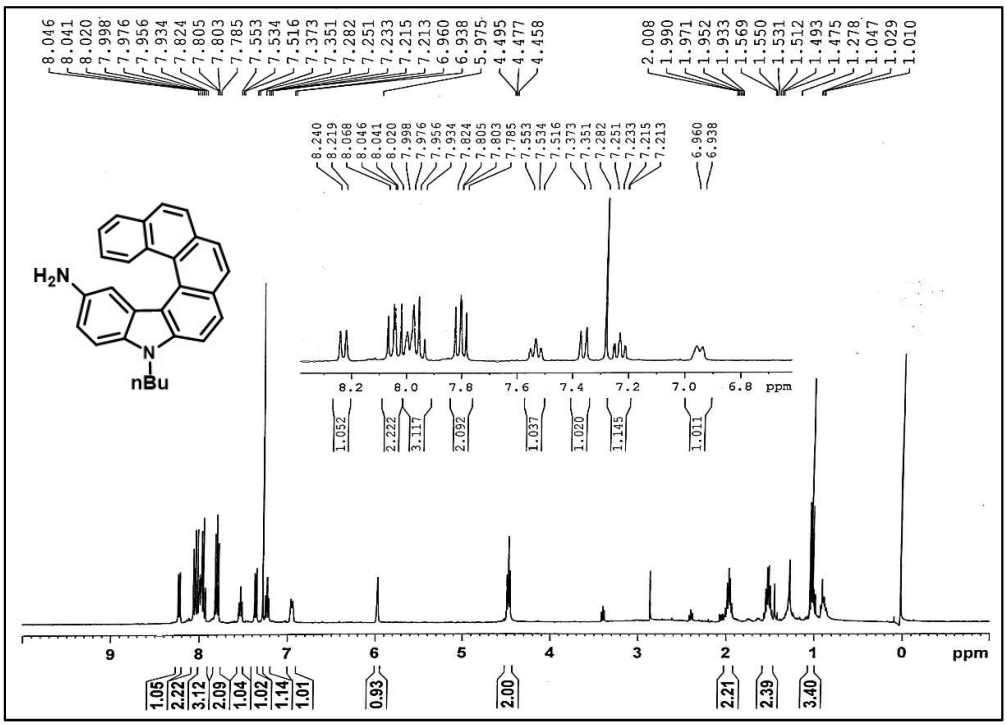

^{1}H NMR Spectrum of 49 ($CDCl_3$, 400 MHz)

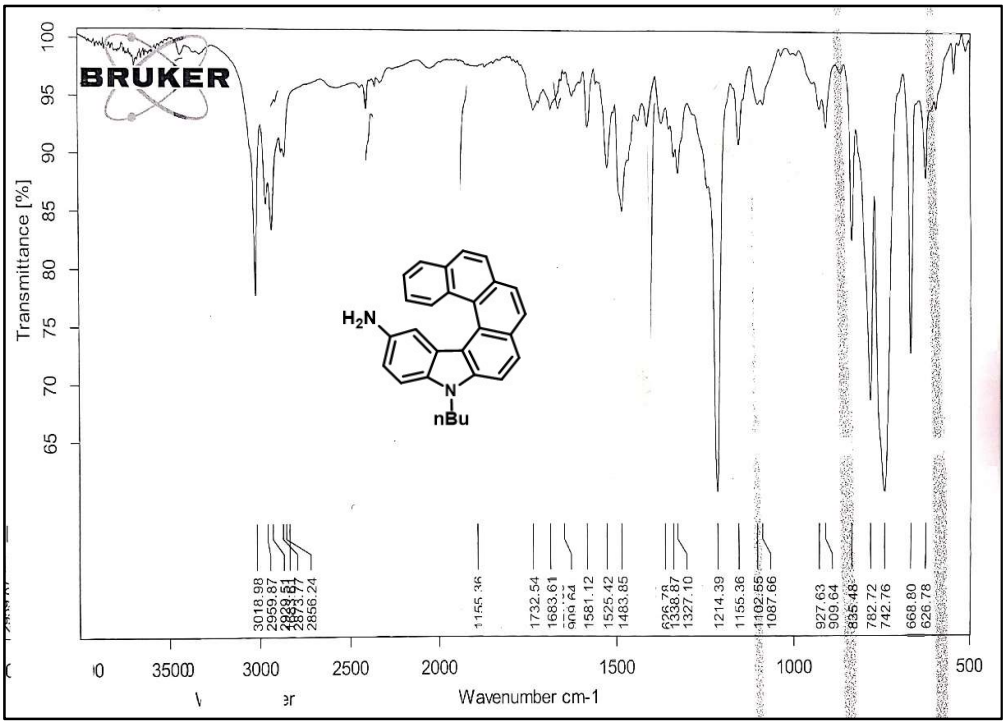

IR Spectrum of 49

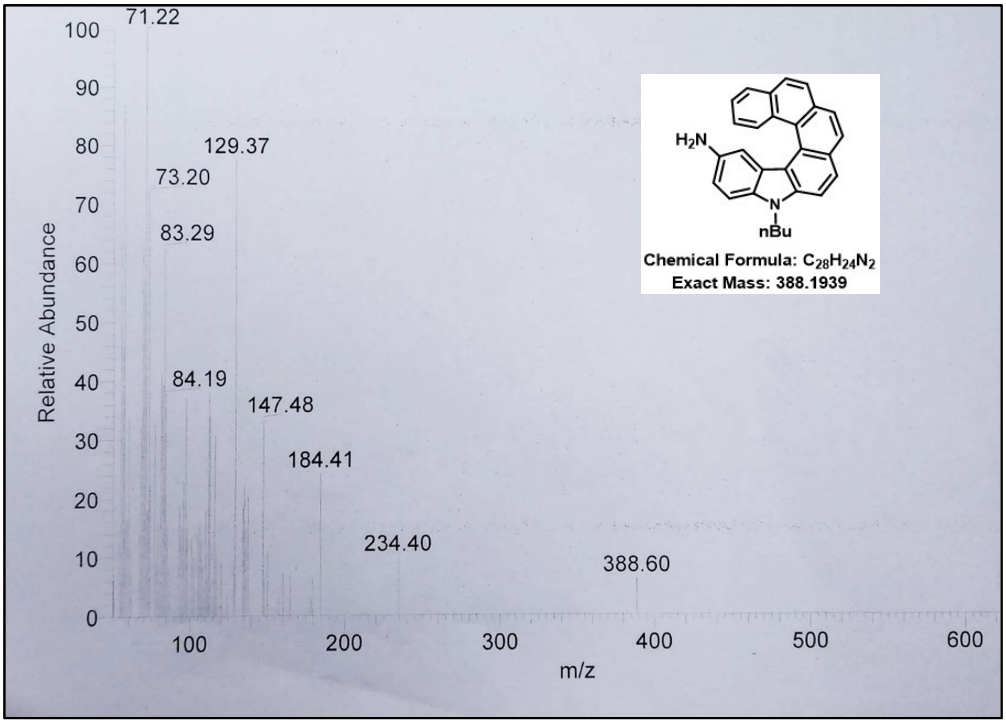

Mass Spectrum of 49

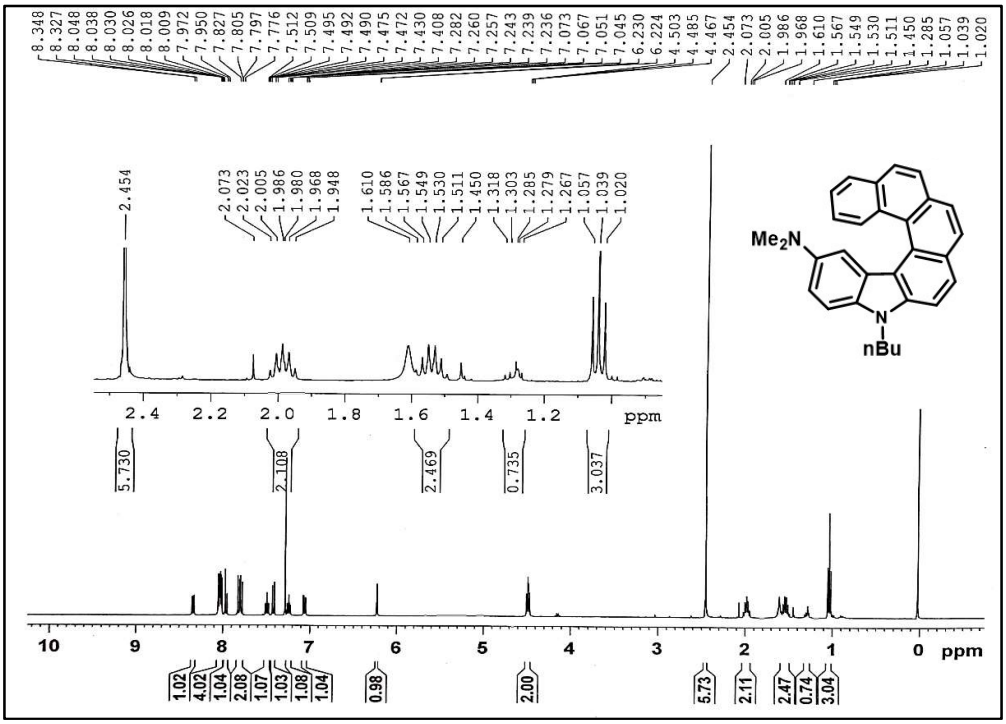

^{1}H NMR Spectrum of 50 ($CDCl_3$, 400 MHz)

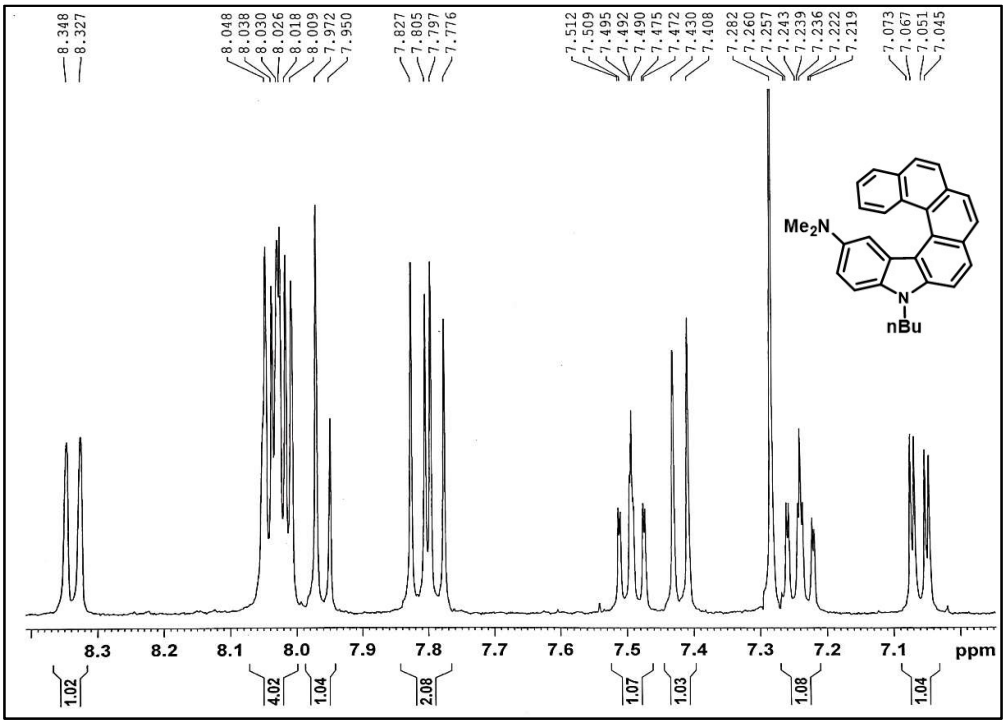

^{1}H NMR Spectrum of 50 (aromatic region) ($CDCl_3$, 400 MHz)

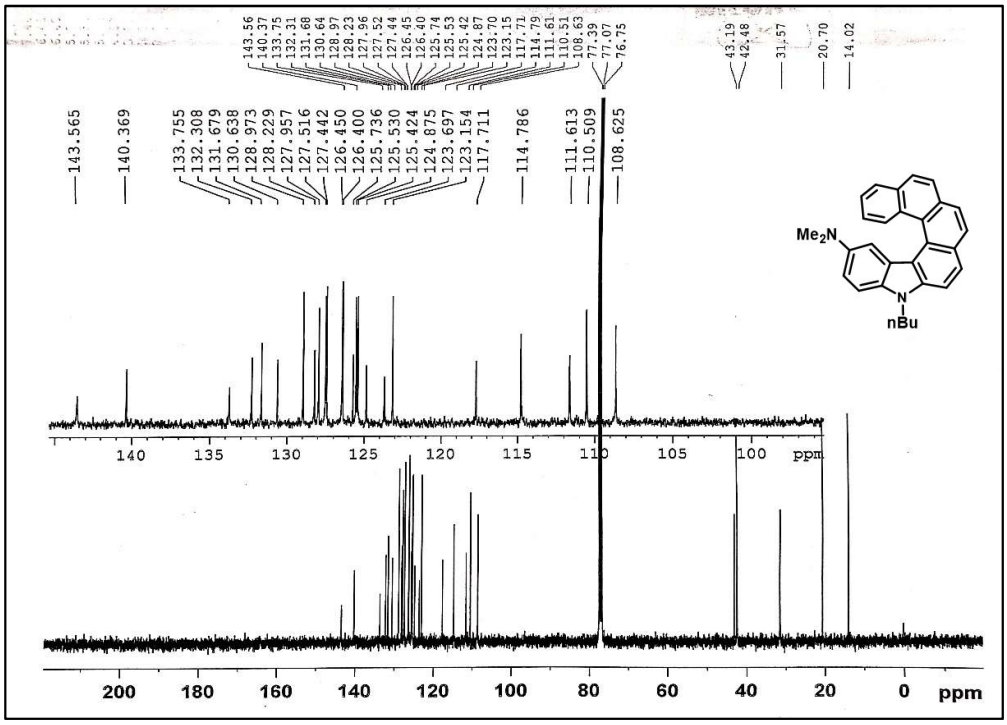

^{13}C NMR Spectrum of 50 ($CDCl_3$, 100 MHz)

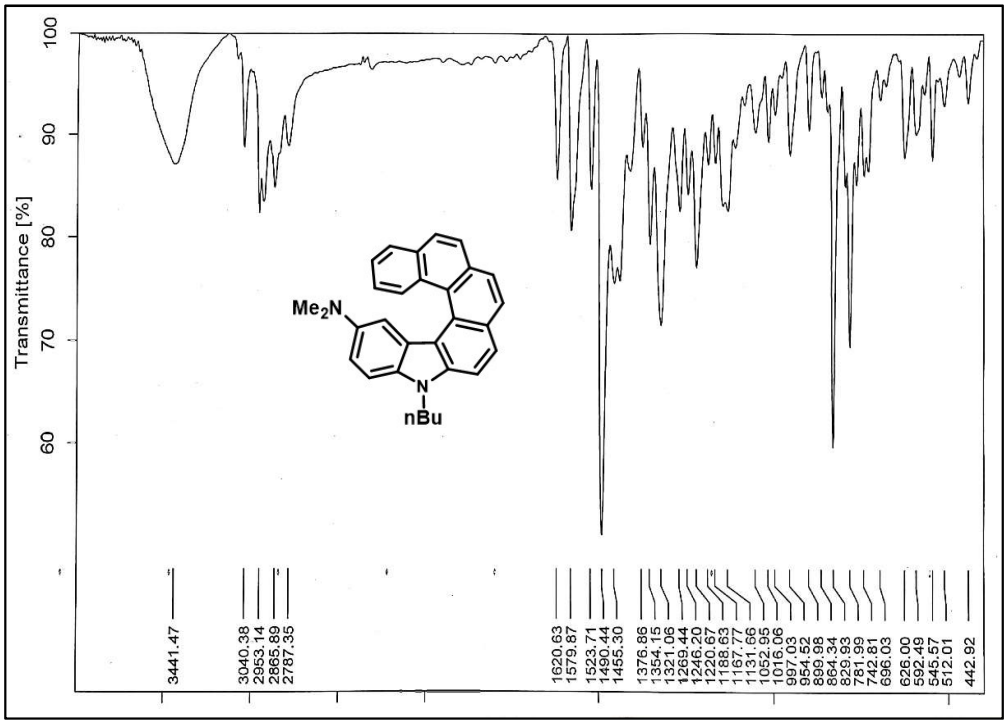

IR Spectrum of 50

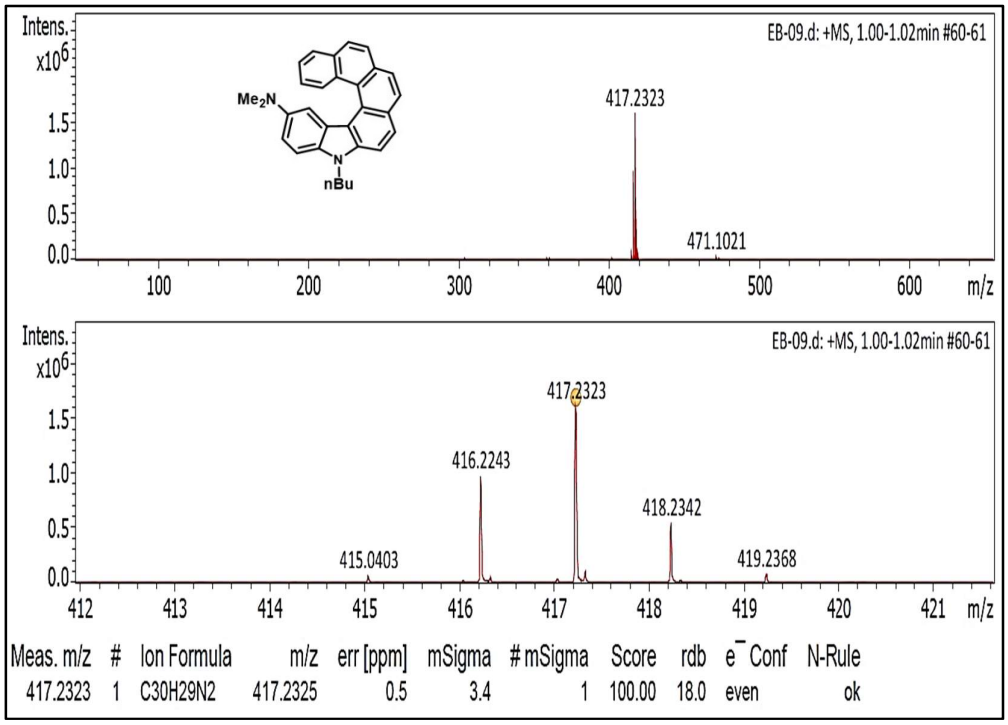

HRMS Spectrum of 50

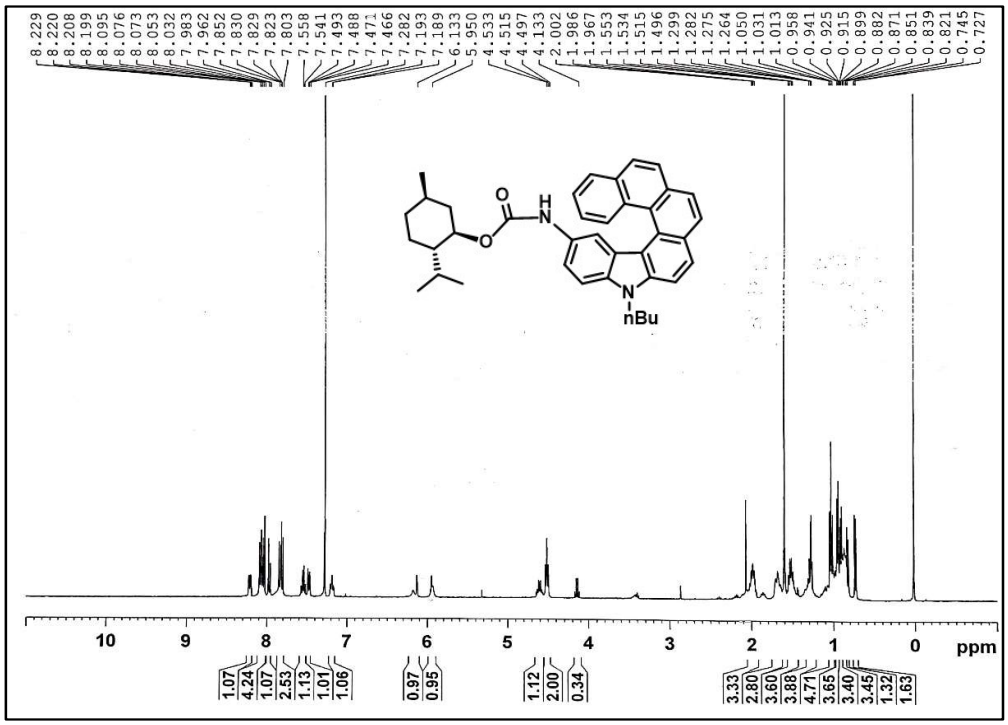

^{1}H NMR Spectrum of mixture of diastereomeric menthylcarbamates ($CDCl_3$, 400 MHz)

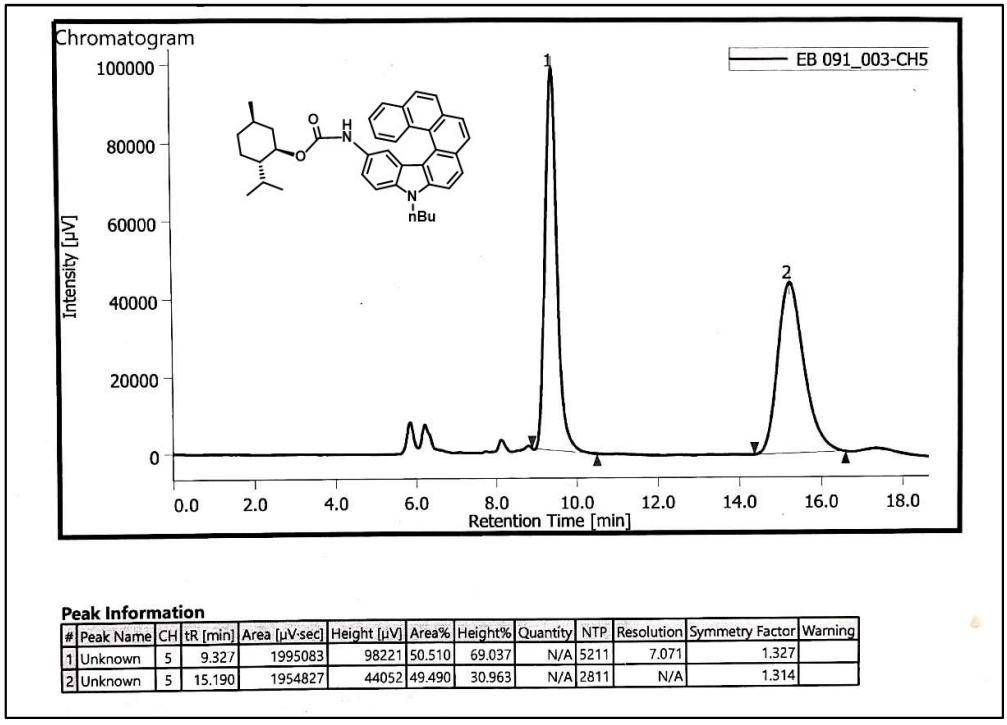

Peak Information

#	Peak Name	CH	tR [min]	Area [µV·sec]	Height [µV]	Area%	Height%	Quantity	NTP	Resolution	Symmetry Factor	Warning
1	Unknown	5	9.327	1995083	98221	50.510	69.037	N/A	5211	7.071	1.327	
2	Unknown	5	15.190	1954827	44052	49.490	30.963	N/A	2811	N/A	1.314	

HPLC chart of mixture of diastereomeric menthylcarbamates

Chiralcel OD-H; isopranol/n-hexane (30/70), 0.5 mL/min, UV 254 nm

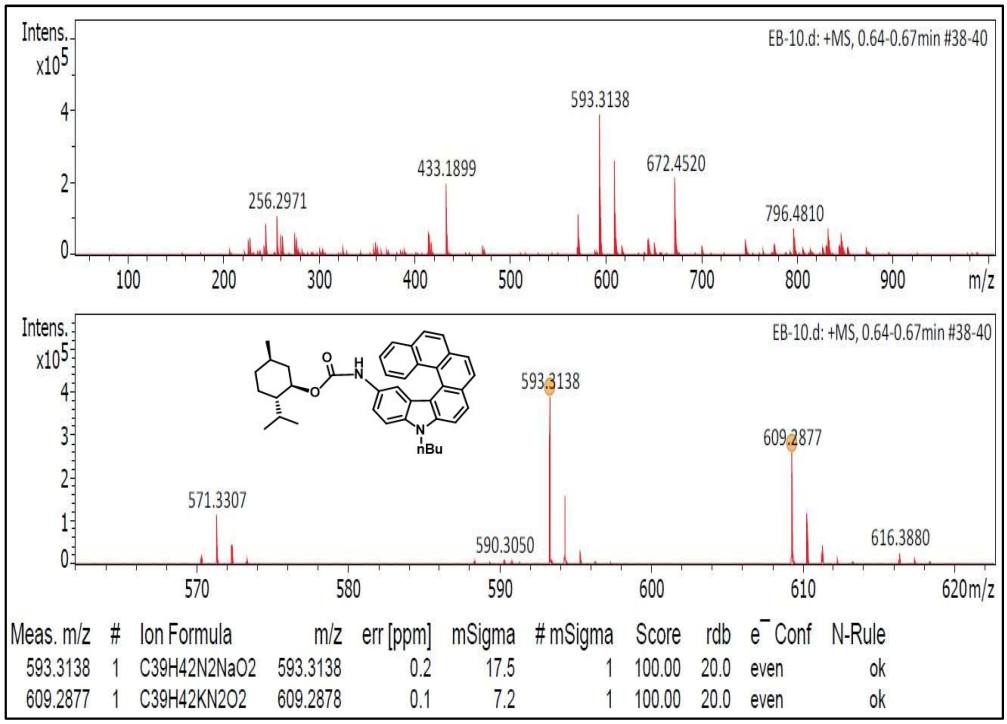

Meas. m/z	#	Ion Formula	m/z	err [ppm]	mSigma	# mSigma	Score	rdb	e⁻ Conf	N-Rule
593.3138	1	C39H42N2NaO2	593.3138	0.2	17.5	1	100.00	20.0	even	ok
609.2877	1	C39H42KN2O2	609.2878	0.1	7.2	1	100.00	20.0	even	ok

HRMS Spectrum of mixture of diastereomeric menthylcarbamates

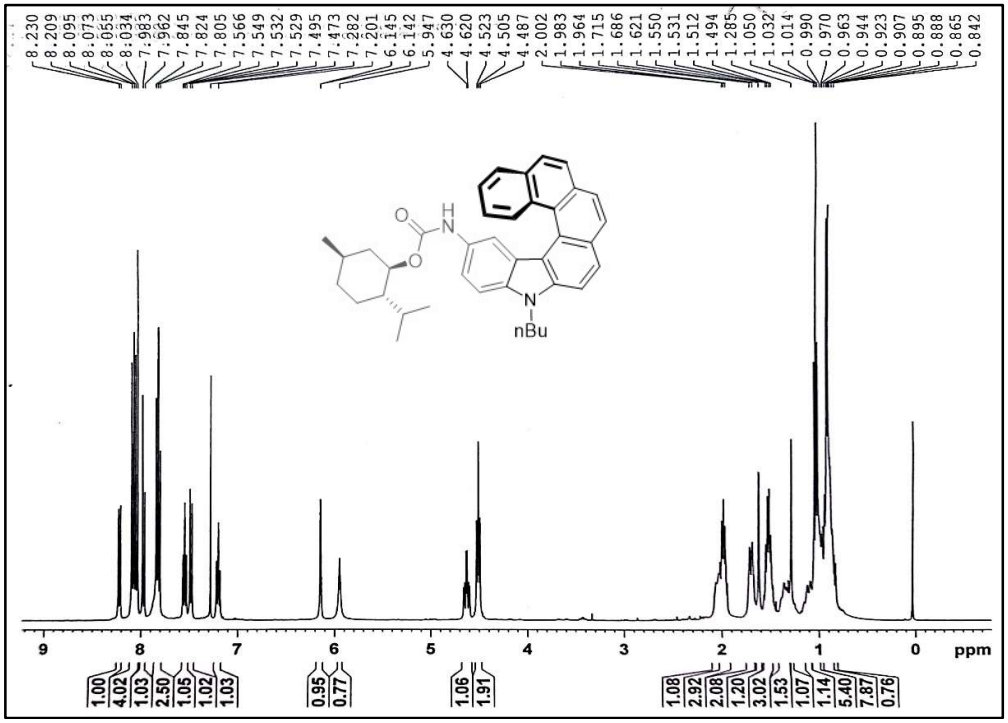

^{1}H NMR Spectrum of (*P*)-51 ($CDCl_3$, 400 MHz)

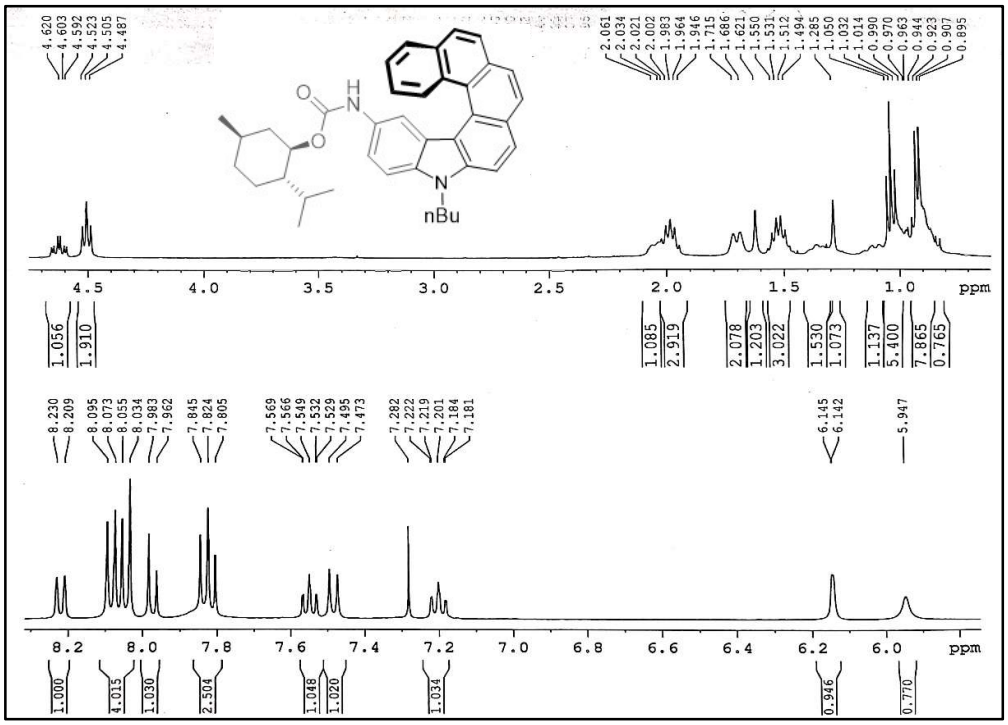

^{1}H NMR Spectrum of (*P*)-51 (enlarged aliphatic and aromatic region) ($CDCl_3$, 400 MHz)

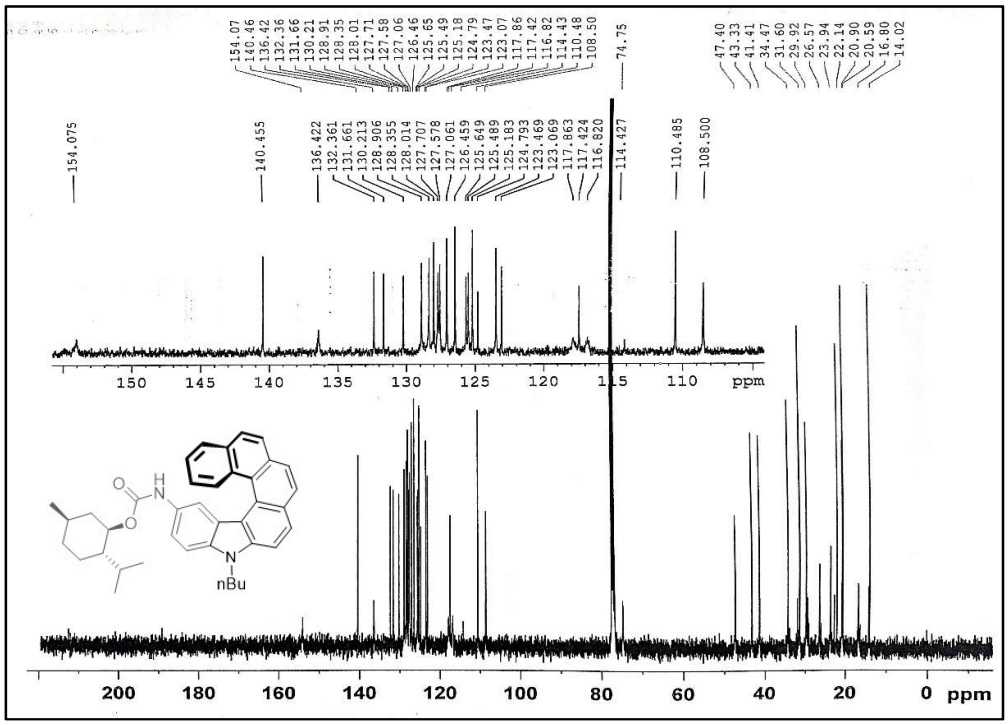

^{13}C NMR Spectrum of (*P*)-51 ($CDCl_3$, 100 MHz)

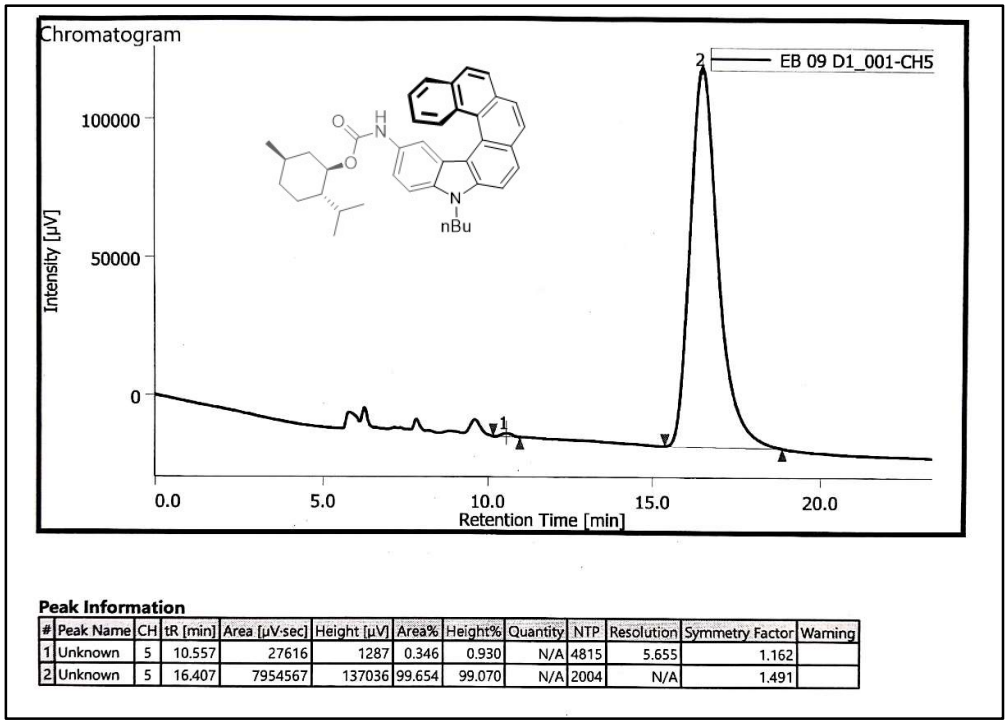

Peak Information

#	Peak Name	CH	tR [min]	Area [µV·sec]	Height [µV]	Area%	Height%	Quantity	NTP	Resolution	Symmetry Factor	Warning
1	Unknown	5	10.557	27616	1287	0.346	0.930	N/A	4815	5.655	1.162	
2	Unknown	5	16.407	7954567	137036	99.654	99.070	N/A	2004	N/A	1.491	

HPLC chart of (*P*)-51

99.3% de (Chiralcel OD-H; isopranol/n-hexane (30/70), 0.5 mL/min, UV 254 nm)

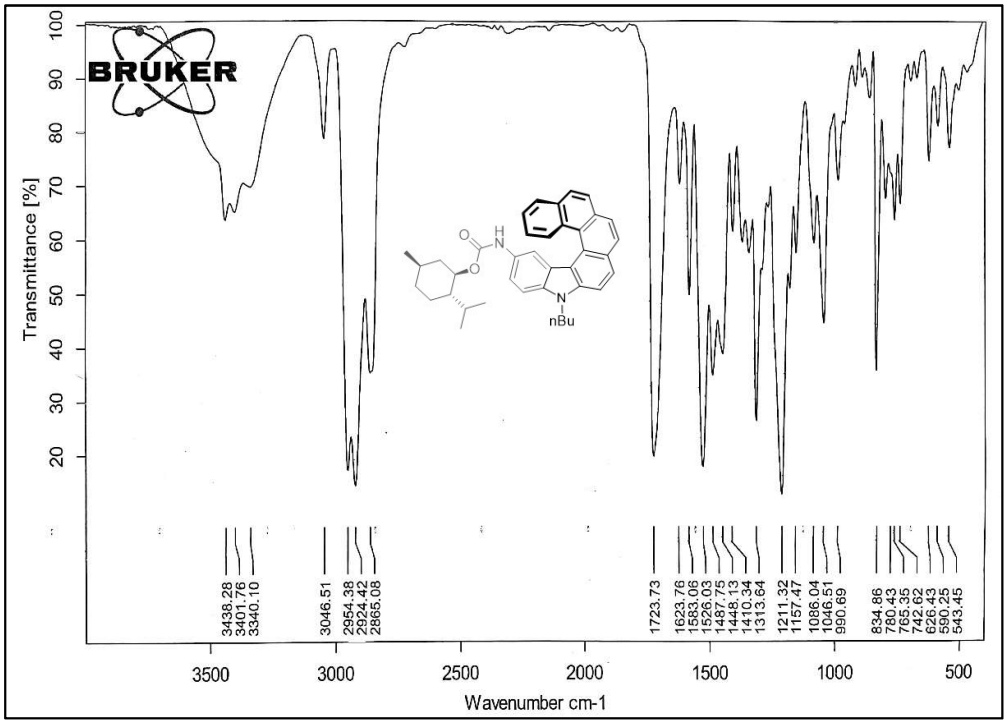

IR Spectrum of (*P*)-51

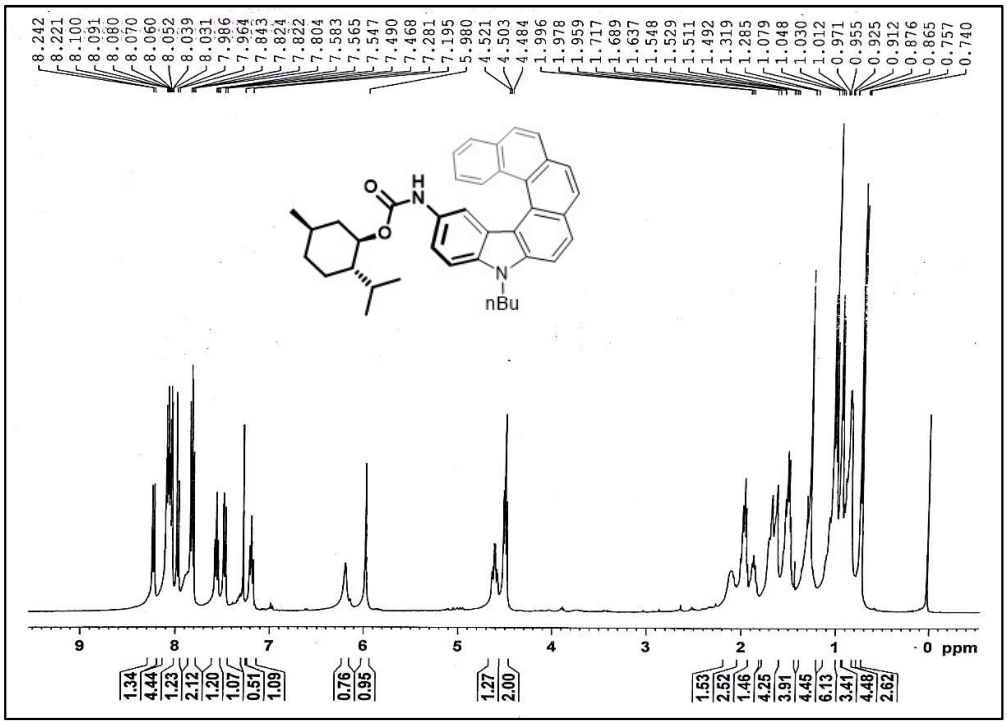

^{1}H NMR Spectrum of (*M*)-51 ($CDCl_3$, 400 MHz)

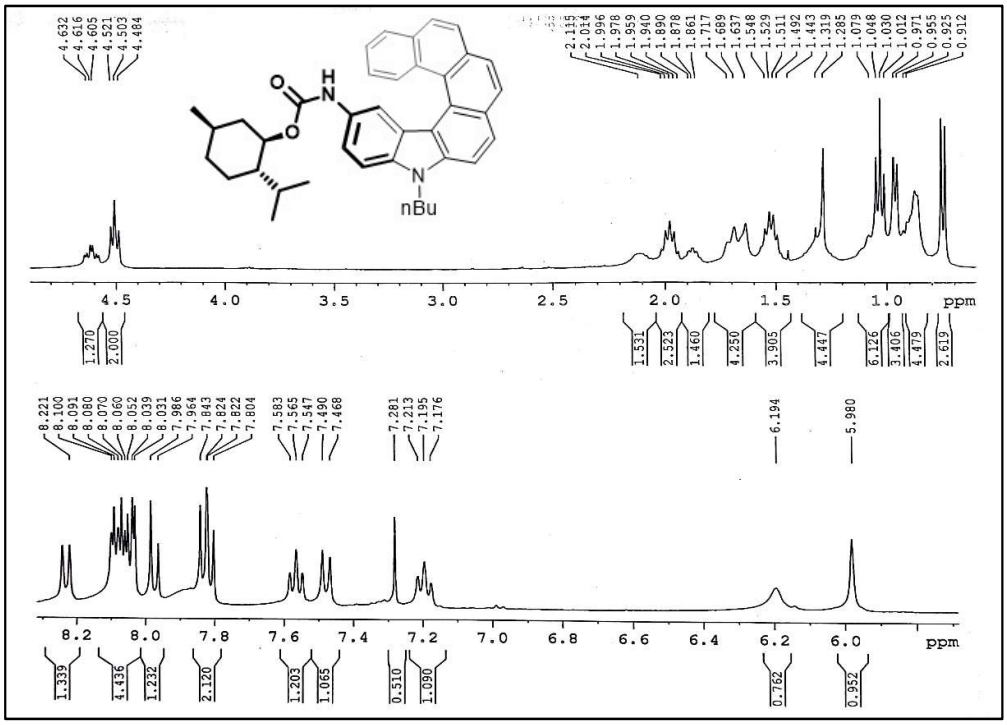

^{1}H NMR Spectrum of (*M*)-51 (enlarged aliphatic and aromatic region) ($CDCl_3$, 400 MHz)

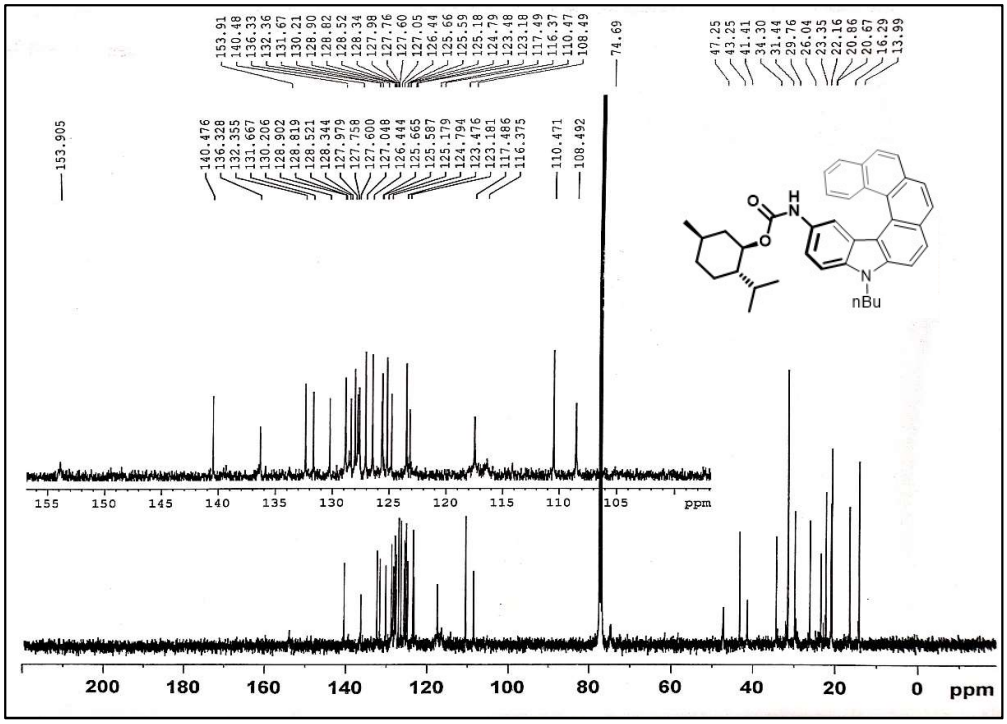

^{13}C NMR Spectrum of (*M*)-51 ($CDCl_3$, 100 MHz)

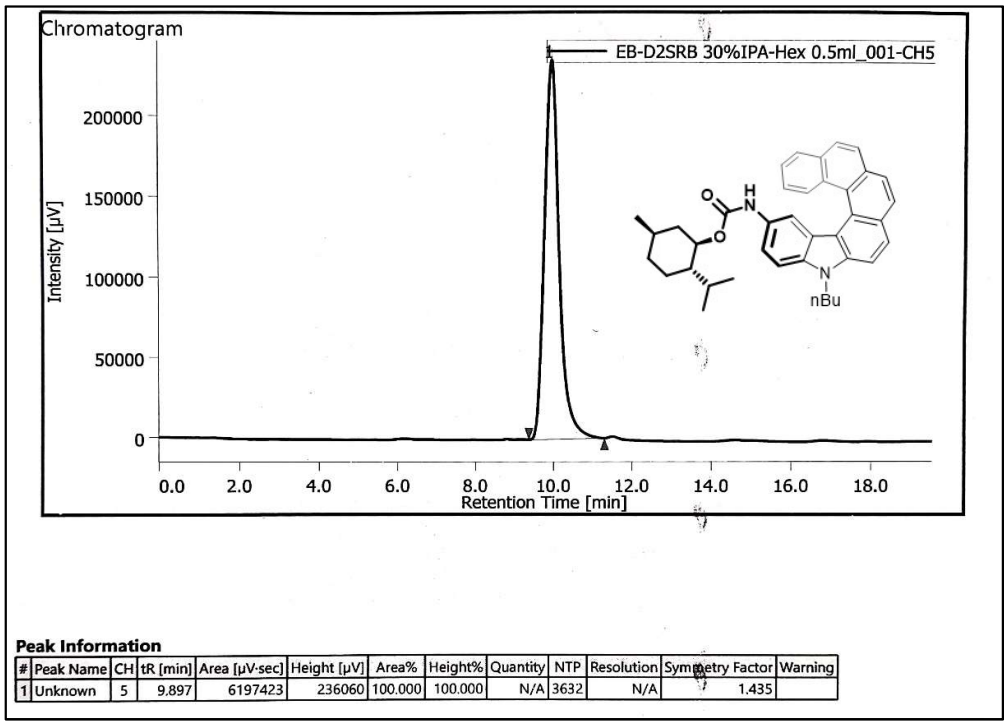

Peak Information

#	Peak Name	CH	tR [min]	Area [μV·sec]	Height [μV]	Area%	Height%	Quantity	NTP	Resolution	Symmetry Factor	Warning
1	Unknown	5	9.897	6197423	236060	100.000	100.000	N/A	3632	N/A	1.435	

HPLC chart of (*M*)-51

100% de (Chiralcel OD-H; isopranol/n-hexane (30/70), 0.5 mL/min, UV 254 nm)

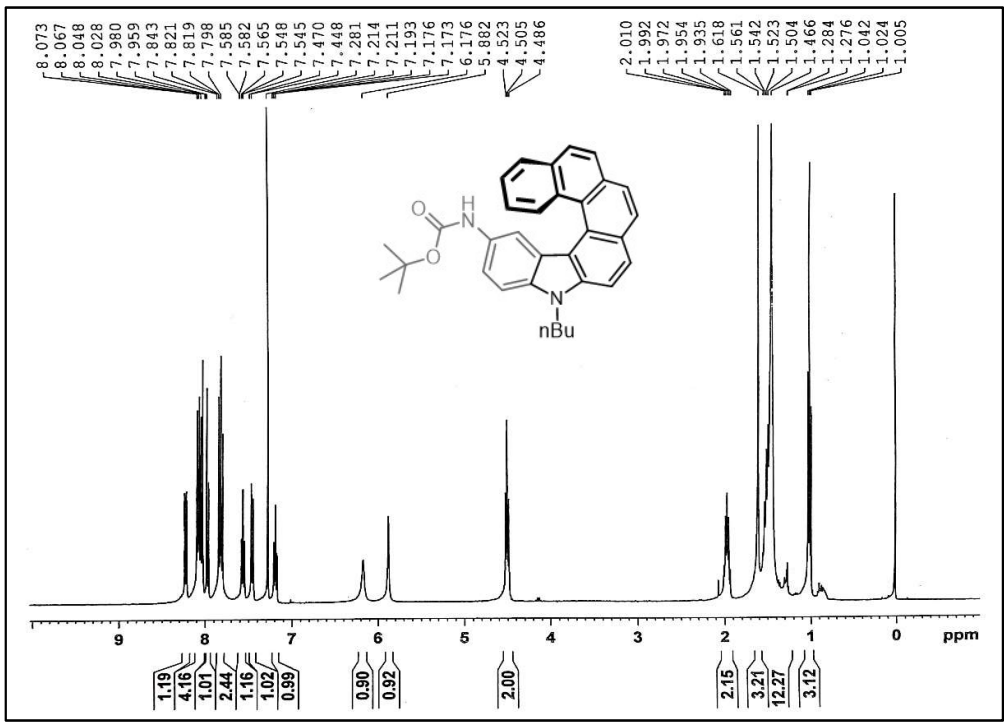

^{1}H NMR Spectrum of (*P*)-52 ($CDCl_3$, 400 MHz)

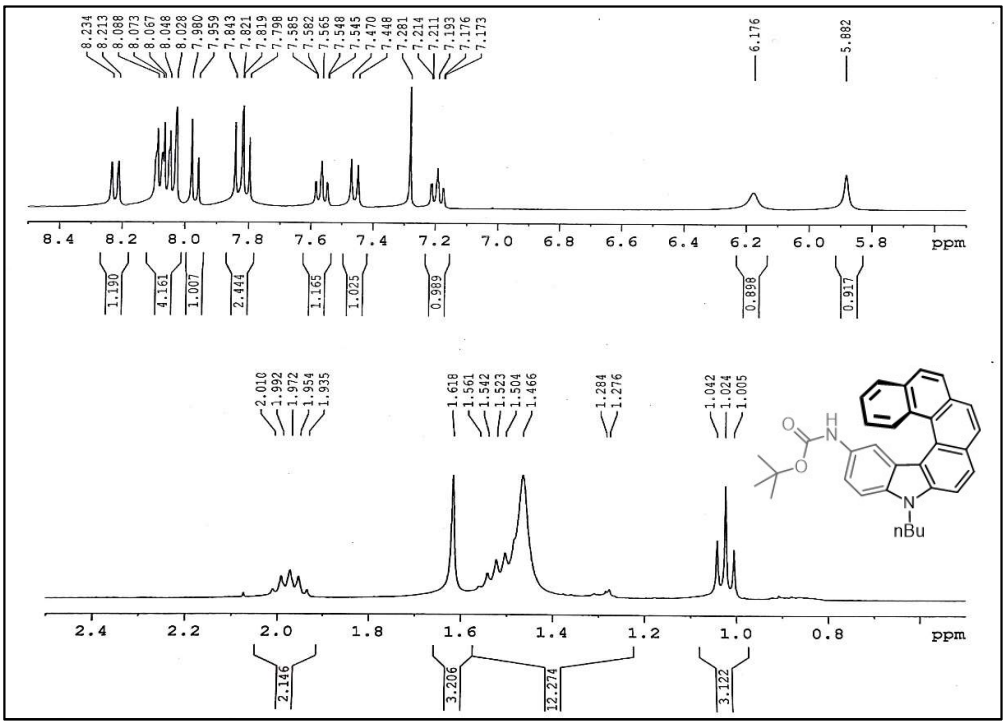

^{1}H NMR Spectrum of (*P*)-52 (enlarged aliphatic and aromatic region) ($CDCl_3$, 400 MHz)

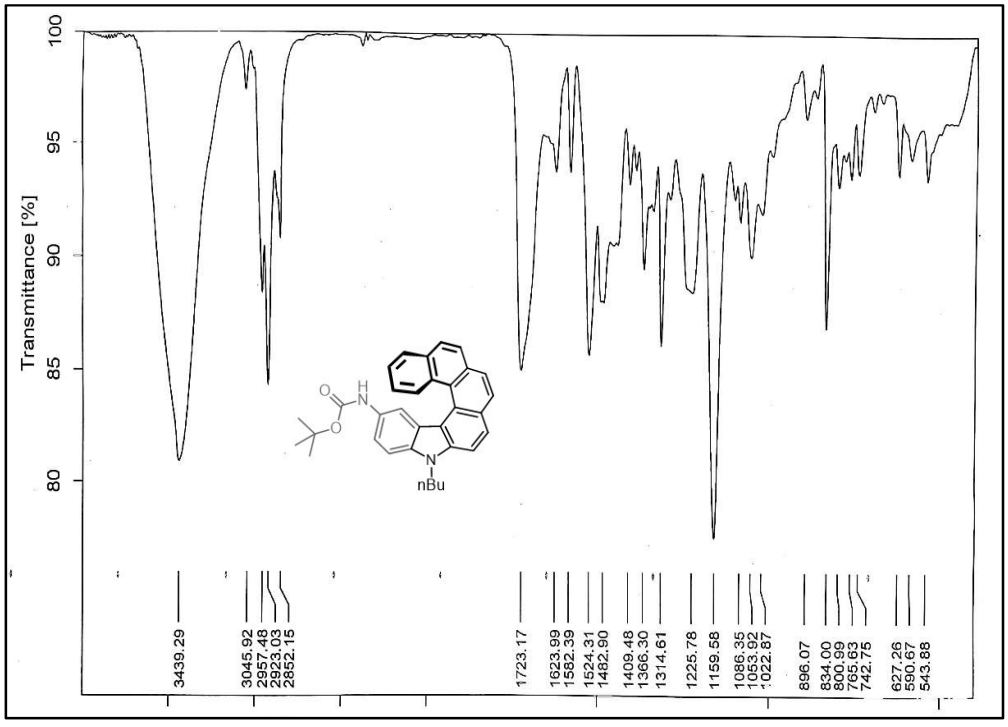

IR Spectrum of (*P*)-52

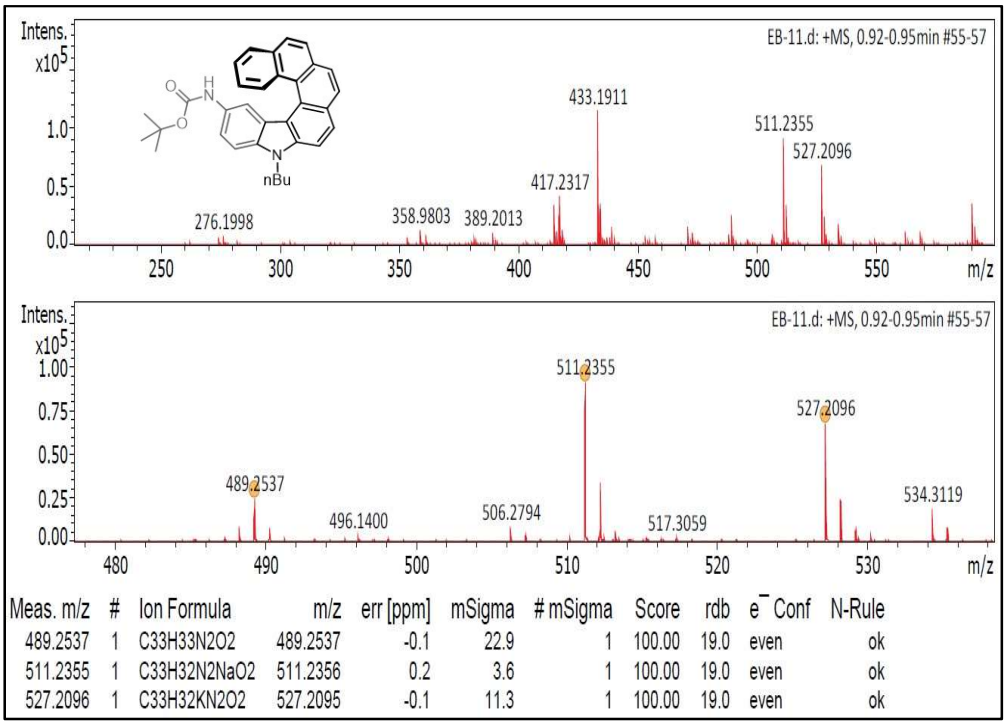

Meas. m/z	#	Ion Formula	m/z	err [ppm]	mSigma	# mSigma	Score	rdb	e⁻ Conf	N-Rule
489.2537	1	C33H33N2O2	489.2537	-0.1	22.9	1	100.00	19.0	even	ok
511.2355	1	C33H32N2NaO2	511.2356	0.2	3.6	1	100.00	19.0	even	ok
527.2096	1	C33H32KN2O2	527.2095	-0.1	11.3	1	100.00	19.0	even	ok

HRMS Spectrum of (*P*)-52

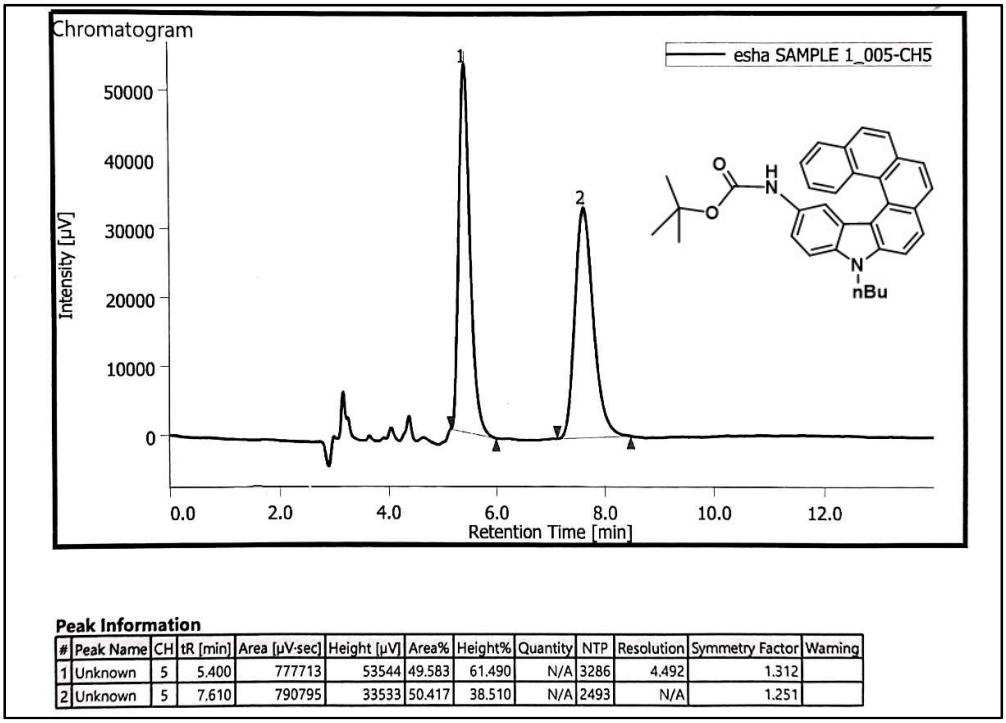

Peak Information

#	Peak Name	CH	tR [min]	Area [µV·sec]	Height [µV]	Area%	Height%	Quantity	NTP	Resolution	Symmetry Factor	Warning
1	Unknown	5	5.400	777713	53544	49.583	61.490	N/A	3286	4.492	1.312	
2	Unknown	5	7.610	790795	33533	50.417	38.510	N/A	2493	N/A	1.251	

HPLC chart of rac-52

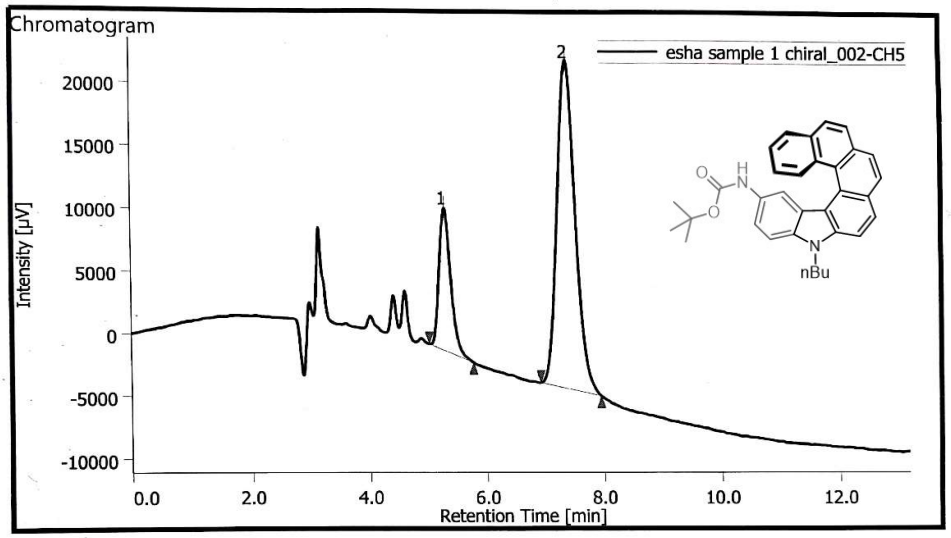

Peak Information

#	Peak Name	CH	tR [min]	Area [µV·sec]	Height [µV]	Area%	Height%	Quantity	NTP	Resolution	Symmetry Factor	Warning
1	Unknown	5	5.267	157403	11355	21.757	30.225	N/A	3447	4.507	1.304	
2	Unknown	5	7.343	566048	26213	78.243	69.775	N/A	2701	N/A	1.203	

HPLC chart of (*P*)-52

56% ee (Chiralcel OD-H; isopranol/n-hexane (30/70), 1.0 mL/min, UV 254 nm)

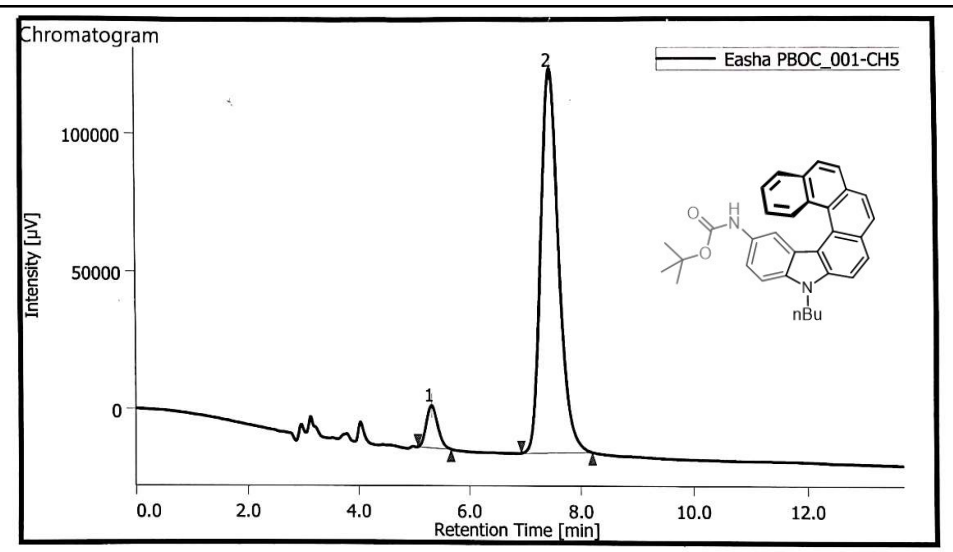

Peak Information

#	Peak Name	CH	tR [min]	Area [µV·sec]	Height [µV]	Area%	Height%	Quantity	NTP	Resolution	Symmetry Factor	Warning
1	Unknown	5	5.317	218938	15336	6.587	9.905	N/A	3144	4.460	1.163	
2	Unknown	5	7.440	3104739	139489	93.413	90.095	N/A	2675	N/A	1.238	

HPLC chart of (*P*)-52

87% ee (Chiralcel OD-H; isopranol/n-hexane (30/70), 1.0 mL/min, UV 254 nm)

2A.6 Crystallographic Data

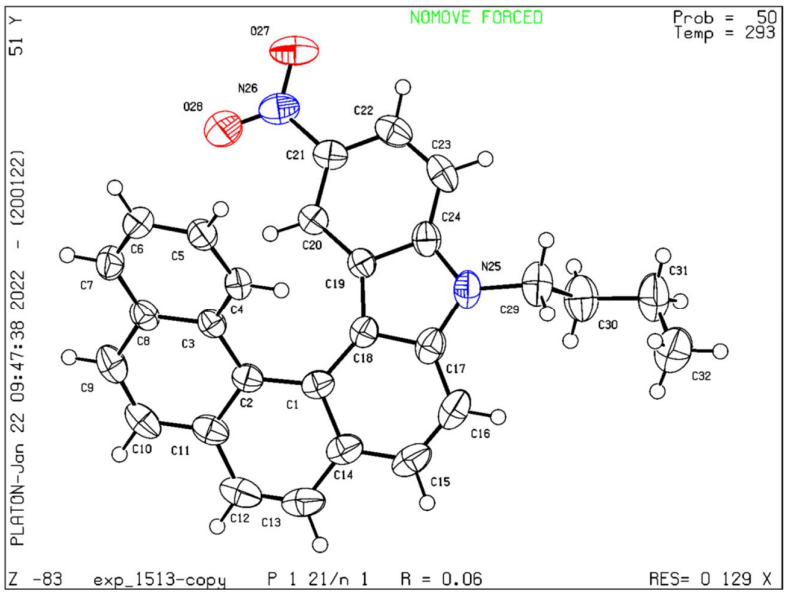

Crystal structure of 47 with an ellipsoid contour at the 50% probability level

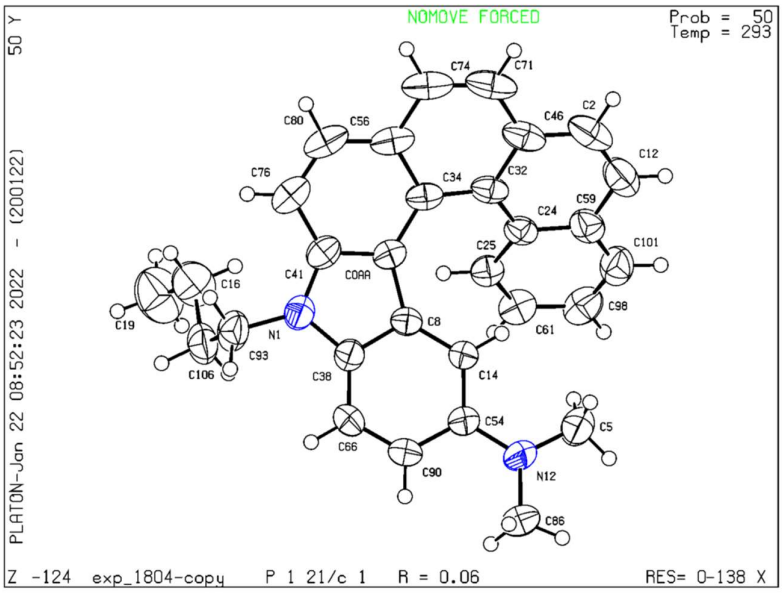

Crystal structure of 50 with an ellipsoid contour at the 50% probability level

	47	**50**
Identification code	exp_1513	exp_1804
Empirical formula	$C_{28}H_{22}N_2O_2$	$C_{30}H_{28}N_2$
Formula weight	418.47	416.54
Temperature/K	293(2)	293(2)
Crystal system	monoclinic	monoclinic
Space group	$P2_1/n$	$P2_1/c$
a/Å	8.2160(12)	9.9079(9)
b/Å	12.6855(13)	11.5192(10)
c/Å	20.018(2)	19.9425(16)
α/°	90	90
β/°	93.636(11)	97.942(8)
γ/°	90	90
Volume/Å^3	2082.1(4)	2254.2(3)
Z	4	4
ρ_{calc}g/cm^3	1.335	1.227
μ/mm^{-1}	0.085	0.071
F(000)	880.0	888.0
Crystal size/mm^3	0.96 × 0.7 × 0.56	0.59 × 0.56 × 0.53
Radiation	MoKα (λ = 0.71073)	MoKα (λ = 0.71073)
2Θ range for data collection/°	6.154 to 57.962	7.074 to 57.91
Index ranges	$-11 \le h \le 11$, $-11 \le k \le 15$, $-27 \le l \le 11$	$-13 \le h \le 12$, $-15 \le k \le 14$, $-25 \le l \le 26$
Reflections collected	8077	25122
Independent reflections	4627 [R_{int} = 0.0243, R_{sigma} = 0.0534]	5404 [R_{int} = 0.0378, R_{sigma} = 0.0358]
Data/restraints/parameters	4627/0/290	5404/0/292
Goodness-of-fit on F^2	1.032	1.025
Final R indexes [I>=2σ (I)]	R_1 = 0.0570, wR_2 = 0.1235	R_1 = 0.0576, wR_2 = 0.1296
Final R indexes [all data]	R_1 = 0.1029, wR_2 = 0.1478	R_1 = 0.1019, wR_2 = 0.1550
Largest diff. peak/hole / e Å^{-3}	0.30/-0.22	0.21/-0.22

Crystal data and structure refinement for 47 and 50

2A.7 References

1. Dhbaibi, K.; Favereau, L.; Crassous, J. Enantioenriched Helicenes and Helicenoids Containing Main-Group Elements (B, Si, N, P), *Chem. Rev.* **2019**, *119*, 8846.
2. Bazzini, C.; Brovelli, S.; Caronna, T.; Gambarotti, C.; Giannone, M.; Macchi, P.; Meinardi, F.; Mele, A.; Panzeri, W.; Recupero, F.; Sironi, A.; Tubino, R. Synthesis and Characterization of Some Aza[5]helicenes, *Eur. J. Org. Chem.* **2005**, *2005*, 1247.
3. Chercheja, S.; Klívar, J.; Jančařík, A.; Rybáček, J.; Salzl, S.; Tarábek, J.; Pospíšil, L.; Chocholoušová, J. V.; Vacek, J.; Pohl, R.; Císařová, I.; Starý, I.; Stará I. G. The Use of Cobalt-Mediated Cycloisomerisation of Ynedinitriles in the Synthesis of Pyridazinohelicenes, *Chem. Eur. J.* **2014**, *20*, 8477.
4. Waghray, D.; Zhang, J.; Jacobs, J.; Nulens, W.; Basarić, N.; Meervelt, L. V.; Dehaen, W. Synthesis and Structural Elucidation of Diversely Functionalized 5,10-Diaza[5]Helicenes, *J. Org. Chem*. **2012**, *77*, 10176.
5. Aloui, F.; El Abed, R.; Marinetti, A.; Ben Hassine, B. Synthesis and resolution of a new helically chiral azahelicene, *Tetrahedron Lett*. **2008**, *49*, 4092.
6. Howarth, J.; Finnegan, J. Synthesis of 9,10-dimethyl[7]helicene and 8,11-diaza[7]helicene, *Synth. Commun.* **1997**, *27*, 3663.
7. Murase, T.; Suto, T.; Suzuki, H. Azahelicenes from the oxidative photocyclization of boron hydroxamate complexes, *Chem. Asian J*. **2017**, *12*, 726.
8. Kos, M.; Žádný, J.; Storch, J.; Církva, V.; Cuřínová, P.; Sýkora, J.; Císařová, I.; Kuriakose, F.; Alabugin, I. V. Oxidative photocyclization of aromatic schiff bases in synthesis of phenanthridines and other aza-PAHs, *Int. J. Mol. Sci*. **2020**, *21*, 5868.
9. Fuchs, W.; Niszel, F. Über die Tautomerie der Phenole, IX.: Die Naphtho-carbazol-Bildung aus Naphtholen, *Ber. Dtsch. Chem. Ges. B* **1927**, *60*, 209.
10. Pischel, I.; Grimme, S.; Kotila, S.; Nieger, M.; Vögtle, F. A Configurationally Stable Pyrrolohelicene: Experimental and Theoretical Structure-Chiroptic Relationships, *Tetrahedron Asymmetry* **1996**, *7*, 109.
11. (a) Jančařík, A.; Rybáček, J.; Cocq, K.; Vacek Chocholoušová, J.; Vacek, J.; Pohl, R.; Bednárová, L.; Fiedler, P.; Císařová, I.; Stará, I. G.; Starý, I. Rapid access to dibenzohelicenes and their functionalized derivatives, *Angew. Chem. Int. Ed.* **2013**, *52*, 9970. (b) Teplý, F.; Stará, I. G.; Starý, I.; Kollárovič, A.; Šaman, D.; Rulíšek, L.; Fiedler, P. Synthesis of [5]-, [6]-, and [7]Helicene via Ni(0)- or Co(I)-Catalyzed Isomerization of Aromatic *cis*,*cis*-Dienetriynes, *J. Am. Chem. Soc*. **2002**, *124*, 9175.

12. Míšek, J.; Teplý, F.; Stará, I. G.; Tichý, M.; Šaman, D.; Císařová, I.; Vojtíšek, P.; Starý, I. A Straightforward Route to Helically Chiral N-Heteroaromatic Compounds: Practical Synthesis of Racemic 1,14-Diaza[5]helicene and Optically Pure 1- and 2-Aza[6]helicenes, *Angew. Chem. Int. Ed.* **2008**, *47*, 3188.

13. (a) Takenaka, N.; Sarangthem, R. S.; Captain, B. Helical Chiral Pyridine *N*-Oxides: A New Family of Asymmetric Catalysts, *Angew. Chem. Int. Ed*. **2008**, *47*, 9708. (b) Chen, J.; Takenaka, N. Helical Chiral Pyridine *N*-Oxides: A New Family of Asymmetric Catalysts, *Chem. Eur. J.* **2009**, *15*, 7268.

14. Weimar, M.; Correa da Costa, R.; Lee, F.-H.; Fuchter, M. J. A Scalable and Expedient Route to 1-Aza[6]helicene Derivatives and Its Subsequent Application to a Chiral-Relay Asymmetric Strategy, *Org. Lett*. **2013**, *15*,1706.

15. Nakano, K.; Hidehira, Y.; Takahashi, K.; Hiyama, T.; Nozaki, K. Stereospecific Synthesis of Hetero[7]helicenes by Pd-Catalyzed Double N-Arylation and Intramolecular O-Arylation, *Angew. Chem.Int. Ed.* **2005**, *44*, 7136.

16. Kötzner, L.; Webber, M. J.; Martínez, A.; De Fusco, C.; List, B. Asymmetric Catalysis on the Nanoscale: The Organocatalytic Approach to Helicenes, *Angew. Chem Int. Ed.* **2014**, *53*, 5202.

17. Chen, F.; Tanaka, T.; Mori, T.; Osuka, A. Synthesis, Structures, and Optical Properties of Azahelicene Derivatives and Unexpected Formation of Azahepta[8]circulenes, *Chem. Eur. J*. **2018**, *24*, 7489.

18. (a) Alkorta, I.; Blanco, F.; Elguero, J.; Schroder, D. Distinction between homochiral and heterochiral dimers of 1-aza[n]helicenes (n = 1-7) with alkaline cations, *Tetrahedron Asymmetry* **2010**, *21*, 962. (b) Bell, T. W.; Hext, N. M. Supramolecular optical chemosensors for organic analytes, *Chem. Soc. Rev*. **2004**, *33*, 589.

19. Karras, M.; Holec, J.; Bednárová, L.; Pohl, R.; Schmidt, B.; Stará, I. G.; Starý, I. Asymmetric Synthesis of Nonracemic 2-Amino[6]- helicenes and Their Self-Assembly into Langmuir Films, *J. Org. Chem*. **2018**, *83*, 5523.

20. van der Meijden, M. W.; Gelens, E.; Quirós, N. M.; Fuhr, J. D.; Gayone, J. E.; Ascolani, H.; Wurst, K.; Lingenfelder, M.; Kellogg, R. M. Synthesis, Properties, and Two-Dimensional Adsorption Characteristics of 5-Amino[6]hexahelicene, *Chem. Eur. J*. **2016**, *22*, 1484.

21. Balandina, T.; van der Meijden, M. W.; Ivasenko, O.; Cornil, D.; Cornil, J.; Lazzaroni, R.; Kellogg, R. M.; De Feyter, S. Self-Assembly of an Asymmetrically Functionalized [6]Helicene at Liquid/Solid Interfaces, *Chem. Commun*. **2013**, *49*, 2207.

22. Ascolani, H.; van der Meijden, M. W.; Cristina, L. J.; Gayone, J. E.; Kellogg, R. M.; Fuhr, J. D.; Lingenfelder, M. Van der Waals Interactions in the Self-Assembly of 5-Amino[6]Helicene on Cu(100) and Au(111), *Chem. Commun*. **2014**, *50*, 13907.

23. Hellou, N.; Mace, A.; Martin, C.; Dorcet, V.; Roisnel, T.; Jean, M.; Vanthuyne, N.; Berree, F.; Carboni, B.; Crassous, J. Synthesis of Carbo[6]helicene Derivatives Grafted with Amino or Aminoester Substituents from Enantiopure [6]Helicenyl Boronates, *J. Org. Chem*. **2018**, *83*, 484.

24. Xu, Y; Zhang, Y. X.; Sugiyama, H.; Umano, T.; Osuga, H.; Tanaka, K. (*P*)-helicene displays chiral selection in binding to Z-DNA, *J. Am. Chem. Soc.* **2004**, *126*, 6566.

25. Teplý, F.; Stará, I. G.; Starý, I.; Kollárovič, A.; Šaman, D.; Vyskočil, S.; Fiedler, P. Synthesis of 3-Hexahelicenol and Its Transformation to 3-Hexahelicenylamines, Diphenylphosphine, Methyl Carboxylate, and Dimethylthiocarbamate, *J. Org. Chem*. **2003**, *68*, 5193.

26. Okubo, H.; Nakano, D.; Anzai, S.; Yamaguchi, M. Synthesis of Symmetrical Polynitrohelicenes and Their Chiral Recognition in the Charge Transfer Complexation, *J. Org. Chem*. **2001**, *66*, 557.

27. Ichinose, W.; Miyagawa, M.; Ito, J.; Shigeno, M.; Amemiya, R.; Yamaguchi, M. Synthesis and Duplex Formation of the Reverse Amidohelicene Tetramer, *Tetrahedron* **2011**, *67*, 5477.

28. Delgado, I. H.; Pascal, S.; Wallabregue, A.; Duwald, R.; Besnard, C.; Guénée, L.; Nançoz, C.; Vauthey, E.; Tovar, R. C.; Lunkley, J. L.; Mullerd, G.; Lacour J. Functionalized cationic [4]helicenes with unique tuning of absorption, fluorescence and chiroptical properties up to the far-red range, *Chem. Sci.* **2016**, *7*, 4685.

29. Sánchez, I. G.; Šámal, M.; Nejedlý, J.; Karras, M.; Klívar, J.; Rybáček, J.; Buděšínský, M.; Bednárová, L.; Seidlerová, B.; Stará I. G.; Starý, I. Oxahelicene NHC ligands in the asymmetric synthesis of nonracemic helicenes, *Chem. Commun*. **2017**, *53*, 4370.

30. Zhao, T.; Liu, Z.; Song, Y.; Xu, W.; Zhang, D.; Zhu, D. Novel Diethynylcarbazole Macrocycles: Synthesis and Optoelectronic Properties, *J. Org. Chem*. **2006**, *71*, 7422.

31. (a) Laarhovan, W.H. Photochemical cyclizations and intramolecular cycloadditions of conjugated arylolefins: Part 2: Photocyclizations without dehydrogenation and photocycloadditions, *Recl. Trav. Chim. Pays-Bas* **1983**, *102*, 241. (b) Newman, M. S.; Wolf, M. A New Synthesis of Benzo(c)phenanthrene: 1,12-Dimethylbenzo(c)phenanthrene, *J. Am. Chem. Soc.* **1952**, *74*, 3225. (c) Liu, L.; Yang, B.; Katz, T. J.; Poindexter, M. K. Improved methodolgy for photocyclization reactions,

J. Org. Chem. **1991**, *56*, 3769.

32. Talele, H. R.; Gohil, M. J.; Bedekar, A. V. Synthesis of Derivatives of Phenanthrene and Helicene by Improved Procedures of Photocyclization of Stilbenes, *Bull. Chem. Soc. Jpn.* **2009**, *82*, 1182.
33. Upadhyay, G. M.; Talele, H. R.; Bedekar, A. V. Synthesis and Photophysical Properties of Aza[n]helicenes, *J. Org. Chem.* **2016**, *81*, 7751.
34. Laarhoven, W. H.; Cuppen, J. H. M.; Nivard, R. J. F. Photodehydrocyclizations in stilbene-like compounds—III : Effect of steric factors, *Tetrahedron* **1970**, *26*, 4865.
35. Mallory, F. B.; Mallory, C. W. *Organic Reactions; Wiley: New York* **1984**; *30*, 49.
36. Roose, J.; Achermann, S.; Dumele, O.; Diederich, F. Electronically Connected [*n*]Helicenes: Synthesis and Chiroptical Properties of Enantiomerically Pure (*E*)-1,2-Di([6]helicen-2-yl)ethenes, *Eur. J. Org. Chem.* **2013**, 3223.
37. Dreher, S. D.; Weix, D. J.; Katz, T. J. Easy Synthesis of Functionalized Hetero[7]helicenes, *J. Org. Chem.* **1999**, *64*, 3671.
38. (a) Ramesh, C. Iron-Acetic Acid: A Versatile Reductive Cyclizing Agent, *Synlett* **2011**, 587-588. (b) Nose, A.; Kudo, T. Reduction with Sodium Borohydride-Transition Metal Salt Systems. I. Reduction of Aromatic Nitro Compounds with the Sodium Borohydride-Nickelous Chloride System *Chem. Pharm. Bull.* **1981**, *29*, 1159. (c) Mallick, T.; Karmakar, A.; Mandal, D.; Pramanik, A.; Sarkar, P.; Begum, N. A. Harnessing carbazole based small molecules for the synthesis of the fluorescent gold nanoparticles: A unified experimental and theoretical approach to understand the mechanism of synthesis, *Colloids Surf. B* **2018**, *172*, 440.
39. Gidley, M. J.; Sanders, J. K. M. Reductive methylation of proteins with sodium cyanoborohydride. Identification, suppression and possible uses of N-cyanomethyl by-products, *Biochem. J.* **1982**, *203*, 331-334.
40. Westley, J. W.; Halpern, B. Use of (-)-menthyl chloroformate in the optical analysis of asymmetric amino and hydroxyl compounds by gas chromatography, *J. Org. Chem*. **1968**, *33*, 3978.
41. (a) Shahabuddin, M.; Hossain, Md. S.; Kimura, T.; Karikomi, M. Diastereomeric process-based chiral resolution of helical quinone derivatives using (−)-menthyl chloroformate, *Tetrahedron Lett*. **2017**, *58*, 4491. (b) Tsukamoto, T.; Sasahara, R.; Muranaka, A.; Miura, Y.; Suzuki, Y.; Kimura, M.; Miyagawa, S.; Kawasaki, T.; Kobayashi, N.; Uchiyama, M.; Tokunaga, Y. Synthesis of a Chiral [2]Rotaxane: Induction of a Helical Structure through Double Threading, *Org. Lett*. **2018**, *20*, 4745.

(c) Upadhyay, G. M.; Mande, H. M.; Pithadia, D. K.; Maradiya, R. H.; Bedekar, A. V. Effect of the Position of the Cyano Group on Molecular Recognition, Supramolecular Superhelix Architecture, and Spontaneous Resolution of Aza[7]helicenes, *Cryst. Growth Des*. **2019**, *19*, 5354. (d) Sundar, M. S.; Klepetářová, B.; Bednárová L.; Muller, G. Synthesis, Chiral Resolution, and Optical Properties of 2,18-Dihydoxy-5,10,15-trioxa[9]helicene, *Eur. J. Org. Chem*. **2021**, 146.

42. Jacquemard, U.; Bénéteau, V.; Lefoix, M.; Routier, S.; Mérour, J. Y.; Coudert, G. Mild and selective deprotection of carbamates with Bu_4NF, *Tetrahedron* **2004**, *60*, 10039.
43. (a) Almallah, H.; Nos, M.; Ayzac, V.; Brenner, E.; Matt, D.; Gourlaouen, C.; Jahjah M. Complexes featuring N-heterocyclic carbenes with bowl-shaped wingtips, *C. R. Chim.* **2019**, *22*, 299. (b) Noshita, M.; Shimizu, Y.; Morimoto, H.; Ohshima, T. Diethylenetriamine-Mediated Direct Cleavage of Unactivated Carbamates and Ureas, *Org. Lett*. **2016**, *18*, 6062. (c) Li, B.; Berliner, M.; Buzon, R.; Chiu, C. K.-F.; Colgan, S.T.; Kaneko, T.; Keene, N.; Kissel, W.; Le, T.; Leeman, K. R.; Marquez, B.; Morris, R.; Newell, L.; Wunderwald, S.; Witt, M.; Weaver, J.; Zhang, Z.; Zhang, Z. Aqueous Phosphoric Acid as a Mild Reagent for Deprotection of *tert*-Butyl Carbamates, Esters, and Ethers, *J. Org. Chem.* **2006**, *71*, 9045.
44. Xu, T. H.; Lu, R.; Tan, C. H.; Qiu, X. P.; Bao, C. V.; Liu, X.L.; Xue, P. C.; Zhao, Y. Y. Synthesis and Characterization of Carbazole-Based Dendrimers with Porphyrin Cores, *Eur. J. Org. Chem.* **2006**, *17*, 4014.
45. Li, K.; Xue, P.; Shen, Y.; Liu, J. Ultrasound- and protonation-induced gelation of a carbazole-substituted divinylquinoxaline derivative with short alkyl chain, *Dyes Pigm*. **2018**, *151*, 279.
46. Waykole, L.;Rashad, M.; Palermo, S.; Repic, O.; Blacklock, T. *J*. Selective Benzylic Bromination of 2-Methylnaphthalene, *Synth. Commun.* **1997**, *27*, 2159.
47. Hua, W.; Liu, Z.; Duan, L.; Dong, G.; Qiu, Y.; Zhang, B.; Cui, D.; Tao, X.; Cheng, N.; Liu, Y. Deep-blue electroluminescence from nondoped and doped organic light-emitting diodes (OLEDs) based on a new monoaza[6]helicene, *RSC Adv*. **2015**, *5*, 75.

CHAPTER – 2B

Accessing optically pure dimethylaza[7]helicene via hydrogenative deprotection of chiral helical diamines

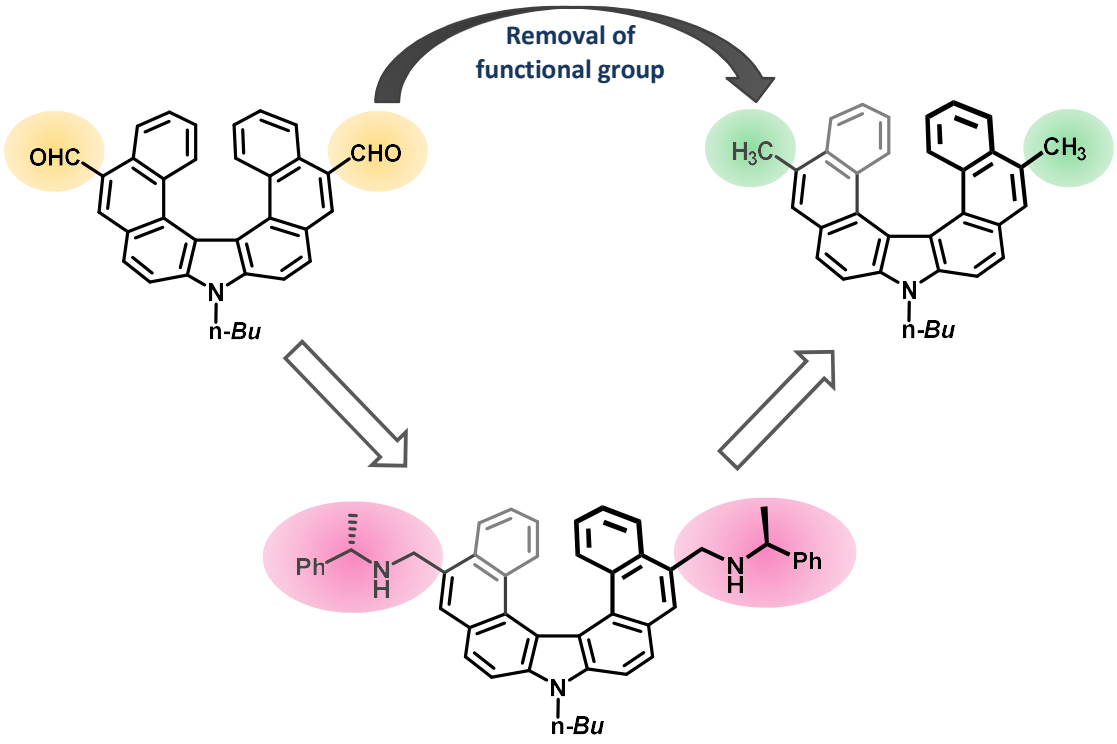

Table of Contents

2B.1 Introduction

Looking at the potential applications of chiral helical molecules in various fields including medicinal chemistry, material science and asymmetric synthesis, it becomes important to separate the enantiomers, which is a big challenge in helicene chemistry. In order to separate the enantiomers, helicenes should be of higher order, as smaller helicenes have a tendency to racemize easily because of reduced steric crowding.

2B.1.1 Methods to obtain optically pure helicene

Several methods have been reported in the literature for resolution of helicenes. One of the widely used methods is separation on chiral HPLC, with different chiral stationary phases to obtain optically pure helicenes from a racemic mixture.[1] The chiral stationary phases used in these method are modified silica prepared by the addition of tetranitro-9-fluorenylidene-aminooxy, substituted organic acids, cellulose or amylose derivatives.[2] This method is sensitive and precise, it has various drawbacks: a continuous need for new chiral stationary phases as certain stationary phases are selective towards the recognition of specific helicenes. Also, the use of expensive chiral columns which makes it less cost effective for separation of sample at higher quantity. Capillary Electrophoresis is another analytical tool which is frequently used for the separation of the enantiomers of helicenes.[3] This method is highly sensitive even towards very minor changes in pH, due to which this technique is not much preferred. Helicenes are good p-donors and can form charge transfer complexes, this concept was first used by Newmann and Lednicer for the resolution of racemic hexahelicene. Electron deficient (–)-TAPA was used to prepare separable charge transfer complexes with the non-functionalized hexahelicene (**Figure 2B.1**).[4]

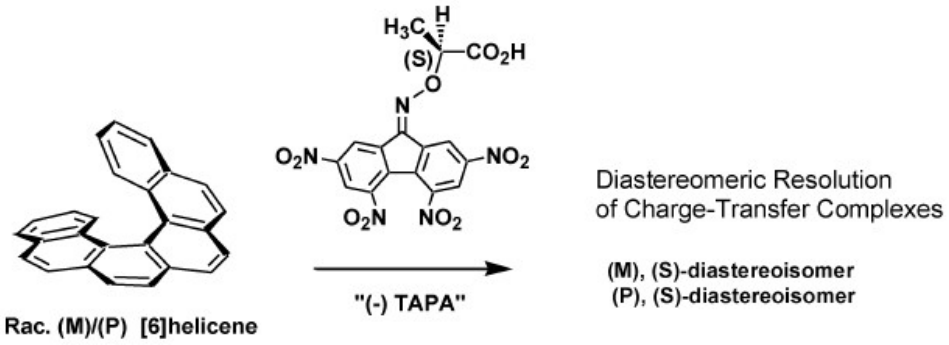

***Figure 2B.1**: Resolution of hexahelicene by formation of charge transfer complex*

Asymmetric synthesis is another technique where stereochemical control is used to access non-racemic products or sometimes a single enantiomer without the need for further resolution. Kagan in 1971 reported the first asymmetric synthesis of helical molecules. A hexahelicene was synthesized in enantio-enriched form with 20 % ee by the use of circularly polarized light (**Scheme 2B.1**).[5]

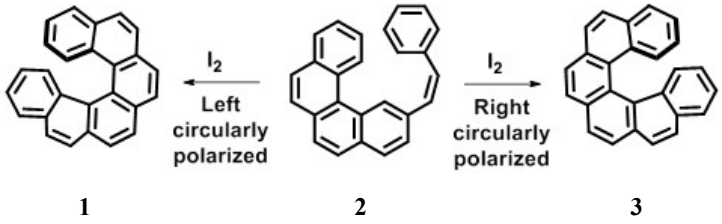

***Scheme 2B.1**: Asymmetric synthesis of hexahelicene using circularly polarized light*

Other examples for asymmetric synthesis of helicenes: Katz methodology for enantioselective synthesis of helical quinones by using Diels-Alder approach,[6] diastereoselective oxy-Cope rearrangement,[7] and the use of chiral phosphine ligands in the palladium catalyzed cyclization reactions[8]. Stará, Starý and co-workers reported the first metal induced enantioselective synthesis of helicene. Here, the cycloisomerization of triyne was carried out with the help of Ni^0 catalyst and a chiral binaphthyl-derived phosphine ligand as a chiral inducer. This enantioselective cyclization afforded 40% ee of (+)-**5** (**Scheme 2B.2**).[9]

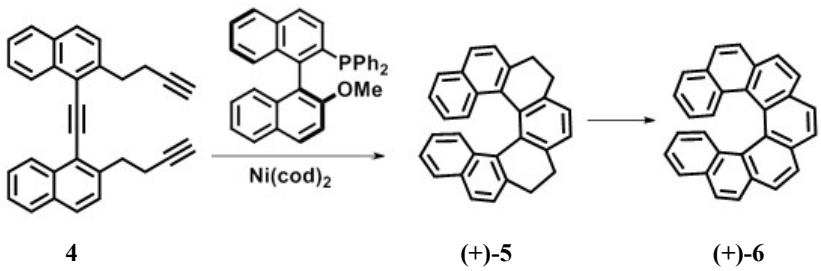

***Scheme 2B.2**: Ni-catalyzed enatioselective synthesis of heptahelicene*

Sako and co-workers reported the use of BINOL-based chiral vanadium complex **7** in the synthesis of oxa[9]helicene **9** in 94% ee from polycyclic phenols. The reaction involves two steps including oxidative coupling, followed by intramolecular cyclization (**Scheme 2B.3**).[10]

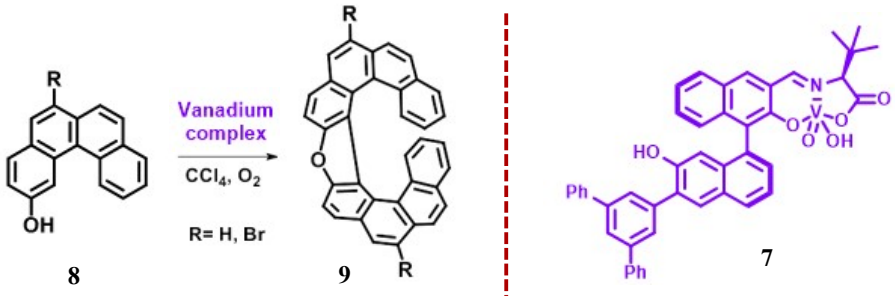

***Scheme 2B.3**: BINOL-Vanadium complex catalyzed asymmetric synthesis of 9*

Spontaneous resolution is also one such phenomena which results in separation of enantiomers by crystallization of the racemic sample.[11] This is relatively a rare phenomena as it works only when a molecule is capable of forming ordered association based on mutual recognition, which may then result in conglomerate formation, effecting in spontaneous resolution. In case of functionalized helicenes, the more frequently used methods for the resolution involves diastereomeric salt formation with chiral reagents,[12] chromatographic separation of diastereomers[13] or enzymatic resolution.[14]

The conventional method of resolution involves the use of chiral auxiliary for the formation of diastereomers. The chiral auxiliary can be regenerated after the separation of diastereomers and can be cleaved using mild conditions which will leave the helicene with the functional group intact.[15] This process can be carried out at an early stage before the construction of helical framework, where a chirally resolved intermediate can be converted to its helicene derivative without any loss of stereochemistry in the process involved, or the resolution of helicene can be carried out after its synthesis.[15] The use of chiral auxiliaries such as (*R*)-menthyl chloroformate,[16] (*S*)-α-methylbenzylamine,[15a,17] (*S*)-camphanic acid,[18] some derivatives of amino acids,[19] etc. for the formation of physically separable diastereomers has been reported in the literature.

For the substituted helicenes bearing free –OH or –COOH group, the use of chiral auxiliaries which can convert them into diastereomeric esters or carbonates or amides have been reported. One such example was shown by Karnik and co-workers. A selective mono esterification of dioxa[6]helicene diol **10** was carried out using chiral (1*S*)-camphor sulphonyl chloride in acetone to obtain diastereomers **11** which were separated with the help of chiral HPLC (**Scheme 2B.4**).[20]

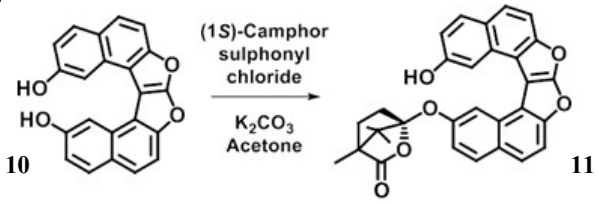

***Scheme 2B.4**: Resolution of dioxa[6]helicene using camphor sulphonyl chloride*

Karikomi and co-workers reported the use of optically pure (*R*)-menthyl chloroformate to resolve the atropisomeric biaryl diol (**Scheme 2B.5**).[16b] The diastereomeric carbonates formed were separated using HPLC, which on mild hydrolysis lead to the pure enantiomers of biaryl diol.

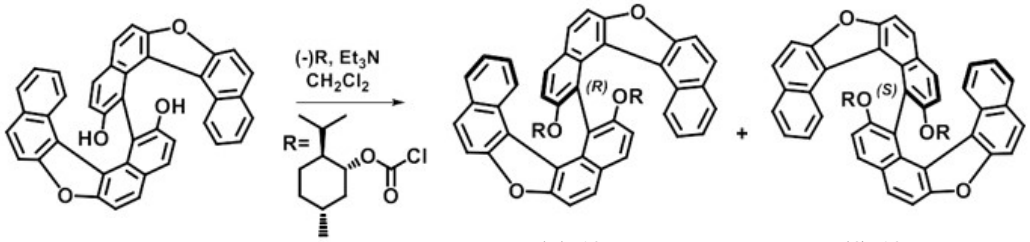

12 (*R*)-**13** (*S*)-**13**

***Scheme 2B.5**: Use of menthyl chloroformate as a chiral resolving agent*

In our earlier work described in Chapter-2A, helicene possessing free amino group was converted to diastereomeric carbamate by the use of (*R*)-menthyl chloroformate as a chiral resolving agent.[16a] In all these cases, detaching a chiral auxiliary after the separartion of diastereomers, may yield the helicene with the functional group intact. The helicenes possessing free halogen group can be converted to diastereomeric amines by subjecting it to Buchwald-Hartwig amination with (*S*)-α-methylbenzylamine. Dehaen and co-workers used this approach to resolve the chloro substituted aza[6]helicene derivative (**Scheme 2B.6**). The diastereomers obtained, were readily separated by using column chromatography.[21]

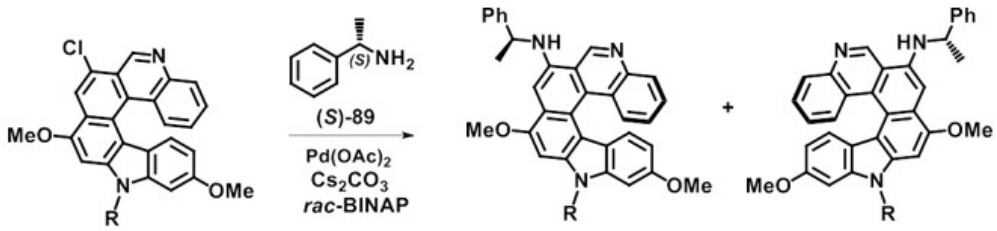

14 **15** **16**

***Scheme 2B.6**: Use of (S)-phenyl ethyl amine as a chiral resolving agent*

However, accessing optically pure isomers of helicenes without any functional group is a daunting task, as by detaching any chiral auxiliary, optically pure helicenes are obtained with original functional group intact. In the chapter we discuss our efforts to synthesize methyl substituted helicene in enantiomerically pure form, where the operation of attachment and removal of chiral auxiliary results in overall transformation of a formyl group to an alkyl moiety.

2B.2 Results and Discussion

The introduction of methyl group on the helical moiety can be achieved by choosing methyl substituted starting material at an early stage of the synthesis.[22] The presence of methyl group makes the separation of the isomers difficult, as it cannot act as a handle for the formation of diastereomers. In the present approach we shall endeavor to achieve the introduction of methyl group by cleavage of chiral auxiliary, and obtain the helicene in optically pure form. The retrosynthetic plan for this approach is as shown in **Figure 2B.2**, where we begin to build the symmetrical 5,13-diformyl-9-aza[7]helicene **17**, as the aldehyde group can assist in the formation of diastereomers with some chiral auxiliary.

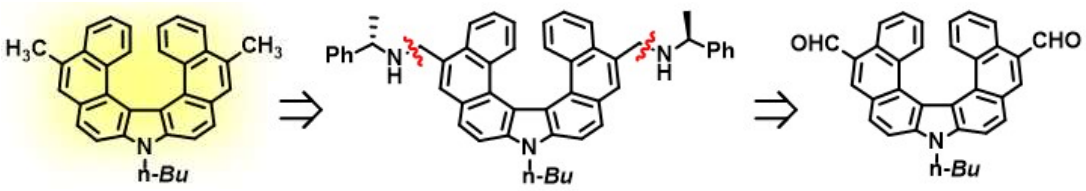

Target molecule

***Figure 2B.2**: Retrosynthetic analysis of dimethylaza[7]helicene*

2B.2.1 Synthesis of 5,13-diformyl-aza[7]helicene

Two different approaches were used for the formation of the helicene **17**.

2B.2.1.1 Approach-1: By formylation of aza[7]helicene

The first approach involved the Vilsmeier-Haack formylation reaction of 9-butyl-9-aza[7]helicene **18**. Here, the starting material **18** was synthesized by a series of steps starting from the iodination of carbazole to obtain 3,6-diiodo-9-butyl-9*H*-carbazole **20**, which was further subjected to *N*-butylation.[23] This 3,6-diiodo-*N*-butylcarbazole **21** was subjected to double Heck olefination reaction with styrene to obtain corresponding 3,6-distyryl-9-butyl-9*H*-carbazole **22** in excellent yields. Oxidative photocyclization of the bis-styryl derivative **22** was carried out in toluene under 125W high pressure mercury vapor lamp, stoichiometric amount of iodine and THF.[24] This resulted in the formation of the desired helicene **18** as a major double angular cyclized product, which was isolated by silica gel column chromatography. (**Scheme 2B.7**).

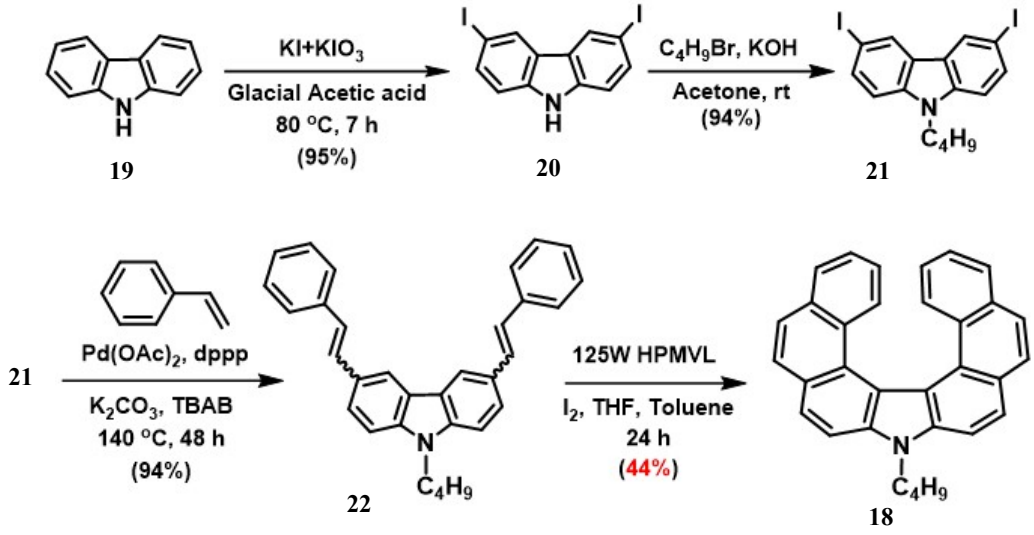

***Scheme 2B.7**: Synthesis of 9-butyl-9H-aza[7]helicene*

Further helicene **18** was subjected to the standard conditions of Vilsmeier-Haack formylation using phosphoryl chloride in DMF[22] (**Scheme 2B.8**). The reaction was monitored by TLC, where a complete disappearance of starting material was observed and formation of multiple new spots were seen.

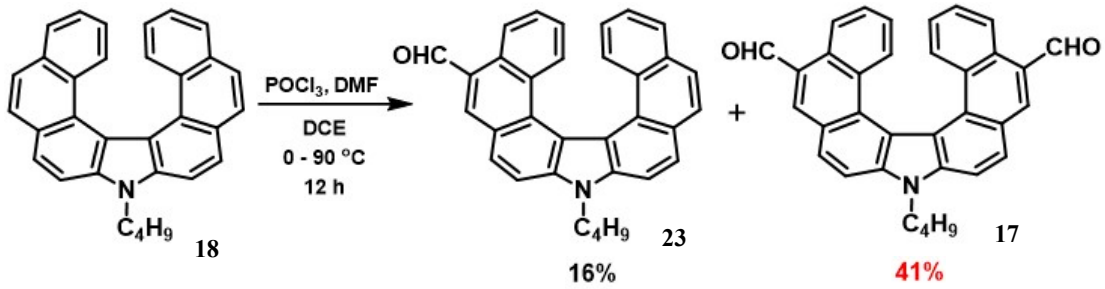

***Scheme 2B.8**: Vilsmeier-Haack formylation of 9-butyl-9H-aza[7]helicene*

The careful column chromatography led to the isolation of two major spots, which were further analyzed by ^{1}H NMR. The ^{1}H NMR of the non-polar compound, showed the presence of number of signals in the aromatic region indicating its unsymmetrical nature. This indicated that the formylation may have occurred at only one position, also the yield of this mono formyl derivative **23** (minor product) was quite low. The polar and major product was the desired diformyl derivative **17** was confirmed by the presence of a much lesser number of signals in the aromatic region of its ^{1}H NMR, as the molecule is symmetrical. The lower yield of **18** during the photocylization step and that of **17** during formylation, were the major limitations of this approach.

2B.2.1.2 *Approach-2: By reduction of 5,13-dicyano-aza[7]helicene*

Another approach was then explored for the synthesis of 5,13-diformyl-9-aza[7]helicene **17** via reduction of 5,13-dicyano-9-aza[7]helicene **24**. The synthesis of dicyano derivative **24** was achieved starting from the formylation of *N*-butylcarbazole to obtain the corresponding diformyl derivative **26** which on Knoevenagel condensation with benzyl cyanide afforded the bis-styryl derivative **27**. Conversion of **27** to the dicyano helicene **24** was done by oxidative photocyclization, where a double, regioselective angular-angular cyclization occurred to afford the **24** in good yield (**Scheme 2B.9**).[11b]

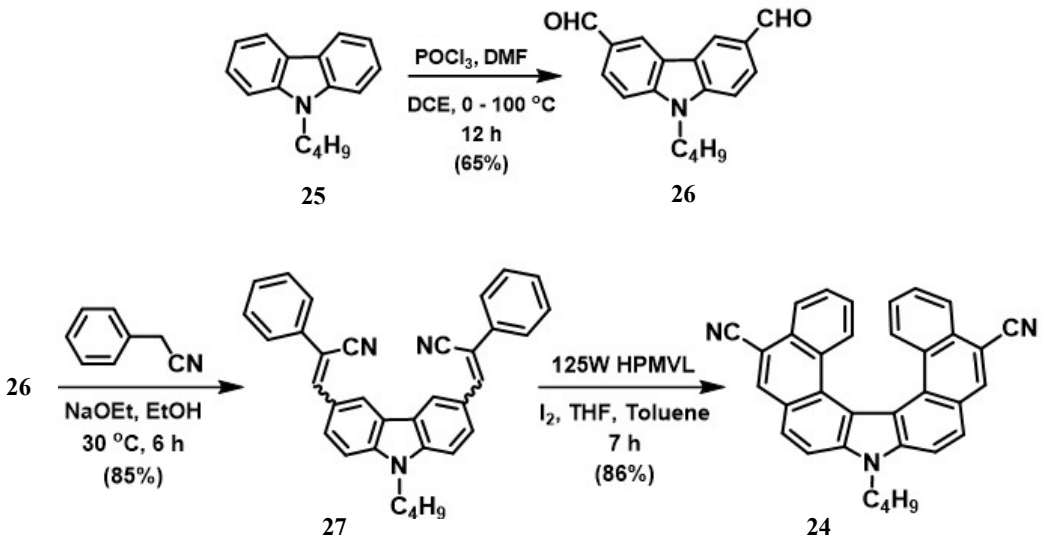

***Scheme 2B.9**: Synthesis of 5,13-dicyano-9-butyl-9H-aza[7]helicene*

The dicyano helicene **24** was selectively reduced to the corresponding diformyl helicene **17** using the known reducing agent diisobutylaluminium hydride in toluene (**Scheme 2B.10**).[23] The reaction was clean and the desired diformyl helicene **17** was obtained in good yield. Appearance of a singlet at 10.53 ppm in a ^{1}H NMR indicated the formation of helicene **17**.

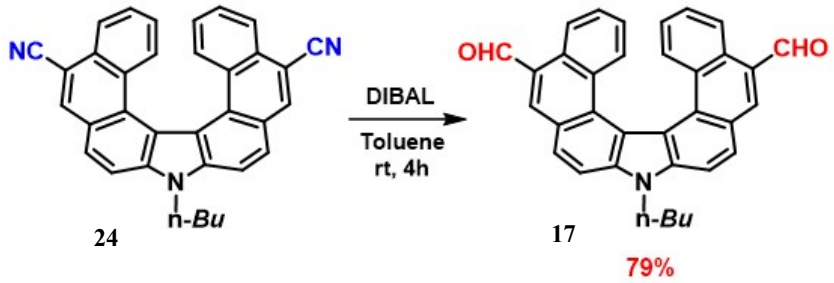

***Scheme 2B.10**: Reduction of 5,13-dicyano-9-butyl-9H-aza[7]helicene*

2B.2.2 *X-ray Structure Analysis of compound 17*

A good quality crystal of compound **17** was obtained in a mixture of dichloroethane in hexane (70%) and the position of the formyl groups in the structure was confirmed by single crystal X-ray diffraction analysis. The ORTEP plot of compound **17** is as shown in **Figure 2B.3 (A)**. The crystal appeared in the Pbca space group, where the unit cell consisted of eight molecules, with equal numbers of *P* and *M* isomers, indicating it to be racemic sample (**Figure 2B.4 (A)**). As expected for the helical structure, the inside carbon-carbon bond lengths were elongated (1.413-1.460 Å) and the outer bonds were compressed (1.362-1.379 Å) compared to the average bond of benzene (1.39 Å). The overall distortion of the molecular structure was found to be 53.21°, indicating good rigidity of the isomers and the dihedral angle was measured to be 34.84° (**Figure 2B.3**). A Cl···H interaction was also observed where Cl atom present in the solvent molecule played a role (**Figure 2B.4 (B)**).

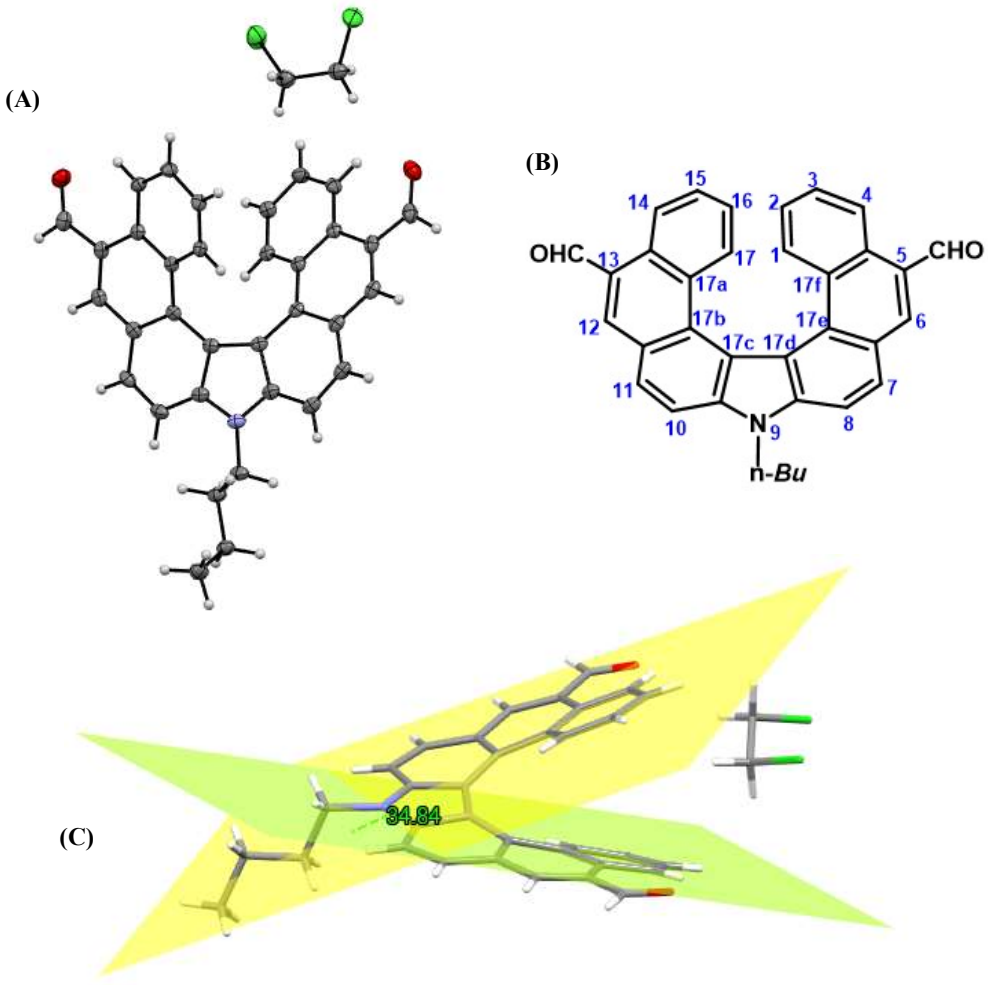

***Figure 2B.3**: (A) ORTEP plot of compound 47 CCDC 2256791 (B) Molecular structure and numbering scheme for 17 (C) figure showing interplanar angle*

Inner carbon-carbon bond length (Å)	
C17c-C17d	1.460
C17d-C17e	1.438
C17e-C17f	1.456
C17f-C1	1.413
Outer carbon-carbon bond length (Å)	
C3-C4	1.379
C5-C6	1.368
C7-C8	1.362
Torsion angle (°)	
φ1 = C17-C17a-C17b-C17c	16.96
φ2 = C17a-C17b-C17c-C17d	14.22
φ3 = C17b-C17c-C17d-C17e	22.03
Distortion of the molecular structure (°)	
φ1 + φ2 + φ3	53.21
Dihedral angle (°)	
θ	34.84

***Table 2B.1**: Crystallographic properties of compound 17*

(A)

(B)

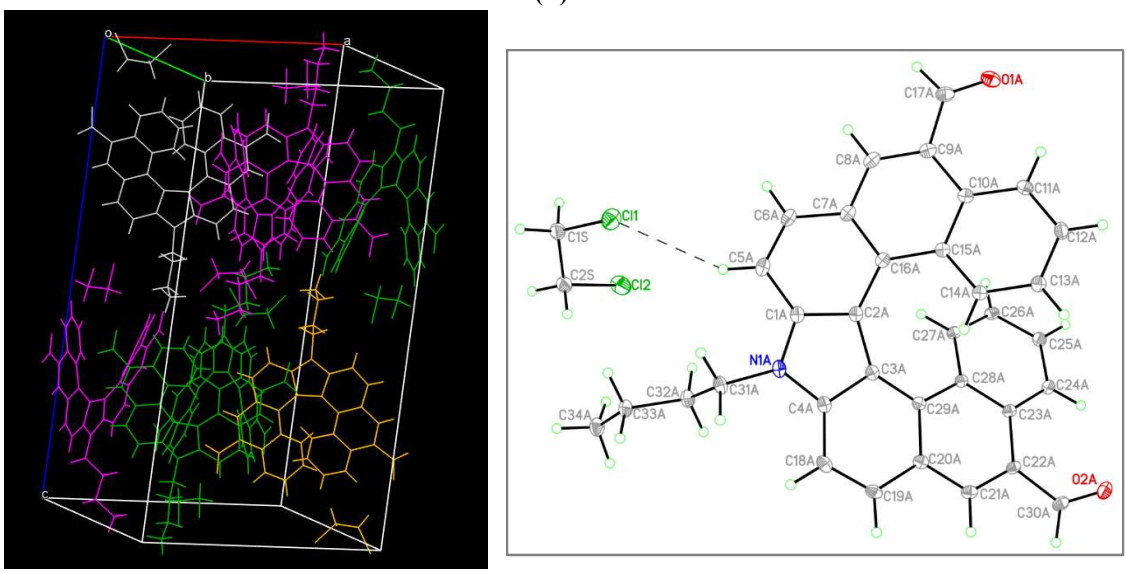

***Figure 2B.4**: (A) Crystal packing in a unit cell (B) figure displaying Cl···H interaction*

2B.2.3 Synthesis of chiral helical diamines

The objective of the present study is to obtain optically pure helicene with methyl substituents placed at the symmetrical positions. With this aim we converted the diformyl helicene **17** to diastereomeric diamine by attaching a chiral auxiliary. Initially we attempted to synthesize the diastereomeric helical diamines (±)-**28** by using the conventional method of refluxing diformyl helicene **17** with (*S*)-(-)-α-methylbenzylamine in presence of acid catalyst using Dean-Stark apparatus (**Scheme 2B.11**). But this resulted in no appreciable conversion of the starting material.

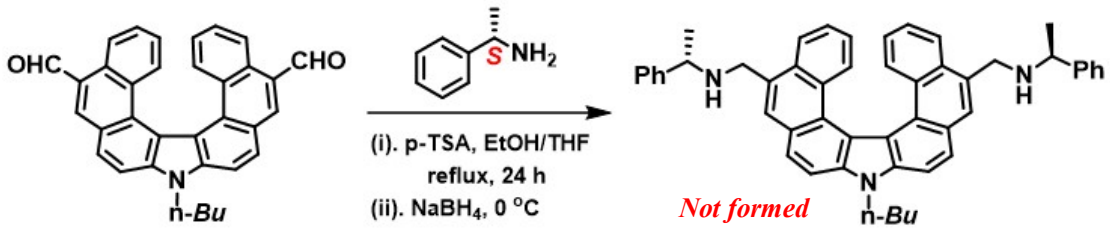

17 **28**

Scheme 2B.11: *Conventional method of reductive amination*

Another method of reductive amination was employed, where diformyl helicene **17** was reacted with the chiral auxiliary (*S*)-(-)-α-methylbenzylamine in presence of titanium(IV)isopropoxide and sodium borohydride[26] (**Scheme 2B.12**). Here, a diastereomeric mixture of helical diamines (±)-**28** was obtained in a good combined yield (88%).

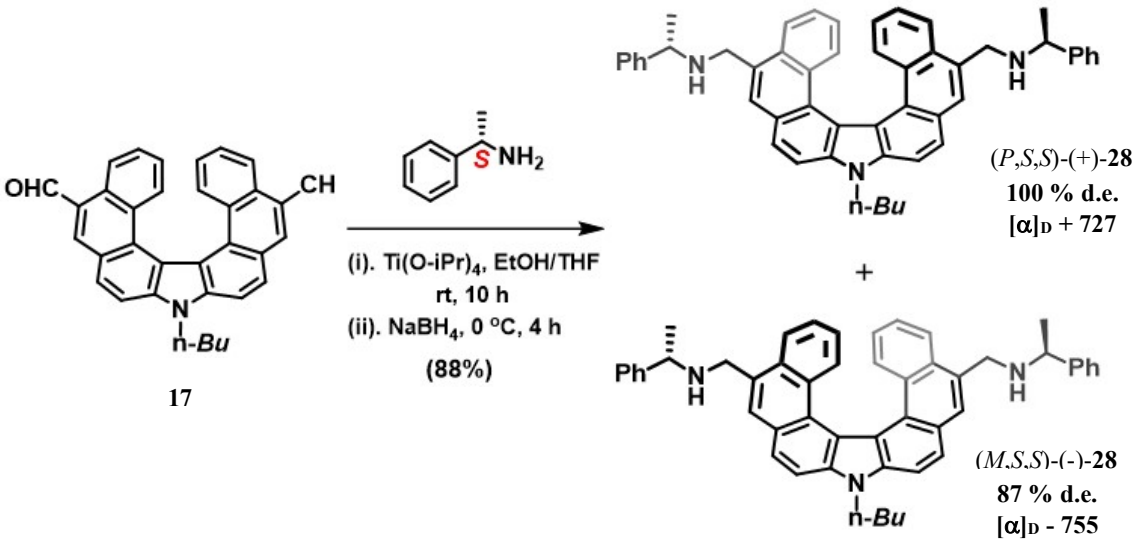

17

Scheme 2B.12: *Synthesis of diastereomeric amine via reductive amination*

The ^{1}H NMR of the crude mixture indicated that both the diastereomers were present in nearly same proportion (based on the values of integration of the marked protons) (**Figure 2B.5**).

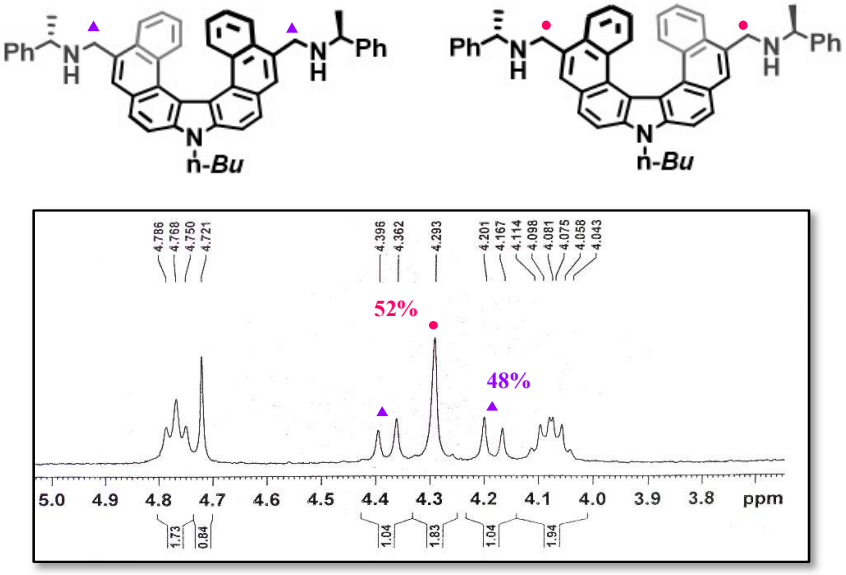

***Figure 2B.5**: ^{1}H NMR spectrum of mixture of diastereomers 28 (enlarged portion of aliphatic region)*

The ratio of the diastereomers was also confirmed by subjecting the mixture to HPLC analysis on chiral stationary phase (CHIRALPAK IC column). The diastereomers were physically separated by column chromatography over alumina. The first eluted isomer showed positive optical rotation, which was designated as the *P* isomer. The separated isomers were further analyzed by HPLC analysis (**Figure 2B.6**).

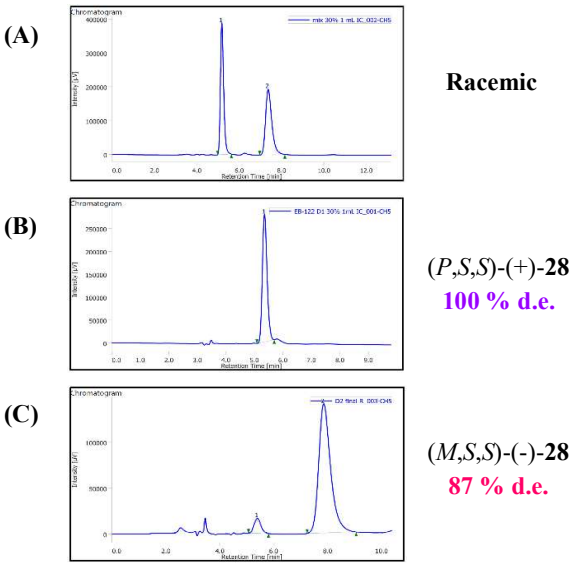

***Figure 2B.6**: HPLC chromatograms of (A) mixture of diastereomers; (B) (P)-28; (C) (M)-28*

HPLC Conditions: Chiral Column: CHIRALPAK IC Column,
Solvent System: Hexane: IPA(70:30), Flow rate: 1.0 mL/min

The separated diastereomers were further analyzed by ^{1}H NMR. It was observed that the signals specific to the helical moiety as well as the α-methylbenzylamine group were present. There was one marked difference between the ^{1}H NMR of the two isomers. The methylene protons next to NH should split into two doublets as they are diastereotopic in nature. In one of the isomers, these protons appeared as two well separated doublets at 4.38 and 4.19 ppm, whereas in the other isomer a merged doublet appeared at 4.29 ppm (**Figure 2B.7**).

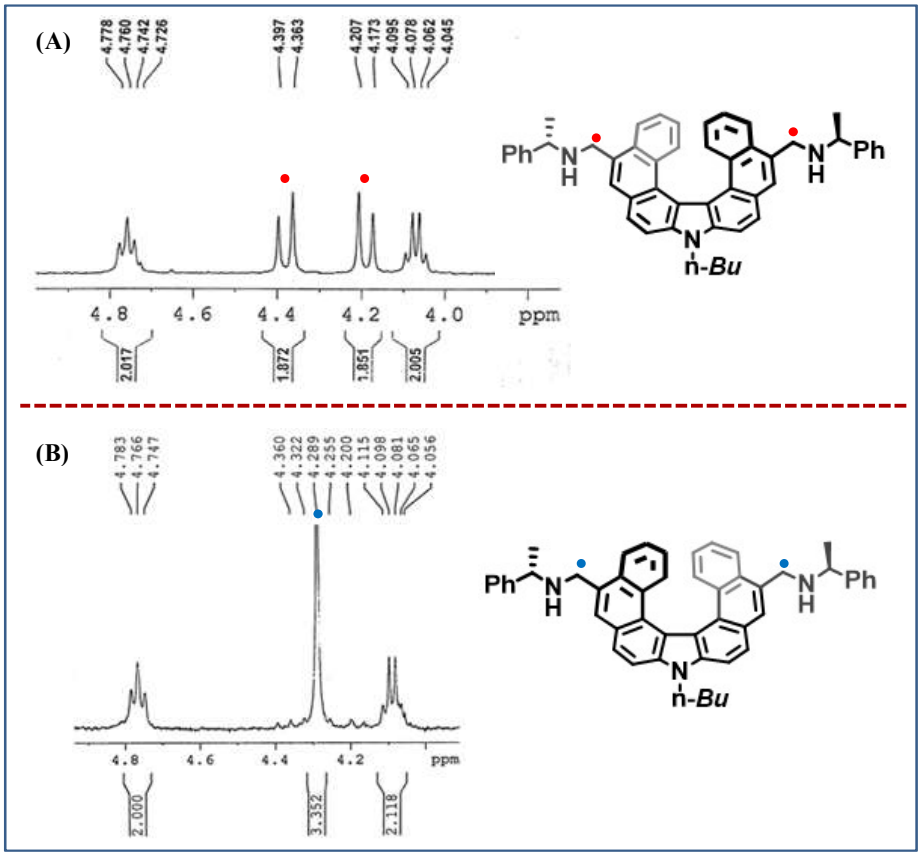

***Figure 2B.7**: Comparision of ^{1}H NMR spectrum of diastereomers after separation: (A) (P,S,S)-(+)-28 and (B) (M,S,S)-(-)-28 (enlarged portion of aliphatic region)*

The optically pure helical isomers show considerably high values of specific optical rotations. The specific and molar rotations of the pure (*P*,*S*,*S*)-(+)-**28** (100% d.e.): $[\alpha]_D$ = +727, $[\phi]_D$ = + 5009 and (*M*,*S*,*S*)-(-)-**28** (87% d.e.): $[\alpha]_D$ = - 755, $[\phi]_D$ = - 5201, measured as solution in chloroform (c = 2.1 X 10^{-3} M). The rotation values are almost opposite with a minor contribution from (*S*)-(-)-α-methylbenzylamine moiety.

2B.2.4 *Selective hydrogenation of helical diamines*

In order to obtain optically pure helicene with methyl substituents, we investigated the hydrogenative deprotection of these diastereomeric helical diamines (±)-**28**. The diamine has two benzyl carbon-carbon bonds which can get cleaved during hydrogenation, in which case either 5,13-dimethyl or 5,13-diamino methyl helicene can be obtained. The pure isomer (*P*,*S*,*S*)-(+)-**28** (100% d.e.) was subjected to the standard conditions of hydrogenation by using 10% Pd/C as a catalyst under hydrogen atmosphere[27] (**Scheme 2B.13**). It was observed that the hydrogenolysis of one of the *N*-benzyl bonds occurred selectively which led to the formation of the 5,13-dimethyl-9-aza[7]helicene (*P*)-(+)-**29** in moderate yield. Thus, hydrogenative cleavage occurred at the less hindered C-N bond thus causing selective removal of the chiral attachment, (*S*)-(-)-α-methylbenzylamine. The formation of the dimethyl helicene **29** was confirmed by the ^{1}H NMR analysis. The protons of the methyl group appeared as a singlet at 2.88 ppm and also the specific signals of the helicene moiety were present. The protons attached to C2 and C16 appeared at 6.24 ppm, most upfield compared to other aromatic protons as they lie under the shielding zone of the terminal benzene ring. Similarly, the other isomer (*M*,*S*,*S*)-(-)-**28** (87% d.e.) was also subjected to hydrogenative deprotection under the same reaction conditions used earlier (**Scheme 2B.13**).

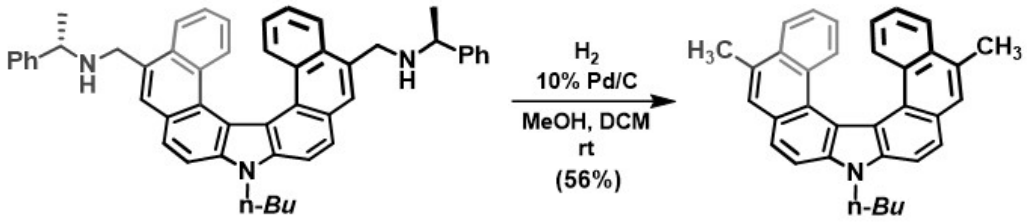

(*P*,*S*,*S*)-(+)-**28**
100 % de

(*P*)-(+)-**29**
97 % ee

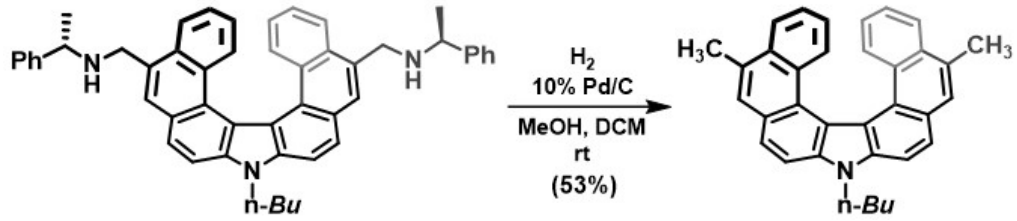

(*M*,*S*,*S*)-(-)-**28**
87 % de

(*M*)-(-)-**29**
85 % ee

***Scheme 2B.13**: Hydrogenative deprotection of the diastereomeric helical diamines (P,S,S)-(+)-28 and (M,S,S)-(-)-28*

The optical purity of the isomers of 5,13-dimethyl-9-aza[7]helicene **29** was studied by HPLC analysis over chiral stationary phase (CHIRALPAK IC column) and their specific optical rotations were recorded. The isomer (*P*)-(+)-**29** was isolated in 97% ee, whereas (*M*)-(-)-**29** was obtained in 85% ee (**Figure 2B.8**).

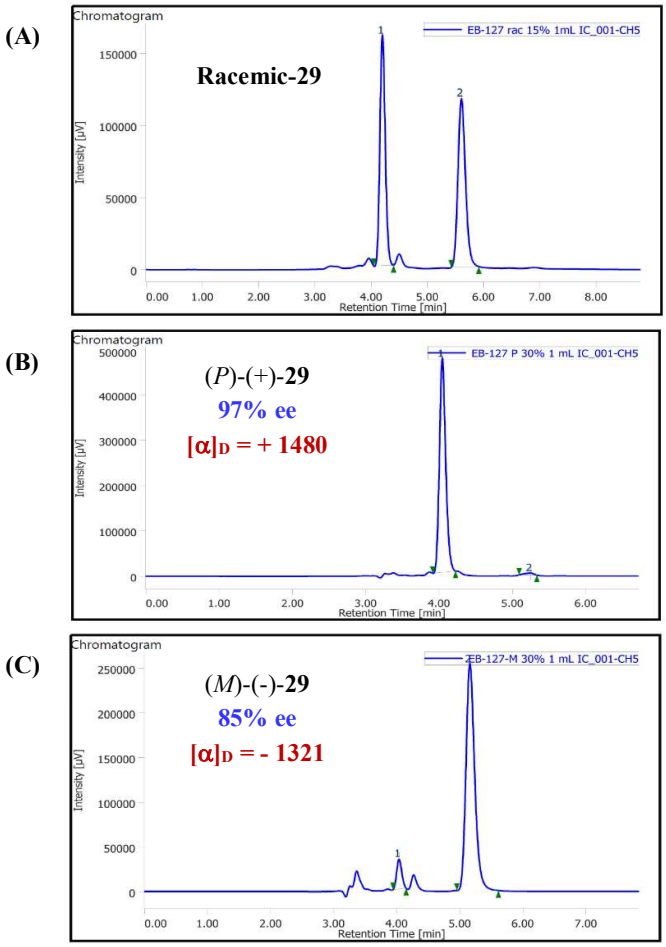

***Figure 2B.8**: HPLC chromatograms of (A) racemic-29; (B) (P)-29; (C) (M)-29*

HPLC Conditions: Chiral Column: CHIRALPAK IC Column, Solvent System: Hexane: IPA(70:30), Flow rate: 1.0 mL/min

The specific and molar rotations of the (*P*)-(+)-**29** (97% ee) was $[\alpha]_D$ = + 1480, $[\phi]_D$ = + 6674 and for (*M*)-(-)-**29** (85% ee) it was $[\alpha]_D$ = - 1321, $[\phi]_D$ = - 5957, measured as solution in dichloromethane (c = 2.1 X 10^{-3} M).

The isomers of **29** were further analyzed by circular dichroism (CD) spectroscopy (**Figure 2B.9**). The two isomers showed opposite Cotton effect in the spectra, as expected for such type of compounds.[11b,15b] The intensity of the CD curves were not same for both the isomers. This difference in their intensities may be attributed to the difference in their enantiomeric excess.

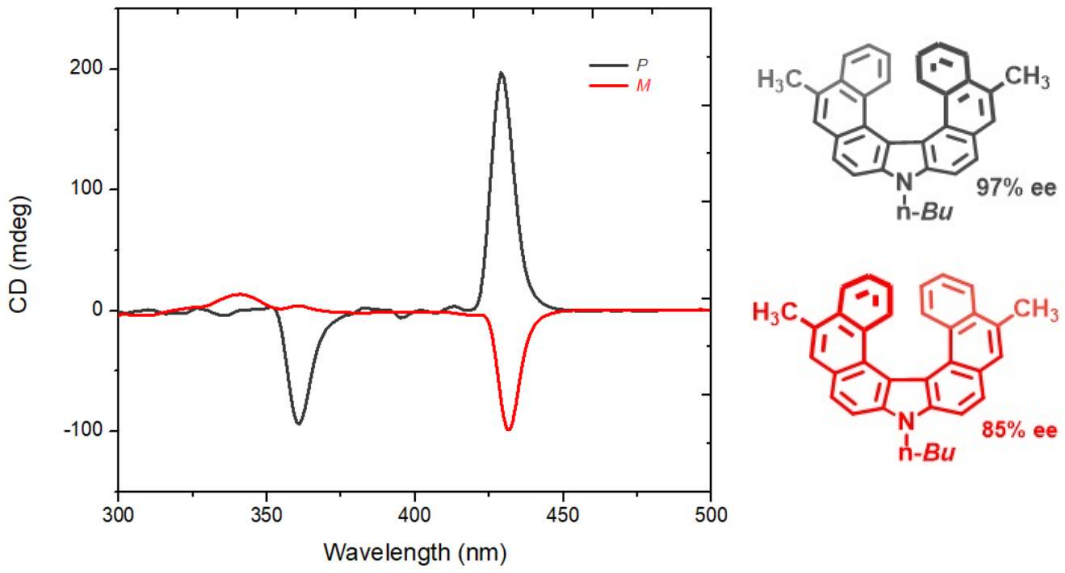

***Figure 2B.9**: CD Spectra of (P)-29 and (M)-29 (1.0 x 10^{-5} M in dichloromethane)*

2B.3 Conclusion

In this chapter we have established a new method for the formation of optically pure helicene with methyl substituents from the corresponding diastereomeric helical diamine *via* selective removal of the (*S*)-(-)-α-methylbenzylamine moiety. Generally, the cleavage of chiral auxiliary from the helical diastereomers leaves the helicenes with the functional group intact, whereas in this method we obtained methyl substituents by cleaving the chiral attachment. The specific optical rotations were measured for the separated diastereomers and for (*P*)-(+)-**29** and (*M*)-(-)-**29**. The isomers of 5,13-dimethyl-aza[7]helicene were further analyzed by CD spectroscopy. The diformyl derivative of aza[7]helicene, a precursor of the helical diamine was synthesized and characterized by single crystal X-ray diffraction analysis.

2B.4 Experimental Data

Materials and Methods: Reagents purchased from standard commercial sources were used without further purification. All the solvents used were stored on oven-dried molecular sieves (4 Å). All reactions were carried out under inert atmosphere (nitrogen) unless other conditions are specified. Thin Layer Chromatography was performed on Merck 60 F254 aluminium coated plates. The spots were visualized under UV light or with iodine vapor. Purification of all the compounds were done by column chromatography using SRL silica gel (60-120 mesh). ^{1}H NMR spectra were recorded on a 400 MHz Bruker Advance 400 spectrometer (100 MHz for ^{13}C) with $CDCl_3$ as solvent and TMS as an internal standard. IR spectra were recorded on a Perkin-Elmer FTIR RXI spectrometer as KBr pellets. High-resolution mass spectra (HRMS) were measured using electronspray ionization (ESI) method. HPLC was performed using CHIRALCEL OD-H column. Specific optical rotations were measured on JASCO P-2000 polarimeter. CD spectra were recorded on a JASCO J-815 Circular Dichroism Spectrometer. Melting points were measured in Thiele's tube using paraffin oil and are uncorrected.

Synthetic procedures and analytical data

3,6 -Diiodo carbazole (20)

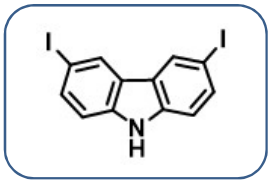

Molecular formula: $C_{12}H_7I_2N$
Molecular weight: 419.00
Physical state: light grey solid

To a round bottom flask (250 mL, two-neck), equipped with a condenser, was loading a solution of carbazole (5.0 g, 29.90 mmol), KI (6.45 g, 38.87 mmol), KIO_3 (6.39 g, 29.90 mmol), acetic acid (100 mL) and deionized water (10 mL). The iodination reaction was continued at 80^{o}C for 24 h. After cooling to room temperature, the mixture was filtered, washed with deionized water, saturated sodium carbonate solution, and methanol to afford a white light grey solid. The analytical data were in complete agreement with the previously published data.[23a]

Yield: 11.91 g (95%)

^{1}H NMR (400 MHz, $CDCl_3$): δ 8.30 (s, 1H), 8.10 (s, 1H), 7.66 (d, *J* = 7.8 Hz), 7.20 (d, *J* = 7.6 Hz, 2H)

9-Butyl-3,6-diiodo-9*H*-carbazole (21)

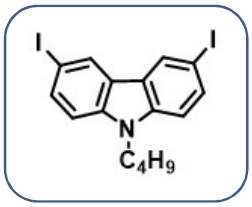

Molecular formula: $C_{16}H_{15}I_2N$
Molecular weight: 475.11
Physical state: white solid

3,6-Diiodocarbazole **20** (2.0 g, 4.77 mmol), powdered potassium hydroxide (1.60 g, 28.65 mmol) were mixed in a flask containing acetone (25 mL). After stirred for 30 minutes, 1-bromobutane (0.98 g, 0.77 mL, 7.16 mmol) was added slowly. The solution was stirred for 5 h at room temperature. After the completion of the reaction, the mixture was poured in ice-cold water and extracted with ethyl acetate (3 x 100 mL). The combined organic phase was washed with water, brine and dried over anhydrous sodium sulfate. The solvent was removed under reduced pressure and the crude product was purified by column chromatography on silica gel using petroleum ether as an eluent to afford **21** as white solid. The analytical data were in complete agreement with the previously published data.[23a] **Yield:** 2.13 g (94%)

^{1}H NMR (400 MHz, $CDCl_3$): δ 8.34 (s, 2H), 7.72 (d, *J* = 8.4 Hz, 2H), 7.19 (d, *J* = 8.4 Hz, 2H), 4.24 (t, *J* = 7.2 Hz, 2H), 1.81 (m, 2H), 1.36-1.34 (m, 2H), 0.93 (t, *J* = 7.2 Hz, 3H).

3,6-Distyryl-9-butyl-9*H*-carbazole (22)

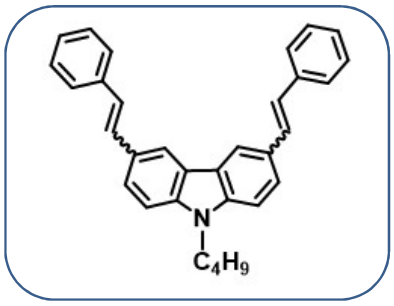

Molecular formula: $C_{32}H_{29}N$
Molecular weight: 479.59
Physical state: light yellow solid
M.p = 152-156 °C

A solution of palladium acetate (0.009 g, 0.042 mmol, 2 mol %) and 1,3-bis(diphenylphosphinopropane) (0.034 g, 0.084 mmol, 4 mol %) was prepared in *N*,*N*-dimethylacetamide (5 mL) under nitrogen atmosphere. The mixture was stirred at room temperature until a homogeneous solution was obtained. This catalyst solution was repeatedly purged by N_2 prior to use. A two-necked round bottom flask was charged with 3, 6-diiodo-*N*-butylcarbazole **21** (1.0 g, 2.1 mmol), dry potassium carbonate (1.16 g, 8.4 mmol), TBAB (0.135 g, 0.42 mmol, 20 mol %), and *N*,*N*-dimethylacetamide (10 mL). The solution was repeatedly

purged with N_2. Styrene (0.546 g, 5.25 mmol) was added at 60 °C and the mixture was heated up to 100 °C. At 100 °C, the previously prepared Pd catalyst solution was added drop wise and the mixture was further heated to 140 °C for 48 h. After the completion of the reaction, the mixture was poured into ice-cold water and extracted with dichloromethane (3 x 100 mL). The combined organic phase was washed with water, brine, and dried over anhydrous sodium sulfate. The solvent was removed under reduced pressure and the crude product was purified by column chromatography on silica gel using petroleum ether–ethyl acetate (98:2) as eluent to afford predominantly *trans* isomer of 3,6-distyryl-*N*-butylcarbazole **22** as light yellow solid. The analytical data were in complete agreement with the previously published data.[24b] **Yield:** 0.845 g (94%)

^{1}H NMR (400 MHz, $CDCl_3$): δ 8.29 (s, 2H), 7.70 (dd, *J* = 8.8 and 1.6 Hz, 2H), 7.62 (d, *J* = 7.6 Hz, 4H), 7.45–7.38 (m, 6H), 7.32-7.28 (m, 4H), 7.21 (d, *J* = 16.4 Hz), 4.29 (t, *J* = 7.2, 2H), 1.90–1.85 (m, 2H), 1.48–1.40 (m, 2H), 0.99 (t, *J* = 7.2 Hz, 3H).

N-butyl aza[7]helicene (18)

Molecular formula: $C_{32}H_{25}N$
Molecular weight: 423.56
Physical state: light brown solid
M.p = 206-208 °C

A solution of 3,6-distyryl-*N*-butylcarbazole **22** (0.350 g, 0.82 mmol), iodine (0.457 g, 1.80 mmol), dry THF (2.95 g, 3.32 mL, 41.3 mmol), and toluene (1.2 L) was irradiated using a 125W HMPV lamp (24 h monitored by TLC). After the completion of the reaction, the excess of iodine was removed by washing the solution with aqueous $Na_2S_2O_3$ and water. The organic layer was concentrated under reduced pressure to obtain the crude product. The crude product was purified by column chromatography over silica gel using petroleum ether–ethyl acetate (98:2) as eluent to obtain title compound **18** as light brown solid. The analytical data were in complete agreement with the previously published data.[24b] **Yield:** 0.151 g (44%)

^{1}H NMR (400 MHz, CDCl3): δ 8.11 (d, *J* = 8.4 Hz, 2H), 8.02 (d, *J* = 8.4 Hz, 2H), 7.95 (d, *J* = 8.4 Hz, 2H), 7.83–7.81 (m, 4H), 7.44 (d, *J* = 8.4 Hz, 2H), 7.25-7.15 (m, 2H), 6.25–6.21 (m, 2H), 4.76 (t, *J* = 7.2 Hz, 2H), 2.10–2.04 (m, 2H), 1.57–1.51(m, 4H signal merged with water peak), 1.01 (t, *J* = 7.2 Hz, 3H).

Vilsmeier-Haack formylation of 18

Phosphoryl chloride (0.725 g, 0.44 mL, 4.72 mmol) was added slowly in dry DMF (0.862 g, 0.91 mL,11.8 mmol) which was purged with nitrogen and cooled at 0 ℃. The reactant was warmed at room temperature, stirred for 1h and then cooled again for 0 ℃. To this mixture was added 9-butyl-9*H*-aza[7]helicene **1** (0.250 g, 0.59 mmol) in dichloroethane (5 mL). In 1h, the reaction temperature was raised to 90 ℃ and then stirred for further 8h. After the completion of the reaction, the mixture was poured into ice-cold water and extracted with dichloromethane (3 x 50 mL). The combined organic phase was removed under reduced pressure and the crude product containing mixture of **3** and **4** were separated and purified by column chromatography on silica gel.

5-formyl-9-butyl-9*H*-aza[7]helicene (23)

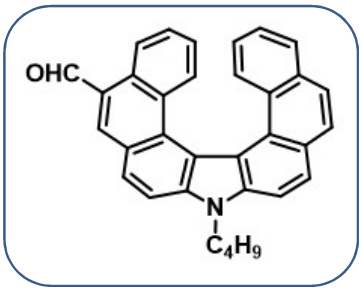

Molecular formula: $C_{33}H_{25}NO$
Molecular weight: 451.56
Physical state: yellow solid
M.p = 127 ℃

Silica gel column chromatography (EtOAc/petroleum ether 10:90) gave **23** as yellow solid. **Yield:** 0.043 g (16%)

^{1}H NMR (400 MHz, $CDCl_3$): δ 10.52 (s, 1H), 9.28 (d, *J* = 8.4 Hz, 1H), 8.57 (s, 1H), 8.24 (d, *J* = 8.4 Hz, 1H), 8.18 (d, *J* = 8.4 Hz, 1H), 8.05-7.97 (m, 3H), 7.88-7.84 (m, 2H), 7.47 (d, *J* = 8.4 Hz, 1H), 7.34-7.31 (m, 2H), 7.22 (t, *J* = 6.8 Hz, 1H), 6.31-6.25 (m, 2H), 4.78 (t, *J* = 7.2 Hz, 2H), 2.15-2.10 (m, 2H), 1.62-1.55 (m, 3H signal merged with water peak), 1.06 (t, *J* = 7.2 Hz, 3H).

^{13}C NMR (100 MHz, $CDCl_3$): δ 193.4, 141.7, 141.3, 139.7, 131.4, 130.7, 130.5, 129.9, 128.2, 127.9, 127.8, 127.5, 127.4, 127.1, 126.9, 123.7, 126.4, 126.3, 124.8, 124.6, 123.7, 123.6, 123.0, 116.9, 116.6, 110.4, 109.7, 43.5, 31.8, 20.7, 13.9.

IR (KBr): 3044, 2953, 2928, 2867, 2717, 1679, 1587, 1519, 1445, 1339, 1284, 1229, 1218, 1108, 824, 746, 647, 511 cm^{-1}.

HRMS (ESI+): *m/z* calcd. for $C_{33}H_{25}NO$ $[M + H]^+$ 452.2014, found 452.2016.

5,13-diformyl-9-butyl-9*H*-aza[7]helicene (17)

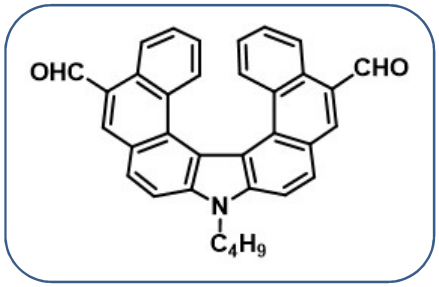

Molecular formula: $C_{34}H_{25}NO_2$
Molecular weight: 479.58
Physical state: yellow solid
M.p = 134 °C

Silica gel column chromatography (EtOAc/petroleum ether 20:80) gave **17** as yellow solid. **Yield:** 0.116 g (41%)

^{1}H NMR (400 MHz, $CDCl_3$): δ 10.52 (s, 2H), 9.27 (d, *J* = 8.4 Hz, 2H), 8.57 (s, 2H), 8.30 (d, *J* = 8.4 Hz, 2H), 8.06 (d, *J* = 8.8 Hz, 2H), 7.35-7.32 (m, 4H), 6.29 (t, *J* = 6.8 Hz, 2H), 4.81 (t, *J* = 7.6 Hz, 2H), 2.15-2.12 (m, 2H), 1.63-1.57 (m, 4H signal merged with water peak), 1.07 (t, *J* = 7.2 Hz, 3H).

^{13}C NMR (100 MHz, $CDCl_3$): δ 193.3, 141.7, 141.2, 130.6, 130.2, 128.7, 128.24, 128.2, 127.8, 127.4, 125.1, 123.9, 123.6, 116.7, 110.5, 43.8, 31.8, 20.7, 13.9.

IR (KBr): 2927, 2855, 2713, 1679, 1587, 1516, 1443, 1337, 1282, 1225, 1164, 1141, 1061, 917, 890, 872, 794, 767, 736, 648, 507 cm^{-1}.

HRMS (ESI+): *m/z* calcd. for $C_{34}H_{25}NO_2$ $[M + H]^+$ 480.1964, found 480.1965.

3,6-Diformyl-9-butyl-9*H*-carbazole (26)

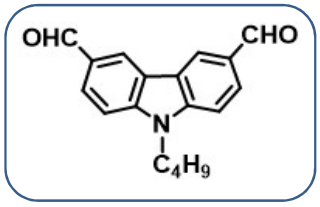

Molecular formula: $C_{18}H_{17}NO_2$
Molecular weight: 279.33
Physical state: Light yellow solid
M.p = 130-133 °C

Synthetic procedure is similar to described for the synthesisof **23** and **17**. **Yield:** 71%

^{1}H NMR (400 MHz, $CDCl_3$): δ 10.14 (s, 2H), 8.68 (d, *J* = 1.2 Hz, 2H), 8.09 (dd, *J* = 8.4 and 1.2 Hz, 2H), 7.56 (d, *J* = 8.4 Hz, 2H), 4.40 (t, *J* = 7.2 Hz, 2H), 1.93 - 1.88 (m, 2H), 1.46 - 1.40 (m, 2H), 0.98 (t, *J* = 7.6 Hz, 3H).

3,3-(9-Butyl-9*H*-carbazole-3,6-diyl)-bis(2-phenylacrylonitrile) (27)

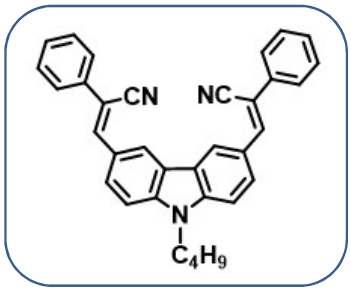

Molecular formula: $C_{34}H_{27}N_3$
Molecular weight: 477.61
Physical state: yellow solid
M.p = 192-194 °C

A solution of 9-butyl carbazole-3,6-dicarbaldehyde (1.0 g, 3.58 mmol) and phenylacetonitrile (1.04 g, 8.96 mmol) in dry ethanol (25 mL) was placed in a single neck R.B. flask fitted with a septum, which is degassed and purged with nitrogen. To this was added drop-wise, with constant stirring, a solution of (0.824 g, 35.8 mmol) sodium dissolved in 25 mL of dry ethanol. This reaction mixture was stirred vigorously for 6 hours at room temperature. After completion of reaction the ethanol was evaporated under reduced pressure the mixture was poured into ice-cold water and extracted with ethyl acetate (3 x 100 mL). The combined organic phase was washed with water, brine, and dried over anhydrous sodium sulfate. The solvent was removed under reduced pressure and the crude product was purified by column chromatography on silica gel using petroleum ether–ethyl acetate (90:10) as eluent to afford **27**. The analytical data were in complete agreement with the previously published data.[11b] **Yield:** 1.47 g (86%)

^{1}H NMR (400 MHz, $CDCl_3$): δ 8.65 (s, 2H), 8.24 (dd, *J* = 8.4 Hz and 1.6 Hz, 2H), 7.76-7.74 (m, 6H), 7.52-7.47 (m, 6H), 7.43-7.39 (m, 2H), 4.37 (t, *J* = 7.2 Hz), 1.95- 1.88 (m, 2H), 1.49-1.39 (m, 2H), 1.0 (t, *J* = 7.2 Hz, 3H).

N-butyl 5,13-dicyano aza[7]helicene (24)

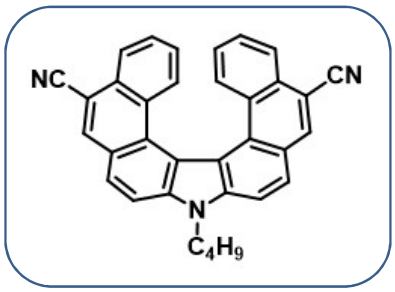

Molecular formula: $C_{34}H_{23}N_3$
Molecular weight: 473.57
Physical state: yellow solid
M.p = 279 °C

In an immersion wall photo reactor (borosilicate glass) equipped with a water cooling jacket and stir bar a solution of 3,3-(9-butyl-9*H*-carbazole-3,6-diyl)-bis(2-phenylacrylonitrile) **27** (0.2 g, 0.42 mmol), iodine (0.185 g, 0.73 mmol), THF (3.02 g, 3.40 mL, 42.0 mmol) and toluene

(350 mL) was irradiated using a 125W HPMV lamp for 7 h monitored by TLC. After the completion of reaction, the excess of iodine was removed by washing the solution with aqueous $Na_2S_2O_3$, followed by distilled water. The organic layer was concentrated under the reduced pressure to obtain the crude product. The crude product purified by column chromatography over silica gel using petroleum ether: ethyl acetate (80:20) as eluent to obtained compound **24** as yellow solid. The analytical data were in complete agreement with the previously published data.[11b] **Yield:** 0.173 g (86%)

^{1}H NMR (400 MHz, $CDCl_3$): δ 8.50 (s, 2H), 8.22 (d, *J* = 8 Hz, 2H), 8.13 (d, *J* = 8.4 Hz, 2H), 8.01 (d, *J* = 8.8 Hz, 2H), 7.34-7.31 (m, 2H),7.16 (d, *J* = 8Hz, 2H), 6.27-6.23 (m, 2H), 4.77 (t, *J* = 7.6 Hz, 2H), 2.13-2.05 (m, 2H), 1.69-1.52 (m, 2H), 1.05 (t, *J* = 7.6Hz,3H).

Reduction of 24.

To a toluene solution (20 mL) of the 5,13-dicyano-9-butyl-9*H*-aza[7]helicene **24** (0.500 g, 1.06 mmol) under nitrogen, DIBAL-H (3.20 mL, 3.17 mmol) was added. This mixture was stirred for 4 hours at room temperature, then a mixture of H_2SO_4/H_2O was added. The mixture obtained was extracted with toluene (3 x 50 mL). The combined organic phase was washed with water and brine and dried over anhydrous sodium sulfate. The solvent was removed under reduced pressure, and the crude product was purified by column chromatography on silica gel using ethyl acetate/petroleum ether (15:85 – 20:80) as eluent to afford compound **17** as yellow solid. **Yield:** 0.400 g (79%).

(1S,1′S)-*N*,*N*′-((9-butyl-9*H*-dinaptho[2,1-*c*:1′,2′-*g*]carbazole-5,13-diyl)bis(methylene))bis(1-phenylethan-1-amine) ((±)-28)

To a solution of 5,13-diformyl-9-butyl-9*H*-aza[7]helicene **17** (0.1 g, 0.21 mmol) in anhydrous EtOH/THF (10 mL) was added (*S*)-(-)-*α*-methylbenzylamine (0.758 g, 0.08 mL, 0.62 mmol) and titanium(IV)isopropoxide (0.356 g, 0.37 mL, 1.25 mmol).The resulting solution was stirred at room temperature for 10 h. Sodium borohydride (0.032 g, 0.83 mmol) was added to the solution at 0 °C and was stirred at room temperature for 4 h before pouring into 2.0 M aqueous ammonia (10 mL). The suspension was filtered through Celite, and to the filtrate was added water. Crude product was extracted with DCM, dried over anhydrous sodium sulphate and solvent was evaporated to obtain crude mass. The crude product was purified by column chromatography over alumina using ethyl acetate/petroleum ether (20:80) as eluent to obtain

mixture of diastereomers as pale yellow solid. **Overall yield:** 0.127 g (88%, mixture of two diastereomers (*P*,*S*,*S*)-(+)-**28** and (*M*,*S*,*S*)-(-)-**28**).

^{1}H NMR (400 MHz, $CDCl_3$): δ 8.12-8.09 (m, 2H), 7.99-7.93 (m, 5H), 7.56-7.45 (m, 9H), 7.39-7.34 (m, 4H), 7.25-7.17 (m, 2H), 6.23-6.16 (m, 2H), 4.77 (t, *J* = 7.2 Hz, 2H), 4.38 (d, *J* = 13.6 Hz, 2H), 4.29 (merged d, 2H), 4.18 (d, *J* = 13.6 Hz, 2H), 4.11-4.04 (m, 2H), 2.12-2.09 (m, 2H), 1.88 (s, 5H), 1.64-1.52 (m, 8H), 1.05 (t, *J* = 7.6 Hz, 3H).
HRMS (ESI+): *m/z* calcd. for $C_{50}H_{48}N_3$ $[M + H]^+$ 690.3843, found 690.3844.
HPLC conditions for (*P*,*S*,*S*)-(+)-**28** and (*M*,*S*,*S*)-(-)-**28**: two well separated peaks [Chiralpak IC; isopropanol/n-hexane (30/70), 1.0 mL/min, UV 254 nm, t_R (*P*,*S*,*S*)-(+)-**28** = 5.17 and t_R (*M*,*S*,*S*)-(-)-**28** = 7.36 min].

(*P*,*S*,*S*)-(+)-28

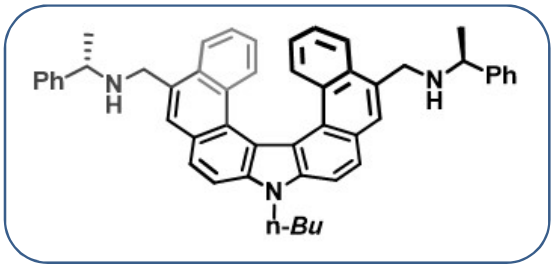

Molecular formula: $C_{50}H_{47}N_3$
Molecular weight: 689.94
Physical state: pale yellow solid
M.p = 107-109 °C

de = 100%. **$[\alpha]_D$** = +727, **$[\phi]_D$** = +5009 ($CHCl_3$, 2.1×10^{-3} mol L^{-1}).

^{1}H NMR (400 MHz, $CDCl_3$): δ 8.09 (d, *J* = 8.8 Hz, 2H), 7.99-7.94 (m, 6H), 7.56-7.45 (m, 10H), 7.38-7.35 (m, 2H), 7.24-7.20 (m, 2H), 6.22-6.18 (m, 2H), 4.76 (t, *J* = 7.2 Hz, 2H), 4.38 (d, *J* = 13.6 Hz, 2H), 4.19 (d, *J* = 13.6 Hz, 2H), 4.09-4.04 (m, 2H), 2.14-2.06 (m, 2H), 1.64-1.53 (m, 8H), 1.05 (t, *J* = 7.2 Hz, 3H).
^{13}C NMR (100 MHz, $CDCl_3$): δ 144.6, 138.3, 130.1, 129.7, 128.6, 127.8, 127.5, 126.0, 125.9, 125.8, 125.7, 125.6, 125.4, 125.1, 125.0, 121.3, 120.7, 108.6, 57.0, 48.5, 42.4, 30.8, 28.7, 23.6, 19.6, 12.9.
IR (KBr): 3648, 3058, 3024, 2957, 2924, 2865, 1589, 1523, 1492, 1448, 1341, 1282, 1160, 1110, 1029, 882, 789, 759, 701, 647 cm^{-1}.

(*M*,*S*,*S*)-(-)-28

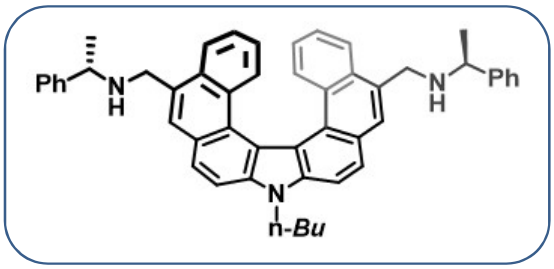

Molecular formula: $C_{50}H_{47}N_3$
Molecular weight: 689.94
Physical state: pale yellow solid
M.p = 110-114 °C

de = 87%. **[α]D** = –755 , **[ϕ]D** = -5201 ($CHCl_3$, 2.1×10^{-3} mol L^{-1}).

^{1}H NMR (400 MHz, $CDCl_3$): δ 8.10 (d, *J* = 8.4 Hz, 2H), 8.03 (s, 2H), 7.96-7.91 (m, 4H), 7.54 (d, *J* = 7.2 Hz, 4H), 7.48-7.44 (m, 6H), 7.37-7.34 (m, 2H), 7.18-7.15 (m, 2H), 6.18-6.14 (m, 2H), 4.76 (t, *J* = 6.8 Hz, 2H), 4.29 (merged d, 4H), 4.11-4.06 (m, 2H), 2.12-2.08 (m, 2H), 1.60-1.52 (m, 8H), 1.05 (t, *J* = 7.2 Hz, 3H).

Hydrogenative deprotection of (±)-28.

To a solution of (±)**28** (0.050 g, 0.072 mmol) in MeOH (5 mL) and CH_2Cl_2 (5 mL), was added 10% Pd/C (0.020 g, 40 %w/w). The inside air was replaced with H_2 (balloon) by three vacuum/H_2 cycles. The reaction mixture was stirred at room temperature until the TLC monitoring indicated maximum conversion of the starting material. Then the reaction mixture was filtered to remove Pd/C and the filtrate was concentrated to obtain crude product which was purified by column chromatography on silica gel using EtOAc/petroleum ether (5:95) as eluent to afford (±)**29** as light yellow solid. **Yield:** 0.018 g (55%).

HRMS (ESI+): *m/z* calcd. for $C_{34}H_{30}N$ $[M + H]^+$ 452.2315, found 452.2384.
HPLC conditions for (*P*)-(+)-**29** and (*M*)-(-)-**29**: two well separated peaks [Chiralpak IC; isopropanol/n-hexane (30/70), 1.0 mL/min, UV 254 nm, t_R (*P*)-**29** = 4.2 and t_R (*M*)-**29** = 5.6 min].

(*P*)-(+)-29

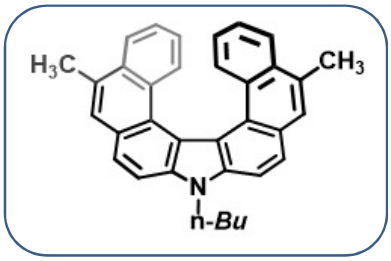

Molecular formula: $C_{34}H_{29}N$
Molecular weight: 451.61
Physical state: light yellow solid
M.p = 124 °C

ee = 97.39%. **[α]D** = +1480, **[ϕ]D** = +6674 (CH_2Cl_2, 2.1×10^{-3} mol L^{-1}).

^{1}H NMR (400 MHz, $CDCl_3$): δ 8.06 (d, *J* = 8.4 Hz, 2H), 7.98 (d, *J* = 8.0 Hz, 2H), 7.94 (d, *J* = 8.4 Hz, 2H), 7.87 (s, 2H), 7.51 (d, *J* = 8.4 Hz, 2H), 7.25 (t, *J* = 7.2 Hz, 2H), 6.24 (t, *J* = 8.4 Hz, 1H), 4.76 (t, *J* = 7.2 Hz, 2H), 2.88 (s, 6H), 2.12-2.08 (m, 2H), 1.58-1.54 (m, 2H), 1.04 (t, *J* = 7.6 Hz, 3H).

^{13}C NMR (100 MHz, $CDCl_3$): δ 206.8, 138.9, 130.9, 130.4, 129.5, 128.7, 126.7, 126.6, 126.4, 125.9, 125.8, 122.2, 116.6, 109.4, 43.3, 31.9, 30.8, 20.7, 19.6, 13.9.

IR (KBr): 3061, 2956, 2922, 2852, 1733, 1591, 1491, 1458, 1441, 1341, 1323, 1197, 1156, 1139, 1034, 873, 787, 757, 735, 647, 616, 508 cm^{-1}.

(*M*)-(-)-29

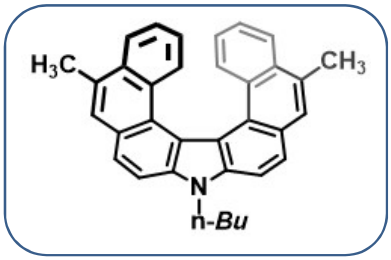

Molecular formula: $C_{34}H_{29}N$
Molecular weight: 451.61
Physical state: light yellow solid
M.p = 124 °C

ee = 85.05%. **[α]D** = –1321, **[ϕ]D** = –5957 (CH_2Cl_2, 2.1×10^{-3} mol L^{-1}).

2B.5 Spectral Data

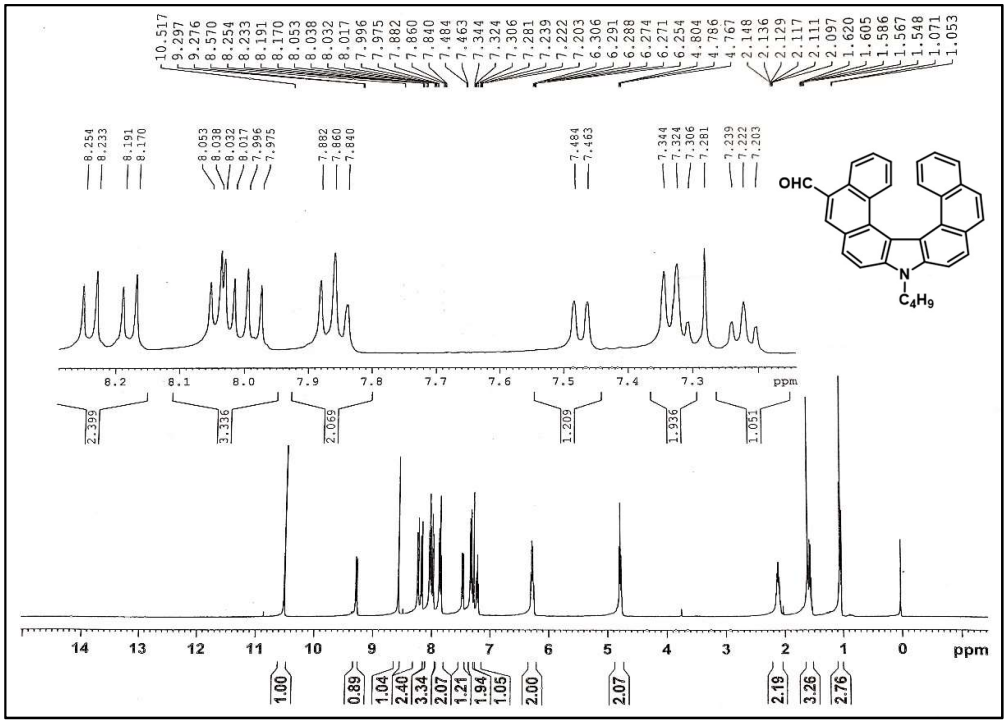

^{1}H NMR Spectrum of 23 ($CDCl_3$, 400 MHz)

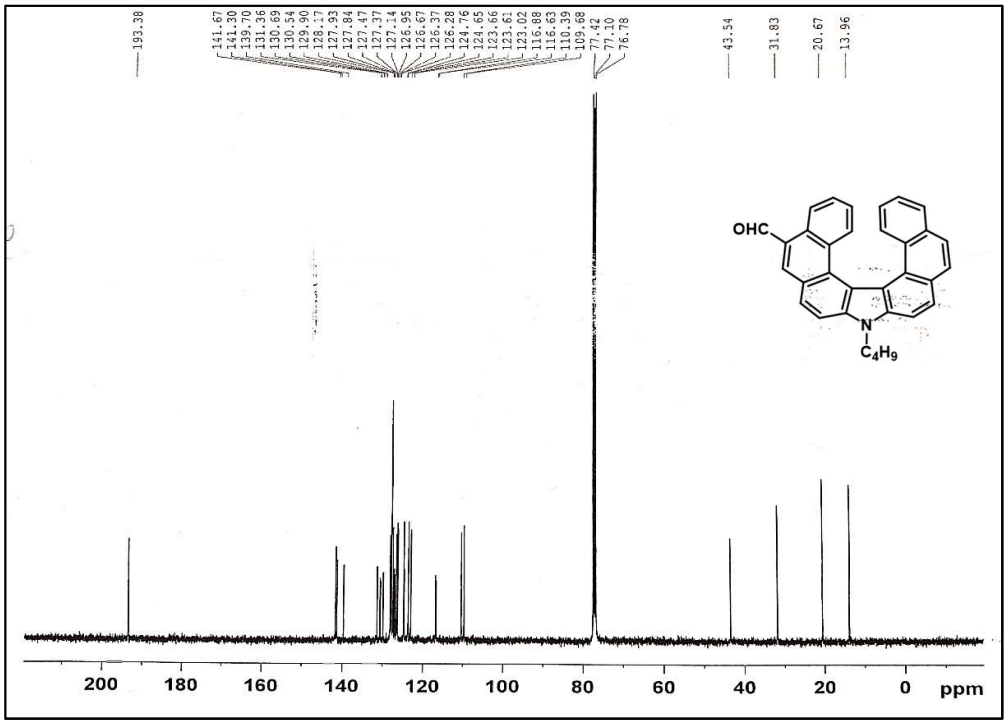

^{13}C NMR Spectrum of 23 ($CDCl_3$, 100 MHz)

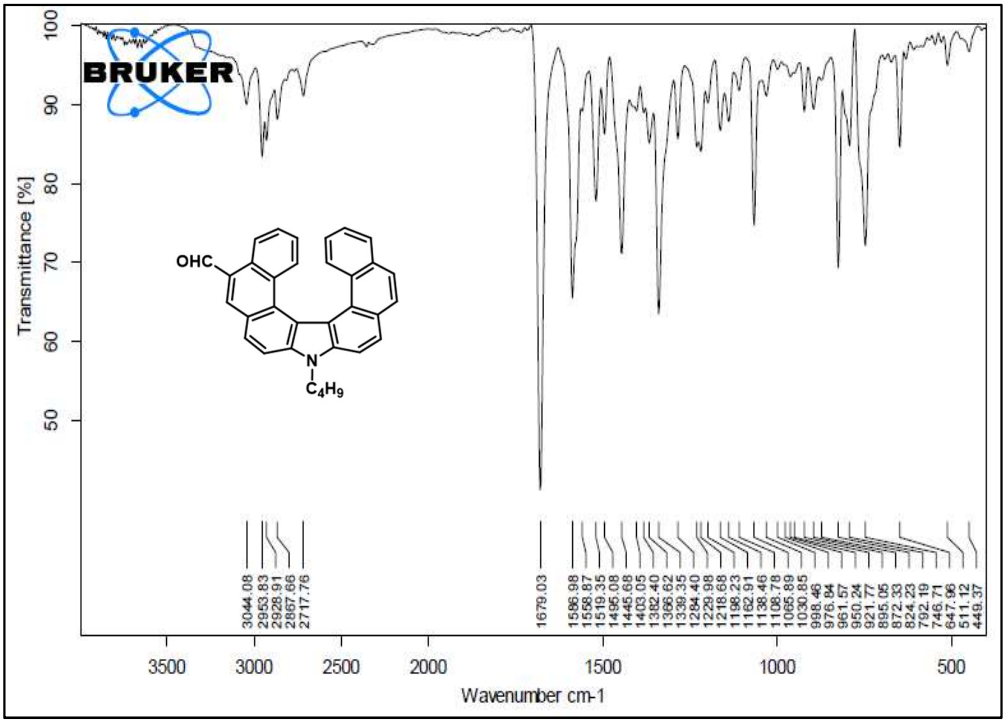

IR Spectrum of 23

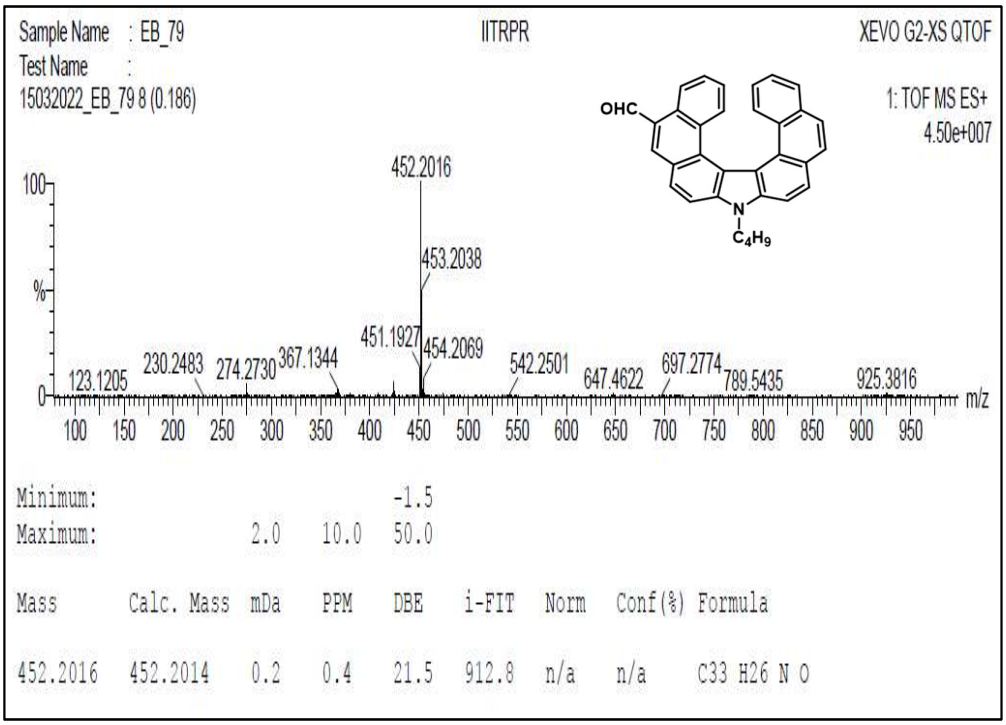

HRMS Spectrum of 23

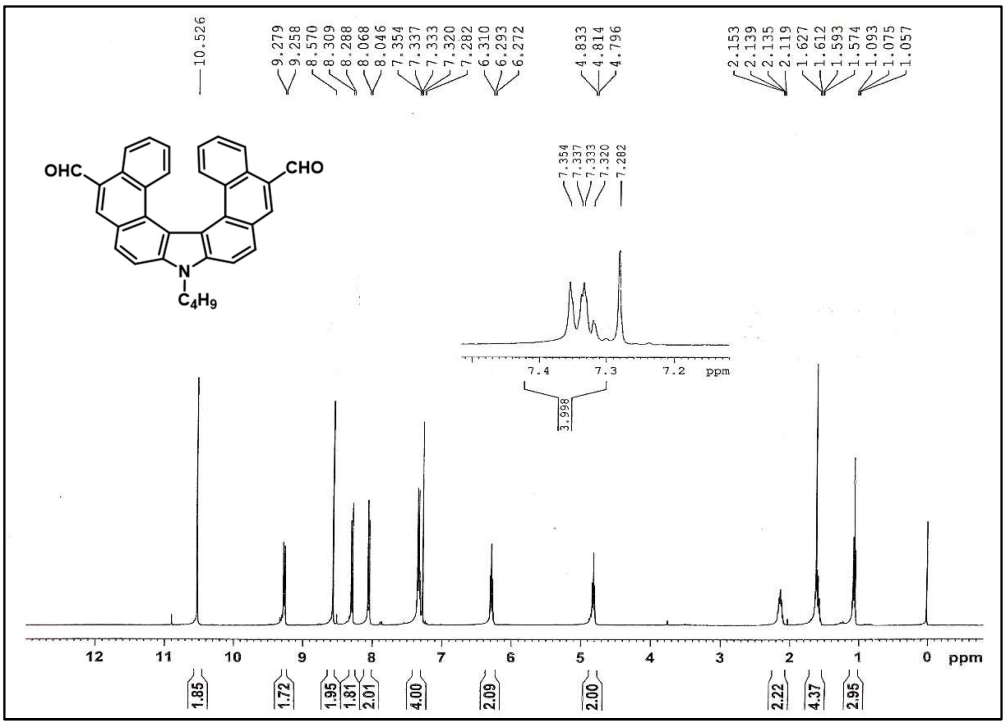

^{1}H NMR Spectrum of 17 ($CDCl_3$, 400 MHz)

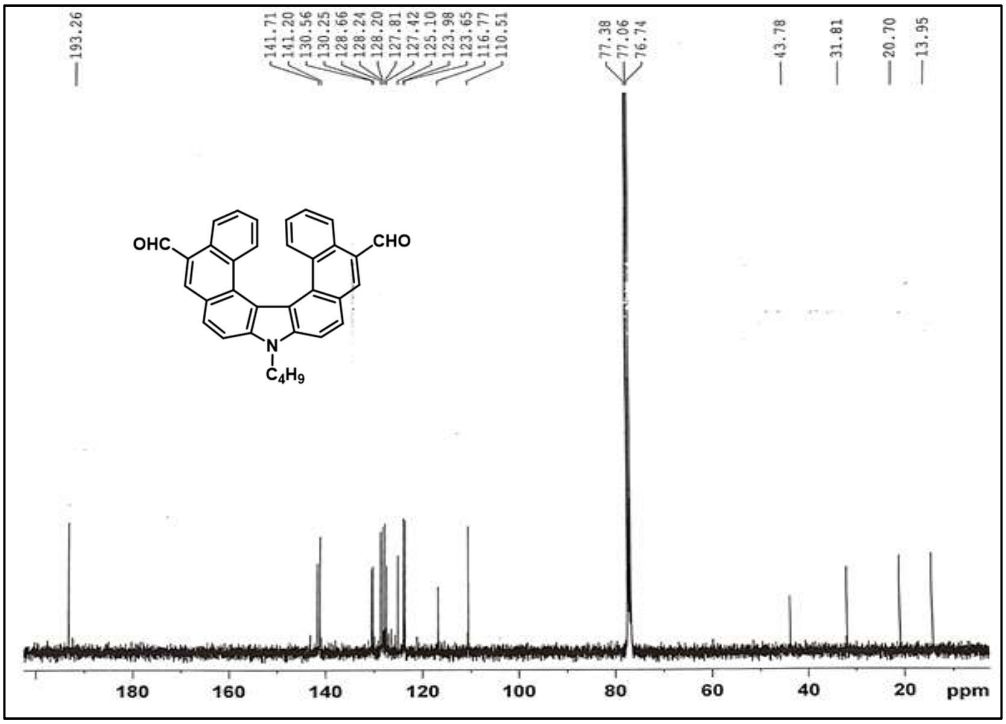

^{13}C NMR Spectrum of 17 ($CDCl_3$, 100 MHz)

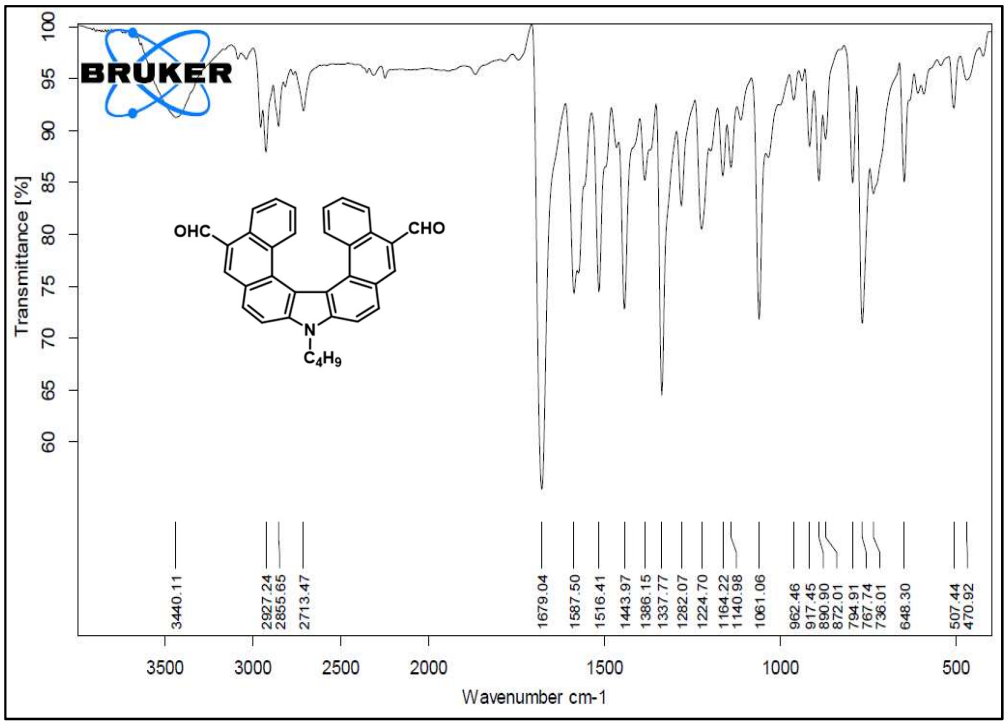

IR Spectrum of 17

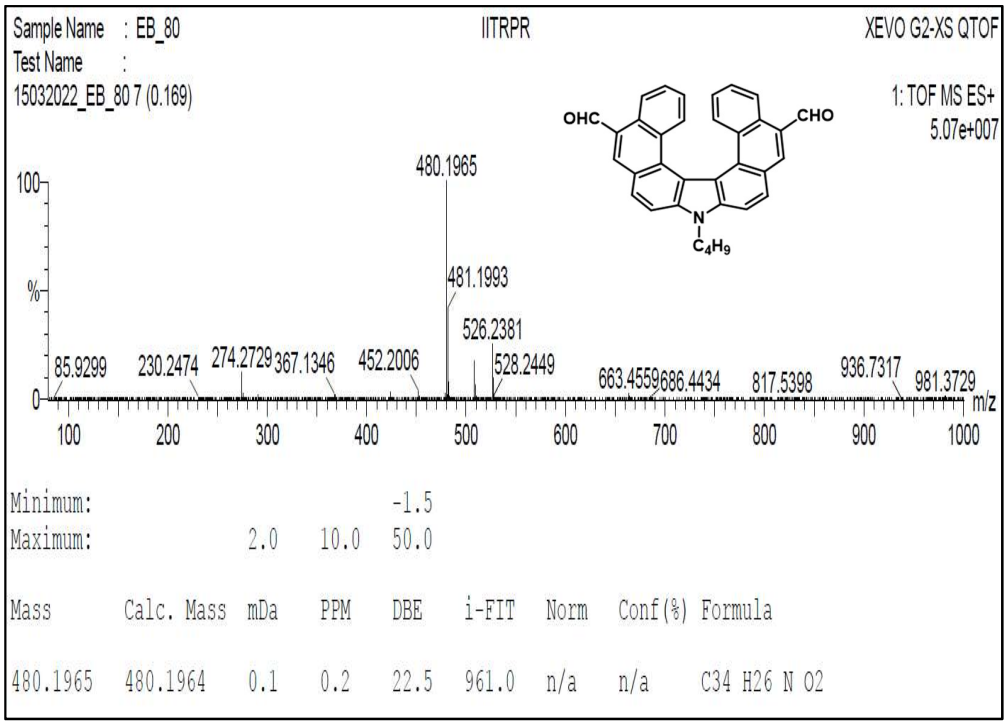

HRMS Spectrum of 17

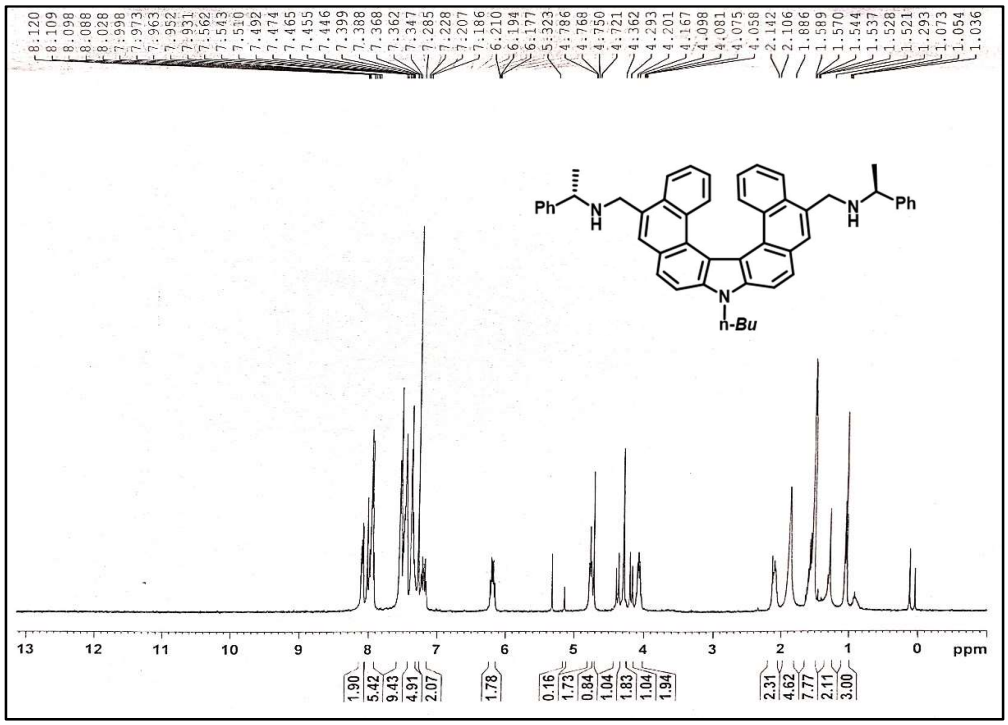

^{1}H NMR Spectrum of crude reaction mixture of diasteoreomeric helical diamines

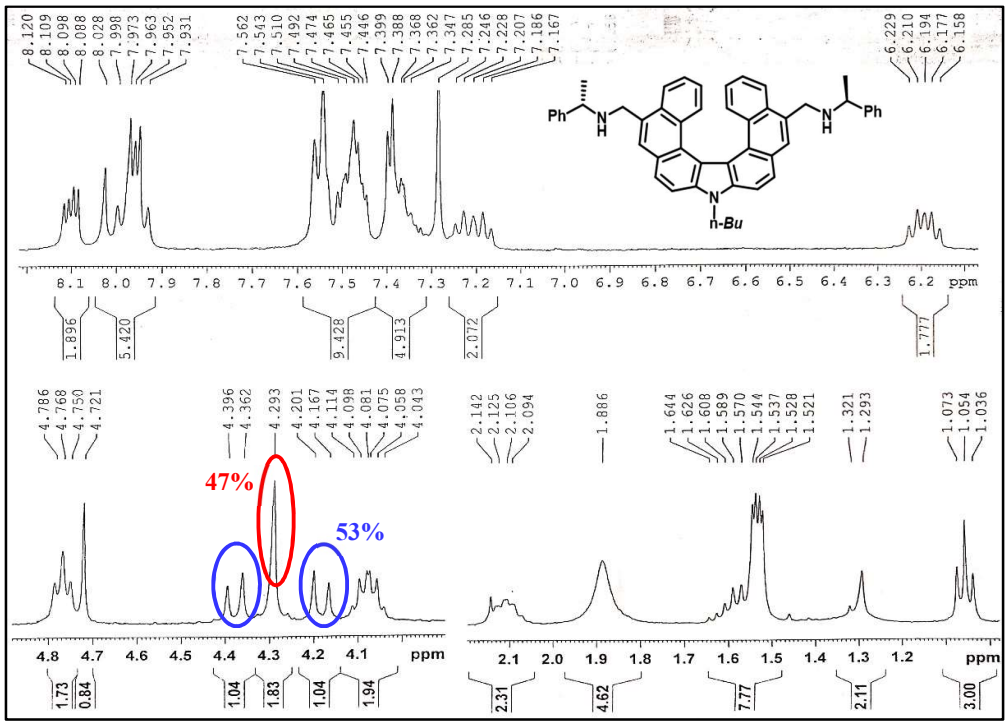

^{1}H NMR Spectrum of mixture of mixture of diastereomeric helical diamines (enlarged portion of aliphatic and aromatic region)

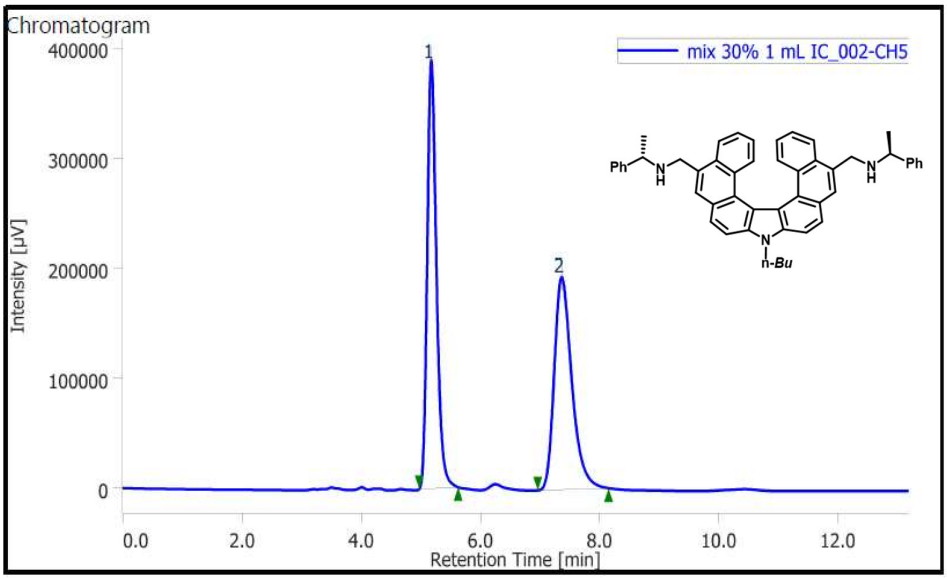

Peak Information

#	Peak Name	CH	tR [min]	Area [µV·sec]	Height [µV]	Area%	Height%	Quantity	NTP	Resolution	Symmetry Factor	Warning
1	Unknown	5	5.173	4164551	389052	51.206	66.813	N/A	5697	5.498	1.291	
2	Unknown	5	7.360	3968444	193251	48.794	33.187	N/A	3163	N/A	1.374	

HPLC chart of mixture of diastereomeric helical diamines

CHIRALPAK IC; isopranol/n-hexane (30/70), 1.0 mL/min, UV 254 nm

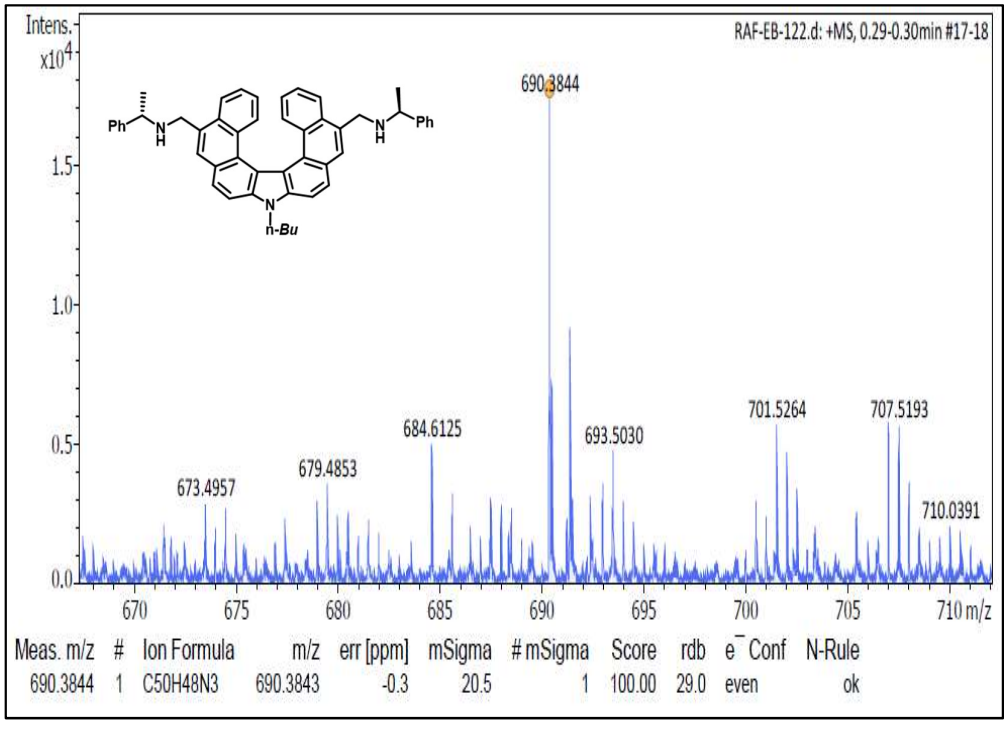

HRMS Spectrum of 28

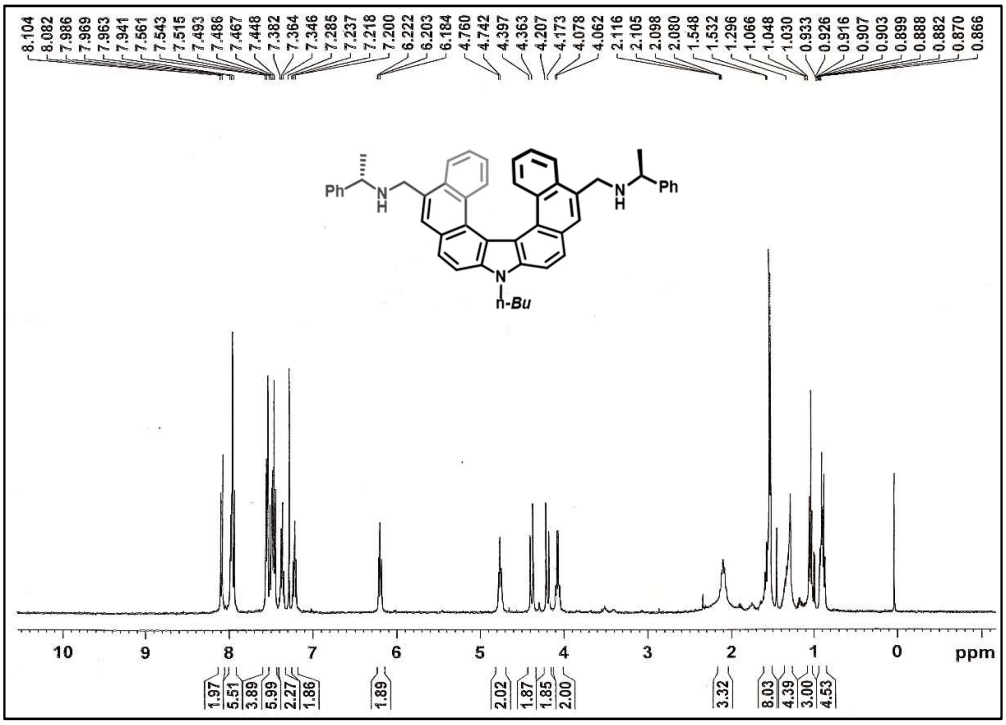

^{1}H NMR Spectrum of (*P,S,S*)-(+)-28 ($CDCl_3$, 400 MHz)

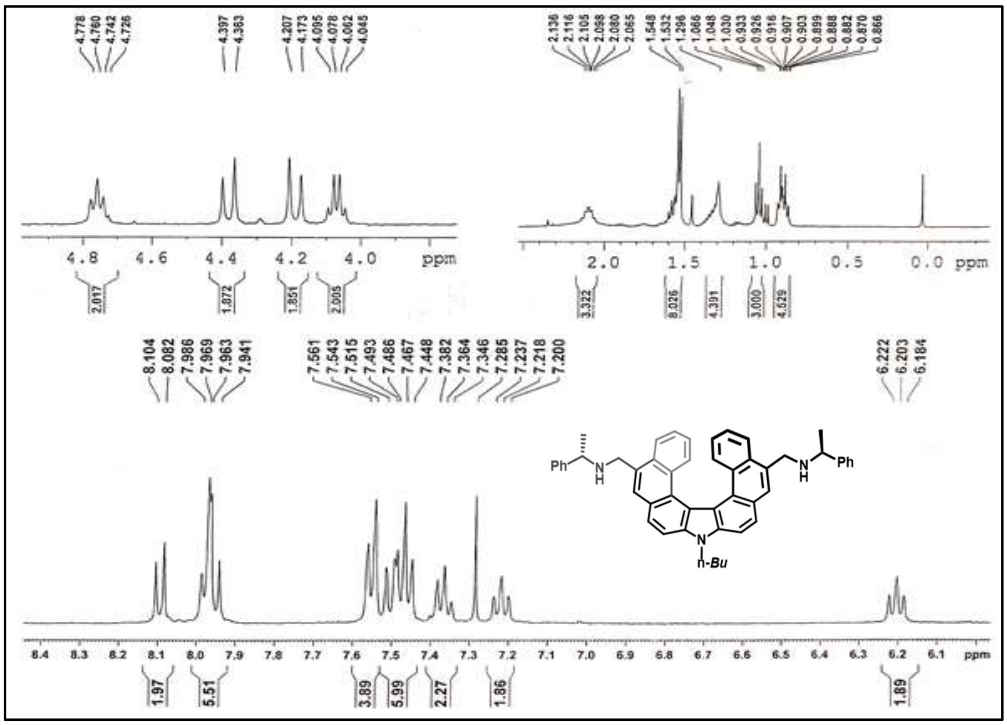

^{1}H NMR Spectrum of (*P,S,S*)-(+)-28 (enlarged aliphatic and aromatic region) ($CDCl_3$, 400 MHz)

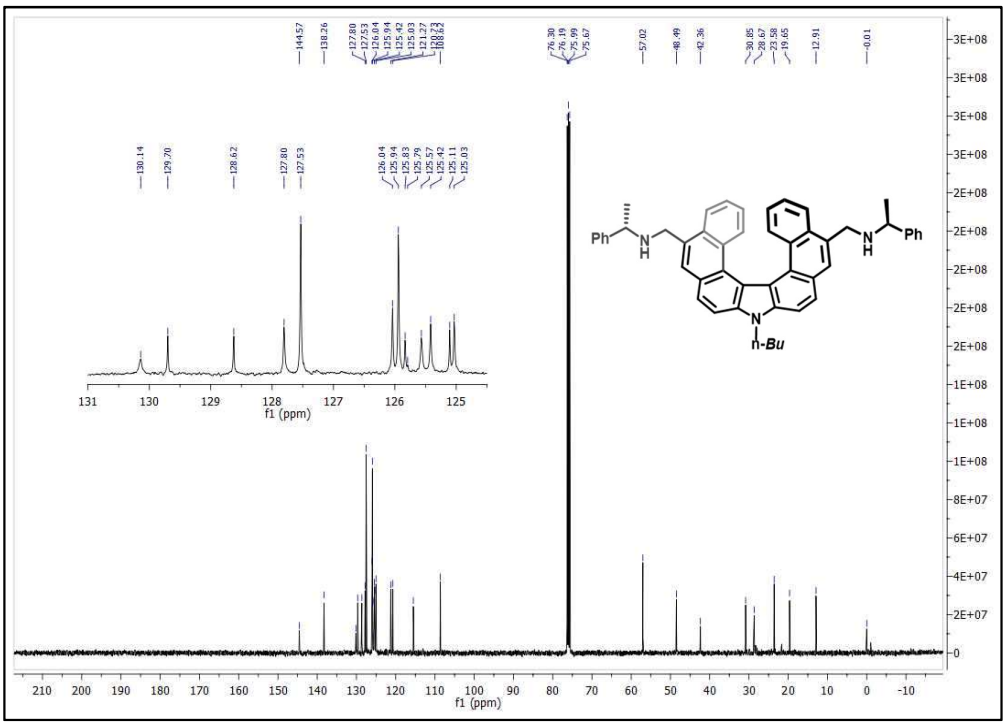

^{13}C NMR Spectrum of (*P,S,S*)-28 ($CDCl_3$, 100 MHz)

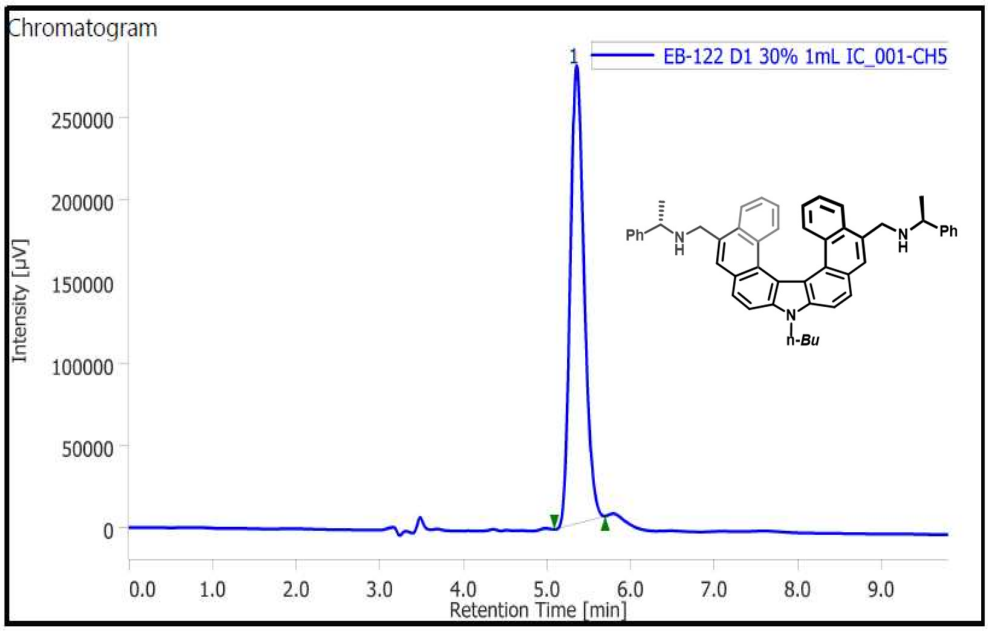

Peak Information

#	Peak Name	CH	tR [min]	Area [µV·sec]	Height [µV]	Area%	Height%	Quantity	NTP	Resolution	Symmetry Factor	Warning
1	Unknown	5	5.350	3203589	278898	100.000	100.000	N/A	5048	N/A	1.203	

HPLC chart of (*P,S,S*)-(+)-28

100% de (CHIRALPAK IC; isopranol/n-hexane (30/70), 1.0 mL/min, UV 254 nm)

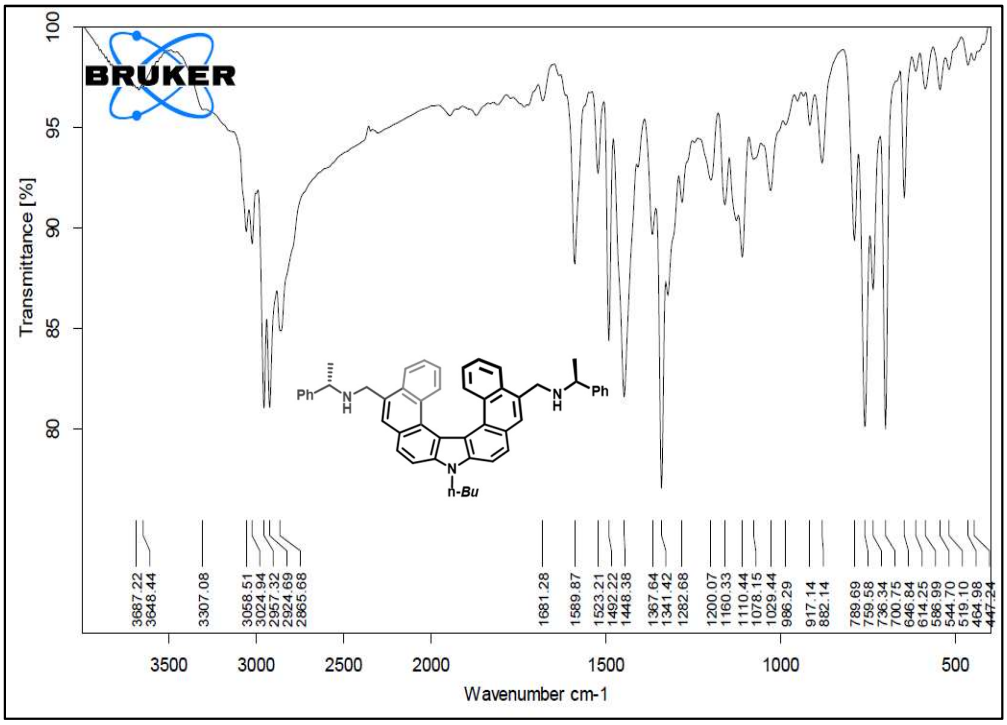

IR Spectrum of (*P,S,S*)-(+)-28

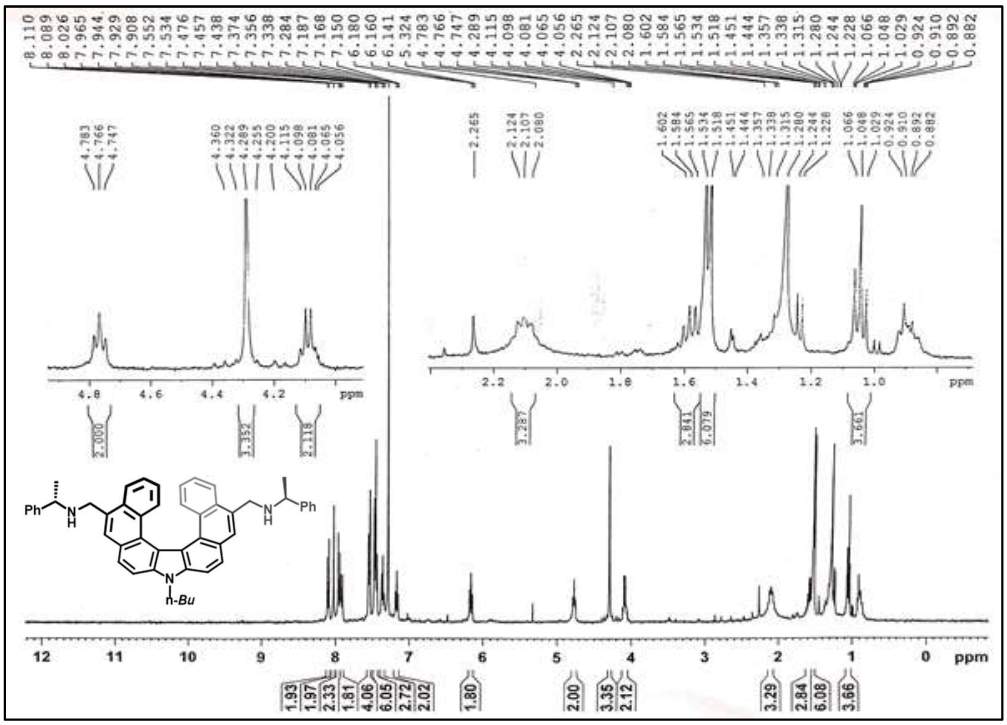

^{1}H NMR Spectrum of (*M,S,S*)-(-)-28 ($CDCl_3$, 400 MHz)

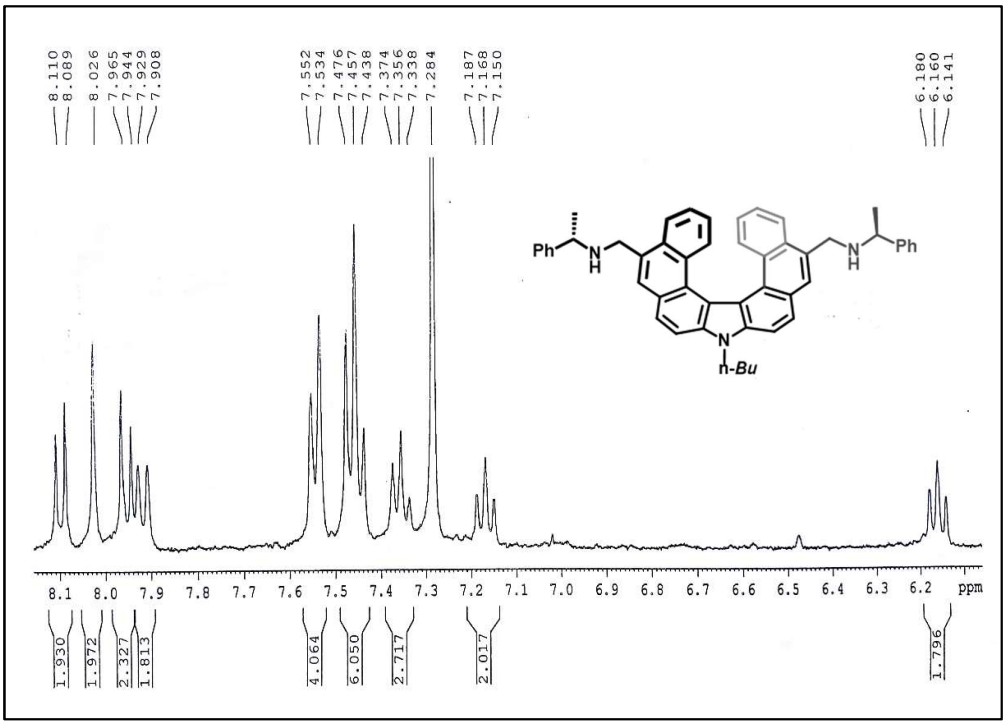

^{1}H NMR Spectrum of (*M,S,S*)-(-)-28 (enlarged aromatic region) ($CDCl_3$, 400 MHz)

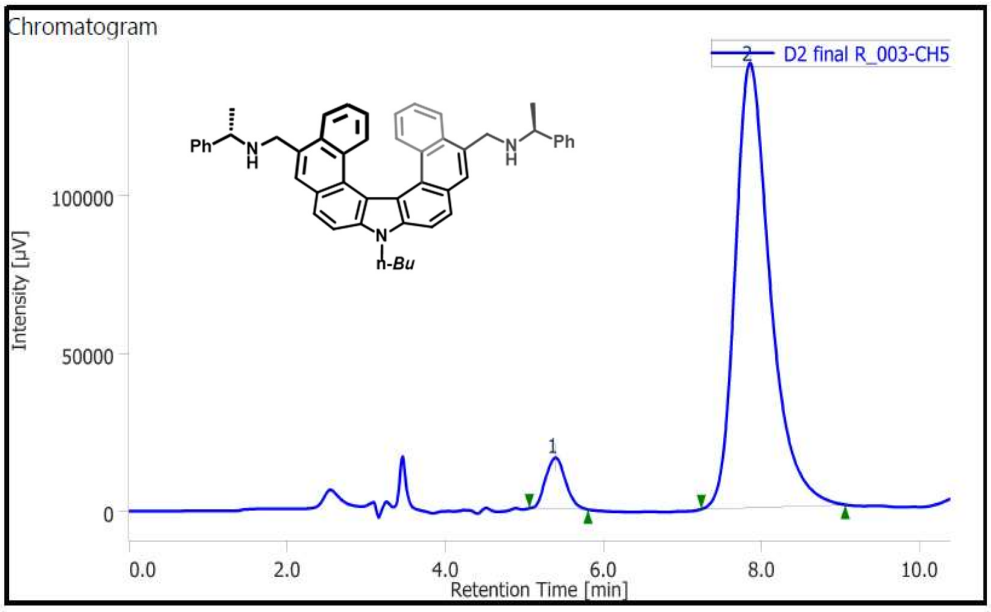

Peak Information

#	Peak Name	CH	tR [min]	Area [µV·sec]	Height [µV]	Area%	Height%	Quantity	NTP	Resolution	Symmetry Factor	Warning
1	Unknown	5	5.393	285421	16281	6.197	10.371	N/A	2073	3.958	1.117	
2	Unknown	5	7.850	4320298	140706	93.803	89.629	N/A	1659	N/A	1.380	

HPLC chart of (*M,S,S*)-(-)-28
87% de (CHIRALPAK IC; isopranol/n-hexane (30/70), 1.0 mL/min, UV 254 nm)

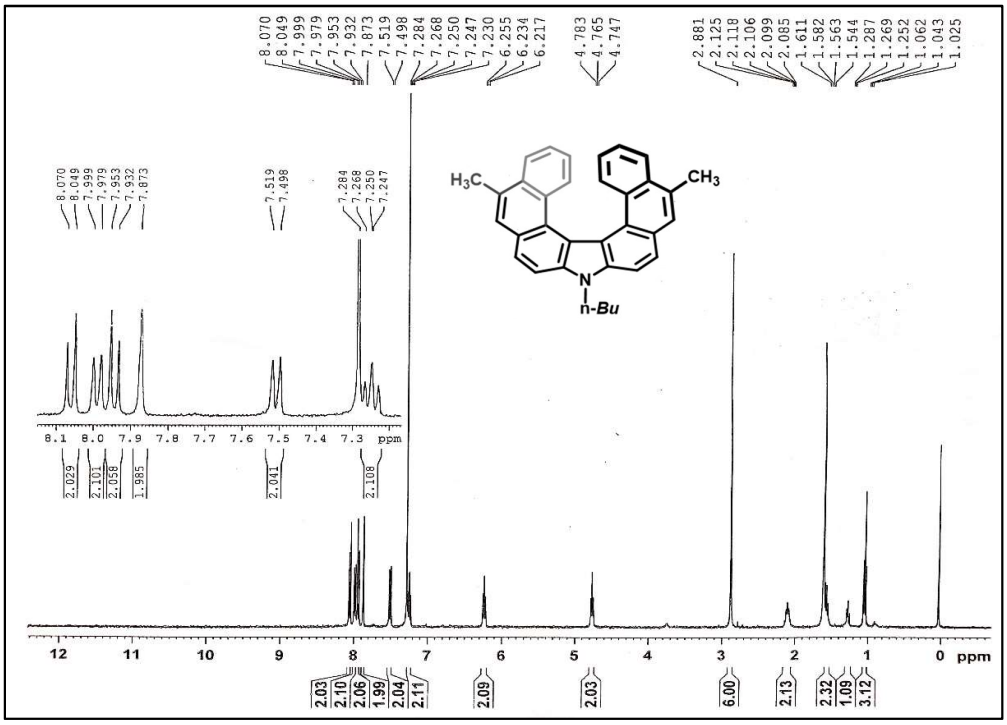

^{1}H NMR Spectrum of (*P*)-(+)-29 ($CDCl_3$, 400 MHz)

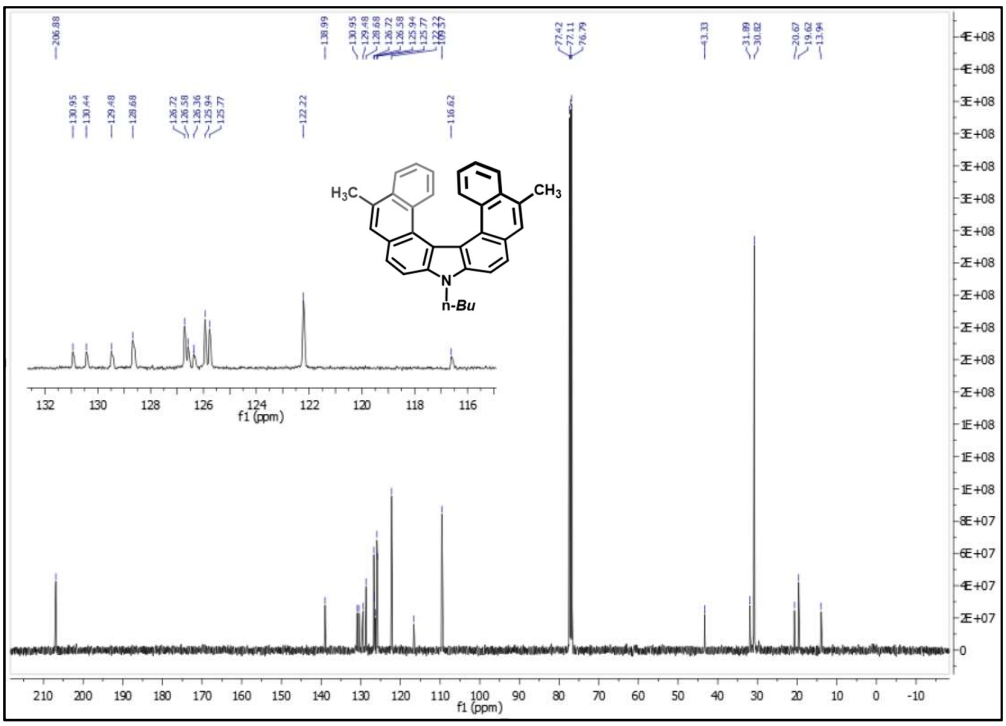

^{13}C NMR Spectrum of (*P*)-(+)-29 ($CDCl_3$, 100 MHz)

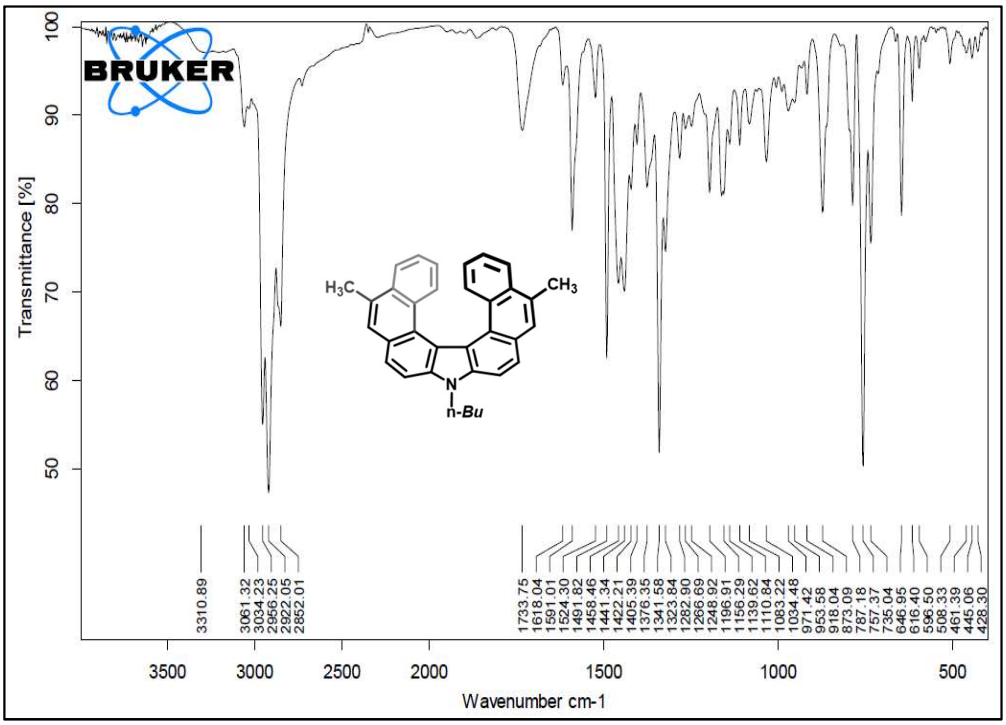

IR Spectrum of (*P*)-(+)-29

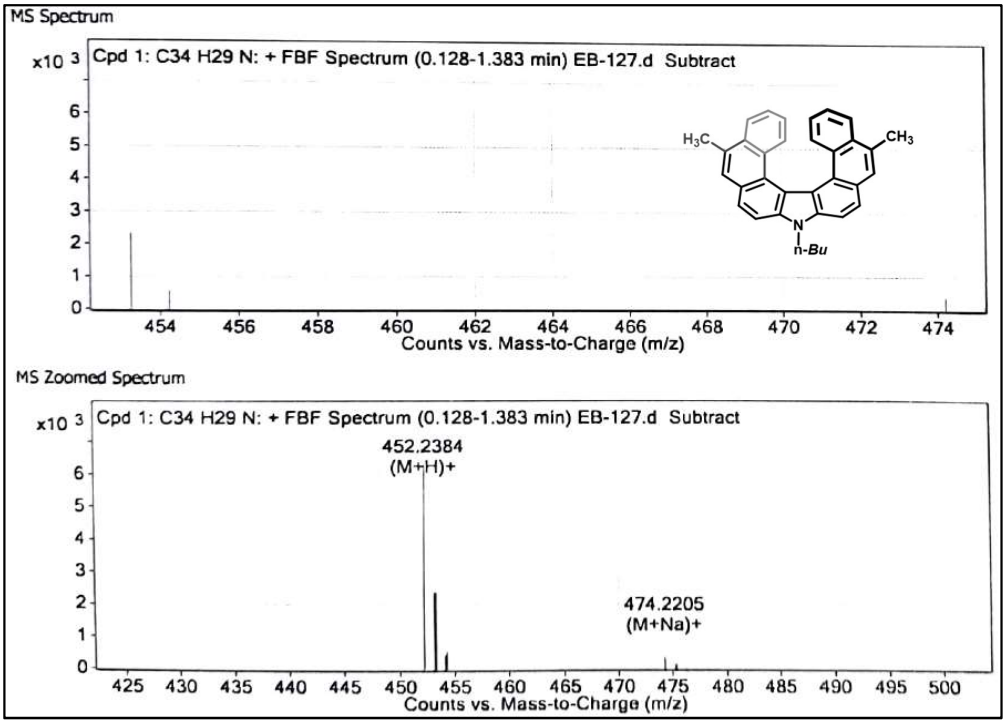

HRMS Spectrum of 29

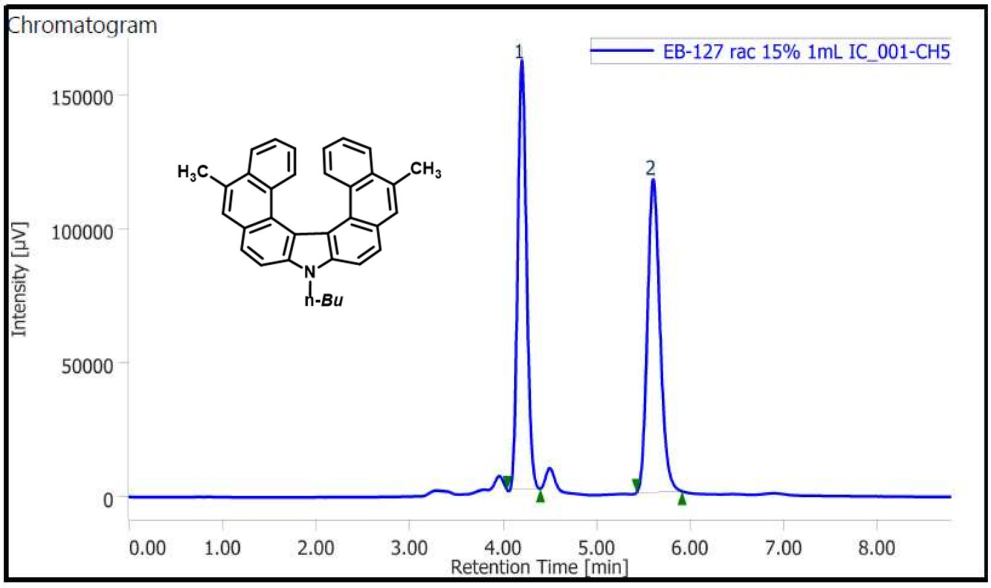

Peak Information

#	Peak Name	CH	tR [min]	Area [µV·sec]	Height [µV]	Area%	Height%	Quantity	NTP	Resolution	Symmetry Factor	Warning
1	Unknown	5	4.200	1051244	159896	49.086	57.837	N/A	9434	6.755	1.126	
2	Unknown	5	5.603	1090405	116564	50.914	42.163	N/A	8463	N/A	1.177	

HPLC chart of rac-29
(CHIRALPAK IC; isopranol/n-hexane (15/85), 1.0 mL/min, UV 254 nm)

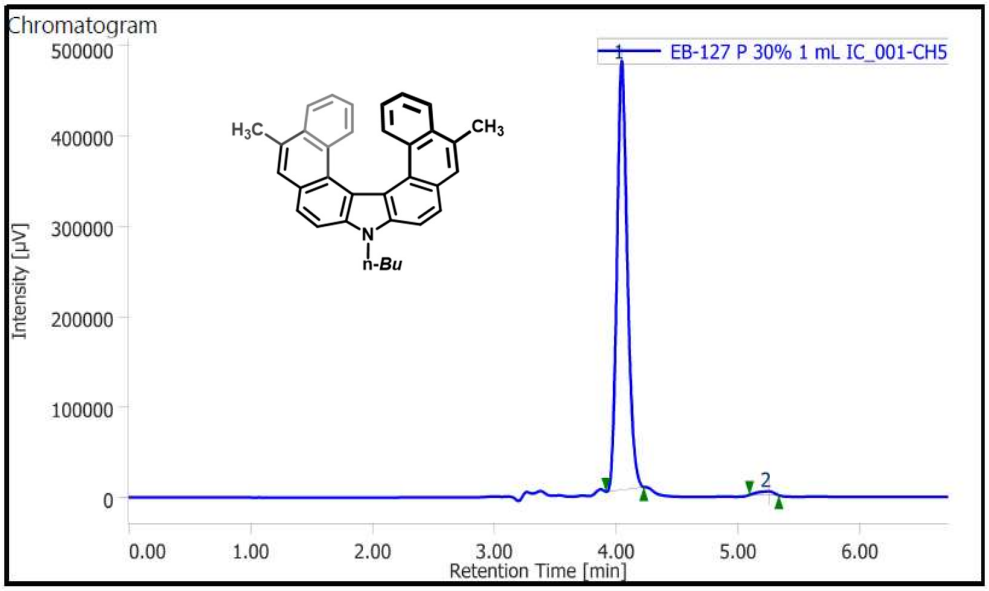

Peak Information

#	Peak Name	CH	tR [min]	Area [µV·sec]	Height [µV]	Area%	Height%	Quantity	NTP	Resolution	Symmetry Factor	Warning
1	Unknown	5	4.043	2809003	473997	98.699	99.159	N/A	11188	5.590	1.180	
2	Unknown	5	5.247	37014	4021	1.301	0.841	N/A	5668	N/A	0.761	

HPLC chart of (*P*)-(+)-29
(CHIRALPAK IC; isopranol/n-hexane (15/85), 1.0 mL/min, UV 254 nm)

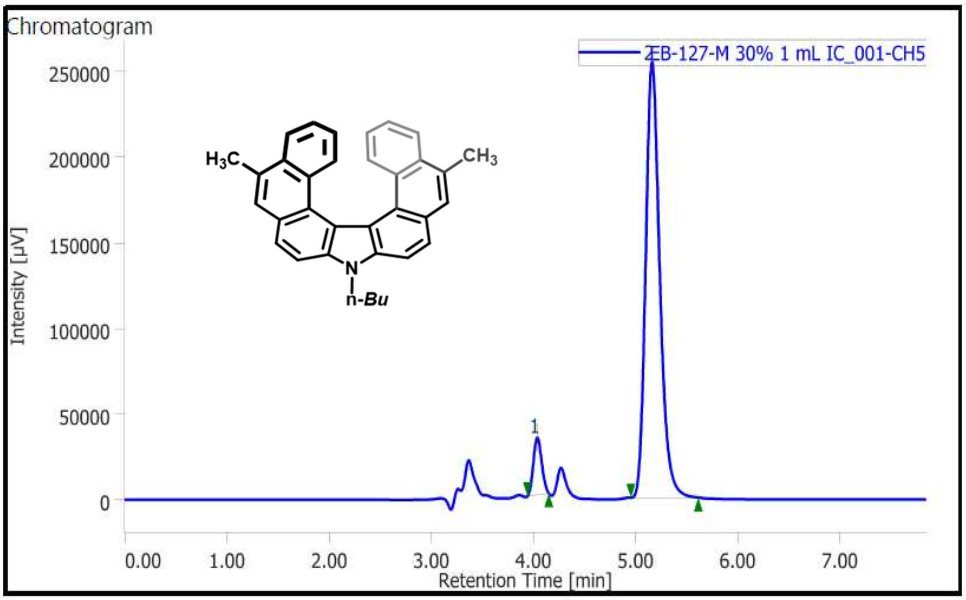

Peak Information

#	Peak Name	CH	tR [min]	Area [µV·sec]	Height [µV]	Area%	Height%	Quantity	NTP	Resolution	Symmetry Factor	Warning
1	Unknown	5	4.037	188534	33304	7.178	11.593	N/A	11098	5.628	1.088	
2	Unknown	5	5.157	2438179	253982	92.822	88.407	N/A	7040	N/A	1.254	

HPLC chart of (*M*)-(-)-29

(CHIRALPAK IC; isopranol/n-hexane (15/85), 1.0 mL/min, UV 254 nm)

2B.6 Crystallographic Data

	17
Identification code	exp_1513
Empirical formula	$C_{36}H_{29}Cl_2NO_2$
Formula weight	578.50
Temperature/K	100(2) K
Crystal system	Orthorhombic
Space group	Pbca
a/Å	16.2579(10)
b/Å	12.1960(8)
c/Å	27.8733(18)
α/°	90
β/°	90
γ/°	90
Volume/Å^3	5526.8(6) Å^3
Z	8
ρ_{calc}g/cm^3	1.391
μ/mm^{-1}	0.271
F(000)	2416
2Θ range for data collection/°	1.925 to 28.338°
Index ranges	-21<=h<=21, -16<=k<=13, -37<=l<=37
Reflections collected	147437
Independent reflections	6877 [R_{int} = 0.1820]
Data/restraints/parameters	6877 / 0 / 371
Goodness-of-fit on F^2	1.085
Final R indexes [I>=2σ (I)]	R_1 = 0.0657, wR_2 = 0.1631
Final R indexes [all data]	R1 = 0.0871, wR2 = 0.1759
Largest diff. peak/hole / e Å^{-3}	0.350 and -0.668 e.Å^{-3}

Crystal data and structure refinement for 17

2B.7 References

1. (a) Misek, J.; Teply, F.; Stara, I. G.; Tichy, M.; Saman, D.; Cisarova, I.; Vojtisek, P.; Stary, I. A Straightforward Route to Helically Chiral N-Heteroaromatic Compounds: Practical Synthesis of Racemic 1,14-Diaza[5]helicene and Optically Pure 1- and 2-Aza[6]helicenes, *Angew. Chemie Int. Ed.* **2008**, *47*, 3188. (b) Reetz, M. T.; Sostmann, S. 2,15-Dihydroxy-hexahelicene (HELIXOL): synthesis and use as an enantioselective fluorescent sensor, *Tetrahedron* **2001**, *57*, 2515. (c) Schweinfurth, D.; Zalibera, M.; Kathan, M.; Shen, C.; Mazzolini, M.; Trapp, N.; Crassous, J.; Gescheidt, G.; Diederich, F. Helicene Quinones: Redox-Triggered Chiroptical Switching and Chiral Recognition of the Semiquinone Radical Anion Lithium Salt by Electron Nuclear Double Resonance Spectroscopy, *J. Am. Chem. Soc.* **2014**, *136*, 13045. (d) Tsuji, G.; Kawakami, K.; Sasaki, S. Enantioselective binding of chiral 1,14-dimethyl[5]helicene-spermine ligands with B- and Z-DNA, *Bioorg. Med. Chem.* **2013**, *21*, 6063.
2. (a) Mikeš, F.; Boshart, G.; Gil-Av, E. Resolution on chiral charge-transfer complexing agents using high performance liquid chromatography, *J. Chem. Soc.* **1976**, 99. (b) Matlin, S. A.; Stacey, V. E.; Lough, W. J. Hexahelicene chiral stationary phase : I. Phase synthesis and use in high-performance liquid chromatographic resolution of enantiomers, *J. Chromatogr. A* **1988**, *450*, 157. (c) Ianni, F.; Scorzoni, S.; Gentili, P. L.; Di Michele, A.; Frigoli, M.; Camaioni, E.; Ortica, F.; Sardella, R. Chiral separation of helical chromenes with chloromethyl phenylcarbamate polysaccharide-based stationary phases, *J. Sep. Sci.* **2018**, *41*, 1266.
3. (a) Severa, L.; Koval, D.; Novotná, P; Ončák, M.; Sázelová, P.; Šaman, D.; Slavíček, P.; Urbanová, M.; Kašička, V.; Teplý, F. Resolution of a configurationally stable [5]helquat: enantiocomposition analysis of a helicene congener by capillary electrophoresis, *New J. Chem*. **2010**, *34*, 1063. (b) Koval, D.; Severa, L.; Adriaenssens, L.; Vávra, J.; Teplý, F.; Kašička, V. Chiral analysis of helquats by capillary electrophoresis: Resolution of helical N-heteroaromatic dications using randomly sulfated cyclodextrins, *Electrophoresis* **2011**, *32*, 2683.
4. (a) Newman, M. S.; Lutz, W. B.; Lednicer, D. A NEW REAGENT FOR RESOLUTION BY COMPLEX FORMATION; THE RESOLUTION OF PHENANTHRO-[3,4-c]PHENANTHRENE, *J. Am. Chem. Soc.* **1955**, *77*, 3420. (b) Newman, M. S.; Lednicer, D. The Synthesis and Resolution of Hexahelicene, *J. Am. Chem. Soc.* **1956**, *78*, 4765.

5. Kagan, H.; Moradpour, A.; Nicoud, J. F.; Balavoine, G.; Tsoucaris, G. Photochemistry with circularly polarized light. Synthesis of optically active hexahelicene, *J. Am. Chem. Soc.* **1971**, *93*, 2353.

6. (a) Carreño, M. C.; García-Cerrada, S.; Urbano, A. From central to helical chirality: synthesis of *P* and *M* enantiomers of [5]helicenequinones and bisquinones from (*S*,*S*)-2-(p-tolylsulfinyl)-1,4-benzoquinone, *J. Am. Chem. Soc.* **2001**, *123*, 7929. (b) Carreño, M. C.; García-Cerrada, S.; Urbano, A. *Chem. – A Eur. J.* **2003**, *9*, 4118. (c) Carreño, M.C.; Gonzlez-López, M.; Urbano, A. Efficient asymmetric synthesis of [7]helicene bisquinones, *Chem*. *Commun*. **2005**, 611.

7. Ogawa, Y.; Toyama, M.; Karikomi, M.; Seki, K.; Haga, K.; Uyehara, T. Synthesis of chiral [5]helicenes using aromatic oxy-Cope rearrangement as a key step, *Tetrahedron Lett.* **2003**, *44*, 2167.

8. Caeiro, J.; Peña, D.; Cobas, A.; Pérez, D.; Guitián, E. Asymmetric Catalysis in the [2+2+2] Cycloaddition of Arynes and Alkynes: Enantioselective Synthesis of a Pentahelicene, *Adv. Synth. Catal*. **2006**, *348*, 2466.

9. Alexandrova, Z.; Sehnal, P.; Stara, I. G.; Stary, I.; Saman, D.; Urquhart, S. G.; Otero, E. Modified Synthesis of Heptahelicene and Its Resolution Into Single Enantiomers, *Collect. Czech. Chem. Commun*. **2006**, *71*, 1256.

10. Sako, M.; Takeuchi, Y.; Tsujihara, T.; Kodera, J.; Kawano, T.; Takizawa, S.; Sasai, H. Efficient Enantioselective Synthesis of Oxahelicenes Using Redox/Acid Cooperative Catalysts, *J. Am. Chem. Soc.* **2016**, *138*, 11481.

11. (a) Stöhr, M.; Boz, S.; Schär, M.; Nguyen, M.-T.; Pignedoli, C.A.; Passerone, D.; Schweizer, W.B.; Thilgen, C.; Jung, T.A.; Diederich, F. Self-Assembly and Two Dimensional Spontaneous Resolution of Cyano- Functionalized [7]Helicenes on Cu(111), *Angew. Chem. Int. Ed.* **2011**, *50*, 9982. (b) Upadhyay, G.M.; Mande, H.M.; Pithadia, D.K.; Maradiya, R.H.; Bedekar, A.V. Effect of the position of the cyano group on molecular recognition, supramolecular superhelix architecture and spontaneous resolution of aza[7]helicenes, *Cryst. Growth Des.* **2019**, *19*, 5354. (c) Sundar, M.S.; Klepetářová, B.; Bednárová, L.; Muller G. Synthesis, Chiral Resolution, and Optical Properties of 2,18-Dihydoxy-5,10,15-trioxa[9]helicene, *Eur. J. Org. Chem.* **2021**, 146.

12. (a) Okubo, H.; Yamaguchi, M.; Kabuto C. Macrocyclic Amides Consisting of Helical Chiral 1,12-Dimethylbenzo[c]phenanthrene-5,8-dicarboxylate, *J. Org. Chem*. **1998**, *63*, 9500. (b) Yamamoto, K.; Shimizu, T.; Igawa, K.; Tomooka, K.; Hirai, G.; Suemune, H.; Usui, K. Rational Design and Synthesis of [5]Helicene-Derived Phosphine Ligands and

Their Application in Pd-Catalyzed Asymmetric Reactions, *Sci. Rep*. **2016**, *6*, 36211.

13. (a) Tsujihara, T.; Inada-Nozaki, N.; Takehara, T.; Zhou, D.-Y.; Suzuki, T.; Kawano, T. Nickel-Catalyzed Construction of Chiral 1-[6]Helicenols and Application in the Synthesis of [6]Helicene-Based Phosphinite Ligands, *Eur. J. Org. Chem*. **2016**, 4948. (b) Yavar, K.; Aillard, P.; Zhang, Y.; Nuter, F.; Retailleau, P.; Voituriez, A.; Marinetti, A. Helicenes with embedded phosphole units in enantioselective gold catalysis, *Angew. Chem. Int. Ed*. **2014**, *53*, 861. (c) Dreher, S.D.; Katz, T.J.; Lam, K.-C.; Rheingold, A.L. Application of the Russig−Laatsch Reaction to Synthesize a Bis[5]helicene Chiral Pocket for Asymmetric Catalysis, *J. Org. Chem*. **2000**, *65*, 815.
14. Tanaka, K.; Osuga, H.; Suzuki, H.; Shogase, Y. Kitahara, Y. Synthesis, enzymic resolution and enantiomeric enhancement of bis(hydroxymethyl)[7]thiaheterohelicenes, *J. Chem. Soc., Perkin Trans.* 1 **1998**, 935.
15. (a) Waghray, D.; Zhang, J.; Jacobs, J.; Nulens, W.; Basaric, N.; van Meervelt, L.; Dehaen, W. Synthesis and structural elucidation of diversely functionalized 5,10-diaza[5]helicenes, *J. Org. Chem.* **2012**, *77*, 10176. (b) Gupta, R.; Cabreros, T.A.; Muller, G.; Bedekar, A.V. Synthesis and study of enantiomerically pure 5,13-dicyano-9-oxa[7]helicene, *Eur. J. Org. Chem.* **2018**, 5397.
16. (a) Bhalodi, E.H.; Patel, K.N.; Bedekar, A.V. Synthesis and resolution of 2-amino-5-aza[6]helicene, *Tetrahedron* **2022**, *114*, 132761. (b) Shahabuddin, M.; Md. Hossain, M.S.; Kimura, T.; Karikomi, M. Diastereomeric process-based chiral resolution of helical quinone derivatives using (-)-menthyl chloroformate, *Tetrahedron Lett.* **2017**, *58*, 4491.
17. Rajan, B.; Goel, N.; Bedekar A.V. Synthesis and characterization of aza[7]helicenes, *J. Mol. Struct.* **2022**, *1261*, 132972.
18. (a) Nakano, K.; Hidehira, Y.; Takahashi, K.; Hiyama, T.; Nozaki, K. Stereospecific synthesis of hetero[7]helicenes by Pd-catalyzed double *N*-arylation and intramolecular *O*-arylation, *Angew. Chem. Int. Ed.* **2005**, *44*, 7136. (b) Tsujihara, T.; Inada-Nozaki, N.; Takehara, T.; Zhou, D.-Y.; Suzuki, T.; Kawano, T. Nickel-Catalyzed Construction of Chiral 1-[6]Helicenols and Application in the Synthesis of [6]Helicene-Based Phosphinite Ligands, *Eur. J. Org. Chem*. **2016**, 4948. (c) Braiek, M.B.; Aloui, F.; Hassine, B.B. Synthesis and resolution of 2-hydroxyhexahelicene, *Tetrahedron Lett.* **2013**, *54*, 424.
19. Tsujihara, T.; Zhou, D.-Y.; Suzuki, T.; Tamura, S.; Kawano, T. Helically Chiral 1-Sulfur-Functionalized [6]Helicene: Synthesis, Optical Resolution, and

Functionalization, *Org. Lett*. **2017**, *19*, 3311.

20. Hasan, M.; Pandey, A.D.; Khose, V.N.; Mirgane, N.A.; Karnik, A.V. Sterically Congested Chiral 7,8-Dioxa[6]helicene and Its Dihydro Analogues: Synthesis, Regioselective Functionalization, and Unexpected Domino Prins Reaction, *Eur. J. Org. Chem*. **2015**, 3702.
21. Bucinskas, A.; Waghray, D.; Bagdziunas, G.; Thomas, J.; Grazulevicius, J.V.; Dehaen, W. Synthesis, functionalization and optical properties of chiral carbazole-based diaza[6]helicenes, *J. Org. Chem.* **2015**, *80*, 2521.
22. Rajan, B.; Bedekar, Effect of methyl substituent in the fjord region on the conformational stability of aza[5]helicenes, A.V. *J. Mol. Struct.* **2021**, *1234*, 130178.
23. (a) Chuang, C. N.; Chuang, H. J.; Wang, Y. X.; Chen, S. H.; Huang, J. J.;Leung, M. K.; Hsieh, K. H. Polymers with alkyl main chain pendent biphenyl carbazole or triphenylamine unit as host for polymer light emitting diodes, *Polymer* **2012**, *53*, 4983. (b) Zhao, T.; Liu, Z.; Song, Y.; Xu, W.; Zhang, D.; Zhu, D. Novel diethynylcarbazole macrocycles: synthesis and optoelectronic properties, *J. Org. Chem.* **2006**, *71*, 7422.
24. (a) Upadhyay, G.M.; Talele, H.R.; Sahoo, S.; Bedekar, A.V. Synthesis of carbazole derived aza[7]helicenes, *Tetrahedron Lett*. **2014**, *55*, 5394. (b) Upadhyay, G.M.; Talele, H.R.; Bedekar, A.V. Synthesis and photophysical properties of aza[n]helicenes, *J. Org. Chem.* **2016**, *81*, 7751.
25. Moussa, M.E.S.; Srebro, M.; Anger, E.; Vanthuyne, N.; Roussel, C.; Lescop, C.; Autschbach, J.; Crassous, J. Chiroptical Properties of Carbo[6]Helicene Derivatives Bearing Extended π-Conjugated Cyano Substituents, *Chirality* **2013***, 25,* 455.
26. (a) Neidigh, K.A.; Avery, M.A.; Williamson, J.S.; Bhattacharyya, S. Facile preparation of *N*-methyl secondary amines by titanium(IV) isopropoxide-mediated reductive amination of carbonyl compounds, *J. Chem. Soc., Perkin Trans.* 1 **1998**, 2527. (b) DiCesare, J.C.; White, C.E.; Rasmussen, W.E.; White, B.M.; McComas, C.B.; Craft, L.E. Modification of the Titanium(IV) Isopropoxide Reductive Amination Reaction: Application to Solid Phase Synthesis, *Synth. Commun.* **2005**, *35*, 663.
27. Wuts, P. G. M. *Protective Groups in Organic Synthesis*, 4th ed.; John Wiley & Sons, Inc: New Jersey, **2014**.